Acta Universitatis Agriculturae Sueciae

Doctoral Thesis No. 2024:80
Faculty of Natural Resources and Agricultural Sciences

Microplastic distribution and transport in agricultural soils

From field to burrow scale

Wiebke Mareile Heinze

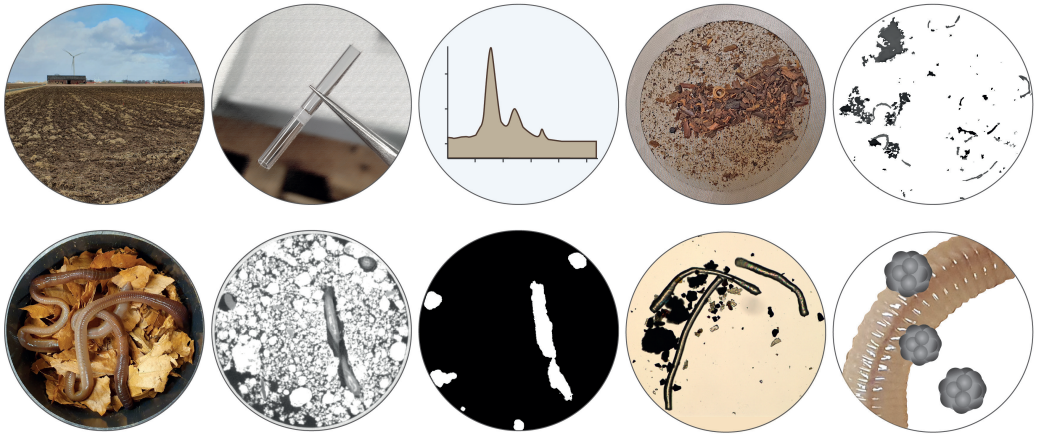

Microplastic distribution and transport in agricultural soils

From field to burrow scale

Wiebke Mareile Heinze
Faculty of Natural Resources and Agricultural Sciences
Department of Soil and Environment
Uppsala

SLU
SWEDISH UNIVERSITY OF AGRICULTURAL SCIENCES

DOCTORAL THESIS
Uppsala 2024

Acta Universitatis Agriculturae Sueciae
2024:80

Cover: Snapshots of field and laboratory procedures and methods for micro- and nanoplastic analysis (photos and figures by Wiebke Mareile Heinze, 2024)

ISSN 1652-6880
ISBN (print version) 978-91-8046-371-3
ISBN (electronic version) 978-91-8046-407-9
https://doi.org/10.54612/a.42s2q72vbg

Swedish University of Agricultural Sciences, Department of Soil and Environment, Uppsala, Sweden

Print: SLU Grafisk service, Uppsala 2024

Microplastic distribution and transport in agricultural soils

Abstract

Micro- and nanoplastics (MNPs) are small plastic particles that are emitted to soils via a range of different pathways with potentially adverse effects on the soil ecosystem. In this thesis, field and laboratory studies were done to investigate the spatial distribution of MNPs in agricultural soils for an improved understanding of input pathways, transport mechanisms and potentially transport limiting factors that modify local exposure levels. Microplastics (MPs) detected in soil profiles taken from long-term field trials revealed that amendments with sewage sludge led to higher exposure to MPs than when conventional mineral fertiliser was applied. Moreover, substantial transport was observed in the field, likely a combined result of macropore transport and bioturbation as influenced by soil management and earthworm activity. Microcosm studies of MNPs with the deep-burrowing earthworm *Lumbricus terrestris* revealed bioturbation as a relevant transport mechanism both for nanoplastics and MP fibres. Relatively small particles were transported faster, but particle aspect ratio and volume likely play decisive roles for the potential ingestion and subsequent transport rate by earthworms. Collectively, the results highlight the need to consider horizontal and vertical MNP mobility in soils, in particular transport by bioturbation, for future monitoring schemes and mass balances. The comparison of a range of analytical methods to quantify and characterise MNPs revealed further need to optimize detection and recovery, as well as improve conversion methods between particle- and mass-based approaches for achieving reliable exposure estimates. Further investigations are necessary to assess the transport potential of other MNP shapes and sizes, by other earthworm ecotypes and under differing soil conditions and soil management systems.

Keywords: pollutant, exposure, bioturbation, organic residues, long-term field trial, μ–FT-IR, Py–GC/MS

Fördelning och transport av mikroplaster i jordbruksmark

Sammanfattning

Mikro- och nanoplaster (MNP) är små plastpartiklar som släpps ut i marken på olika sätt med potentiellt negativa effekter på markens ekosystem. I denna avhandling har fält- och laboratoriestudier gjorts för att undersöka den rumsliga fördelningen av MNP i jordbruksmark för en förbättrad förståelse av ingångsvägar, transportmekanismer och potentiellt transportbegränsande faktorer som påverkar lokala exponeringsnivåer. Mikroplaster (MP) som upptäckts i markprofiler från långliggande fältförsök visade att användning av avloppsslam ledde till högre exponering för MP än när konventionellt mineralgödsel användes. Dessutom observerades betydande transporter i fält, sannolikt ett kombinerat resultat av makroportransport och bioturbation som påverkats av jordbearbetning och daggmaskaktivitet. Mikrokosmosstudier av MNP med den djupt grävande daggmasken Lumbricus terrestris visade bioturbation som en relevant transportmekanism både för nanoplaster och MP fibrer. Relativt små partiklar transporterades snabbare, men partikelstorleksförhållande och volym spelar sannolikt avgörande roller för det potentiella intaget och den efterföljande transporthastigheten av daggmaskar. Sammantaget belyser resultaten behovet av att överväga horisontell och vertikal MNP-rörlighet i mark, särskilt transport genom bioturbation, för framtida övervakningssystem och massbalanser. Jämförelsen av en rad analytiska metoder för att kvantifiera och karakterisera MNP:er avslöjade ytterligare behov av att optimera detektion- och återhämtningsmetoder, samt förbättra konverteringsmetoder mellan partikel- och massbaserade metoder för att uppnå tillförlitliga exponeringsuppskattningar. Ytterligare undersökningar är nödvändiga för att bedöma transportpotentialen för andra MNP-former och -storlekar, av andra typer av daggmaskar och under olika markförhållanden och jordbearbetningssystem.

Sökord: förorenande ämne, organisk återstod, bioturbation, miljöexponering, långvarigt fältförsök, μ–FT-IR, Py–GC/MS

Verteilung und Transport von Mikroplastik in landwirtschaftlich genutzten Böden

Zusammenfassung

Mikro- und Nanoplastik (MNP) sind kleine Kunststoffpartikel, die über verschiedene Wege in den Boden gelangen mit potentiellen negative Auswirkungen für das Bodenökosystem. In dieser Arbeit wurden Feld- und Laborstudien durchgeführt, um die räumliche Verteilung von MNP in landwirtschaftlichen Böden zu untersuchen und so zu einem verbesserten Verständnis der Eintragspfade, Transportmechanismen und transportbegrenzenden Faktoren beizutragen. Mikroplastikmessungen in Bodenprofilen aus Langzeituntersuchungen ergaben, dass die Düngung von Klärschlamm zu einer höheren Belastung mit Mikroplastik (MP) führt als herkömmlicher Mineraldünger. Darüber hinaus wurde im Feld eine erhebliche Translokation von MP beobachtet, vermutlich durch Transport in Makroporen und Bioturbation, die wiederum vom lokale Bodenmanagement und der Aktivität von Regenwürmern beeinflusst werden. Mikrokosmenstudien mit dem tief grabenden Regenwurm *Lumbricus terrestris* bestätigten, dass Bioturbation ein relevanter Transportmechanismus sowohl für Nanoplastik als auch für MP Fasern ist. Kleine Partikel wurden schneller transportiert, aber Längenverhältnis und Volumen sind vermutlich entscheidende Faktoren für die Aufnahme und Transportrate von MP durch Regenwürmer. Insgesamt heben die Ergebnisse die Notwendigkeit hervor, horizontale und vertikale Transportprozesse von MNP, insbesondere die Rolle von Bioturbation, für systematische Überwachungssysteme und Massenbilanzen zu berücksichtigen. Der Vergleich verschiedener analytischer Methoden zur Messung von MNP verdeutlichten, dass zudem weitere analytische Optimierungen von Probenaufbereitung, Analyse und Konvertierung zwischen partikel- und massenbasierten Ansätzen notwendig sind, um potentielle Risiken zuverlässig zu beurteilen. Weitere Untersuchungen sind erforderlich, um das Transportpotenzial von MNP anderer Formen, Größen sowie durch andere Regenwürmer mit anderem Bioturbationsverhalten unter unterschiedlichen Bodenbedingungen und Bodenbewirtschaftungssystemen zu bewerten.

Suchwörter: *Schadstoff, Umweltbelastung, organische Rückstände, Bioturbation, Langzeitfeldversuch, µ–FT-IR, Py–GC/MS*

Preface

I have always had a passion for books. Language is a beautiful tool to create and to think. Over the years, I even started writing my own stories, and I started to dream of the day that I would publish my own book. But as so often with dreams, the seed of doubt gained foot and I abandoned the magical realms of the fantasy world.

That is not to say that my dreams became any less ambitious; but instead of spending days exploring the pages of books I stepped out to discover the real world. After school, I travelled the world for a year, and when I returned home I started studying geography as an idealist, wanting to change the world for the better. But as so often with ambitious aspirations, sooner or later the realization dawned upon me that one person cannot solve all problems in the world; each person can only work on a piece of the puzzle.

Then, one day during my bachelor studies I just happened to find myself attending a lecture on soil geography. Quite frankly, I had very low expectations when I entered the lecture hall and only joined because some friends convinced me to go instead of sitting in a nearby café sipping a coffee and waiting for the next lecture to start. That decision later proved to change everything. Soil is beautifully complex, it affects all aspects of our lives, it interacts with air, water, plants, with a myriad of processes happening at various spatial scales at the same time. Needless to say, when I walked out of the lecture hall, I knew that I wanted to become a soil scientist.

So this is where I stand now: a soil scientist, an author of a book – even if it is a very different one from what I first envisioned all those years ago – and although my research does not solve all our problems in the world I would like to think that it at least helps us to understand part of one problem. The journey took unexpected turns, but it brought me to where I am now, so I am intrigued to see where it takes me next.

To all those who believed in me,
And to all those who work hard to achieve their goal.

Contents

List of publications

This thesis is based on the work contained in the following papers, referred to by Roman numerals in the text:

I. Heinze, W.M., Steinmetz, Z., Klemmensen, N.D.R., Vollertsen, J., Cornelis, G., 2024. Vertical distribution of microplastics in an agricultural soil after long-term treatment with sewage sludge and mineral fertiliser. *Environmental Pollution*. 356, 124343. https://doi.org/10.1016/j.envpol.2024.124343

II. Heinze, W.M., Mitrano, D.M., Lahive, E., Koestel, J., Cornelis, G., 2021. Nanoplastic transport in soil via bioturbation by *Lumbricus terrestris*. *Environmental Science & Technology*. 55, 16423–16433. https://doi.org/10.1021/acs.est.1c05614

III. Heinze, W.M., Leicht, K.A., Mitrano, D.M., Lahive, E., Cornelis, G. Earthworms transport a wide size range of microplastic fibres in soil. (Manuscript)

The contribution by Wiebke Mareile Heinze to the papers included in this thesis was as follows:

I. Conceptualization, methodology, validation, performance of laboratory analyses, data analysis, formal analysis, visualization, manuscript writing.

II. Conceptualization, methodology, sampling, validation, performance of laboratory analyses, data analysis, formal analysis, manuscript writing.

III. Conceptualization, methodology, sampling, validation, performance of laboratory analyses, data analysis, formal analysis, manuscript writing.

Additional papers

Wiebke Mareile Heinze further contributed to the following papers that were not included in this thesis:

I. Thomas, D., Schütze, B., **Heinze, W.M.**, Steinmetz, Z., 2020. Sample preparation techniques for the analysis of microplastics in soil - A review. *Sustainability*. 12, 9074. doi: 10.3390/su12219074

II. Hooge, A., Hauggaard-Nielsen, H., **Heinze, W.M.**, Lyngsie, G., Ramos, T.M., Sandgaard, M.H., Vollertsen, J., Syberg, K., 2023. Fate of microplastics in sewage sludge and in agricultural soils. *Trends in Analytical Chemistry*. 166, 117184. doi: 10.1016/j.trac.2023.117184

III. Schultz, C., Lahive, E., Belinga-Desaunay, M.-F., Green Etxabe, A., **Heinze, W.M.**, Steinmetz, Z., Horton, A.A., Jurkschat, K., Lynch, I., Matzke, M., Roberts, S., Robinson, A., Short, S., Swart, E., Svendsen, C., Spurgeon, D.J. 2024. The uptake and effects of nanomaterials in terrestrial species exposed under realistic field conditions. (Manuscript)

Abbreviations

μ–FT-IR	Micro – Fourier transform infrared spectrometry
ICP–MS	Inductively coupled plasma – mass spectrometry
K	Potassium
MNP	Micro- and nanoplastic
MP/MPs	Microplastic/microplastics
N	Nitrogen
NaCl	Sodium chloride
NP/NPs	Nanoplastic/nanoplastics
P	Phosphorus
Py–GC/MS	Pyrolysis – gas chromatography/mass spectrometry
PA	Polyamide
PE	Polyethylene
PET	Polyethylene terephthalate
PP	Polypropylene
PS	Polystyrene
PU	Polyurethane
PVC	Polyvinyl chloride
TN	Total nitrogen
TOC	Total organic carbon
X-ray CT	X-ray computed tomography
$ZnCl_2$	Zinc chloride

1. Introduction

"*There's always a bit of truth in each rumour,*
the trouble is finding out which bit."
The Novice, Trudi Canavan

Soils are an often overlooked but essential resource for society. We are inevitably dependent on the existential services soils provide – may that be food production, biodiversity or their function as filters of potential pollutants as water passes through the soil profile towards the groundwater. However versatile and valuable, agricultural soils are exposed to various stressors, some of which can have long-lasting adverse effects or result in irreversible changes in its physical, chemical and biological properties. In recent years, there has been an increasing awareness about the release of plastics into the environment. Much attention has initially been on marine ecosystems, but soils are by no means unaffected. Recent mass flow estimates suggest that soils might even receive 40 times more plastics than the aquatic environment (Kawecki and Nowack, 2019), highlighting the need for a better understanding of the scale and impact of plastic pollution of the soil system.

Plastic production and consumption has continuously increased since its broad-scale introduction into common products in the 1950s (Crawford and Quinn, 2017). Since then, plastics have become an essential part of everyday life, not only as packaging to preserve food, but also as a material used in the building industry, in furniture and storage or as textiles. The term *plastics* is used to summarize a wide range of synthetic carbon-based polymeric materials that differ widely in terms of their chemical composition and physical properties (Hartmann et al., 2019). What they have in common, however, is that most plastics are intentionally designed to be highly resistant

to degradation (Chamas et al., 2020). Whilst the high stability is beneficial for the various purposes for which plastics are used in everyday life, it also makes them persistent pollutants when they enter the terrestrial environment. Especially small plastic particles below 5 mm in size, so-called microplastics (MPs) and nanoplastics (NPs, <1 µm), are a major concern because of their anticipated abundance and persistence in soils (Redondo-Hasselerharm et al., 2021). Micro- and nanoplastics (MNPs) can be formed prior to their entry to soils or *in-situ* with the successive fragmentation of larger particles, with potentially adverse effects on soil biota and crops (Arkatkar et al., 2009; Lambert and Wagner, 2016; Ng et al., 2018; Sintim et al., 2019).

In environmental risk assessment of potentially hazardous substances or materials, risk is considered a combination of hazard, i.e. effects on organisms, and exposure. MNPs are ubiquitous in the terrestrial environment and have been found even in remote places as a result of diffuse atmospheric transport (Allen et al., 2019; Bergmann et al., 2019; Tatsii et al., 2024). However, some soils are more prone to MNP pollution due to their exposure to multiple emission pathways. A variety of agricultural practices are thought to be key determinants of emissions of MNPs to soils (Huerta Lwanga et al., 2023). In particular, the re-use of urban organic residues is thought to exacerbate the exposure of agricultural soils to plastic pollution (Corradini et al., 2019; van den Berg et al., 2020). Particles, including MNPs, in soils can be transported with agricultural management practices, such as ploughing, but also by the movement of water and soil biota. Local MNP exposure levels may therefore continuously be altered as transport processes change their distribution in the soil ecosystem with potential implications for effects at a local scale, but also determining potential transfers to fresh- and groundwater reserves.

Uncertainties still persist concerning the presence of MNPs in agricultural soils in response to different fertiliser practices and their subsequent mobility in the soil (Horton et al., 2017). Improving our understanding of their abundance and distribution in the soil environment is, thus, of critical importance for reliable exposure and risk assessments based on relevant MNP concentrations encountered in the soil environment. Understanding the underlying mechanisms that facilitate or inhibit transport processes are therefore essential to support long-term predictions about the presence and spread of MNPs in soil ecosystems.

2. Aim and objectives

The transport of MNPs and their resulting vertical distribution are important for assessing the spatial and temporal dimension of exposure of soils to MNPs, as well as their potential spread in the soil ecosystem. The overall aim of this thesis was to improve our understanding of the spatial distribution of micro- and nanoplastics in agricultural soils with regards to the underlying transport processes and influencing factors that determine their mobility. The main research questions to be addressed were:

- Are MPs added to soil via sewage sludge and how does MP addition compare to soils where mineral fertiliser is added instead? (**Paper I**)
- How are MPs and NPs distributed in the soil and how are they redistributed by transport processes, in particular by bioturbation? (**Paper I**, **II**, **III**)
- How do MNP properties and soil properties affect the vertical transport dynamics in soil? (**Paper I**, **II**, **III**)

To achieve these aims, several objectives were set out related to the different parts of this work, namely to:

- Develop a strategy for MP mass and particle number quantification and characterisation in field soil samples, and identify advantages and disadvantages of the applied methods. (**Paper I**)

- Compare the contamination of MPs in soils in response to sewage sludge application versus mineral fertiliser (horizontal distribution). (**Paper I**)
- Identify vertical distribution patterns of MPs in agricultural soil under long-term field conditions. (**Paper I**)
- Quantify the transport of NPs and MP fibres by earthworm burrowing and understand the underlying transport mechanism. (**Paper II**, **III**)
- Assess the impact of MP type, size and shape on transport dynamics. (**Paper I**, **II**, **III**)

To achieve these objectives, the distribution and transport of MPs was investigated in field- (**Paper I**) and laboratory-based studies (**Paper II**, **III**). The abundance and spatial distribution of MPs in agricultural soils provided insights into input sources of different fertiliser sources, as well as their potential horizontal and vertical dispersal under environmental conditions at the field scale (**Paper I**). The laboratory studies served to explain field observations by improving the mechanistic understanding of the transport of MP and NP by bioturbation (**Paper II**, **III**).

3. Background

"The fool strikes. The wise man smiles and watches, and learns. Then strikes."
Half a King, Joe Abercrombie

3.1 A definition of micro- and nanoplastics

The term *plastic* refers to carbon-based synthetic polymers that are mouldable, solid at ambient conditions, insoluble in water and resistant to degradation (Hartmann et al., 2019). As evident from this description, the term loosely summarizes a diverse group of chemically differing materials. As a consequence, chemical and physical properties, such as their degree of crystallinity, density or surface charge, vary between plastic polymer types. A plastic product can even comprise different polymers, which is then referred to as a co-polymer or polymer blend depending on the synthesis technique. To add to the complexity, plastics can contain a range of additives to enhance their properties, including flame retardants, metals, plasticizers and stabilizers, some of which can have toxic or endocrine-disrupting effects themselves (Chen et al., 2021). Although some biodegradable plastics have been developed, these still constitute only a small fraction of the overall production of plastics (Geyer et al., 2017). The most commonly produced plastics and a selection of properties are presented in Figure 1.

The terms *microplastic* and *nanoplastic* refer to small plastic particles that are either intentionally produced in their size range or are unintentionally released from fragmenting plastic products during their life cycle, the so-called primary and secondary MNPs. There are still ongoing debates on specific size thresholds defining MNPs (Hartmann et al., 2019). As proposed by Gigault et al. (2018) and inspired by the established classification of

colloidal particles (1 µm to 1 nm), the terms micro- and nanoplastics here refer to particles smaller than 5 mm and 1 µm respectively in their widest dimension. MPs occur in a wide range of shapes that are commonly distinguished as spheres, fragments, films, foams and fibres based on their aspect ratio and geometry (Liu et al., 2023). It is this complex combination of variable sources and the resulting high heterogeneity of chemical and physical properties that makes MPs and NPs a unique contaminant group (Gigault et al., 2021). Each of the aforementioned factors – chemical composition, physical properties, particle size and shape – can potentially modify the behaviour and the effects of MPs and NPs in the soil ecosystem, but are to date poorly understood (Ji et al., 2021; Shafea et al., 2023).

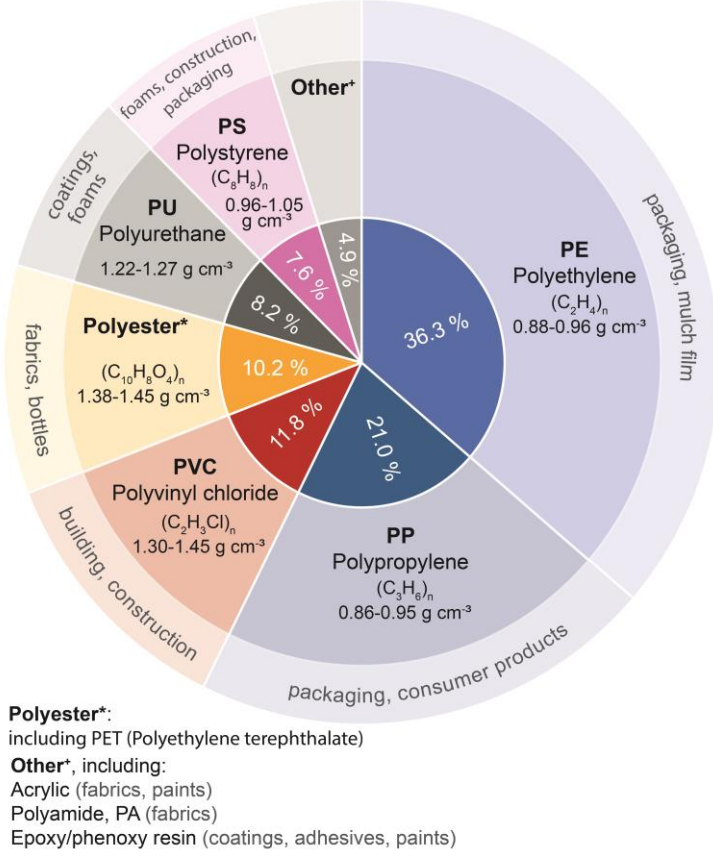

Figure 1: Overview of the most commonly produced plastics, including their common densities and uses. The global production share (%) is based on Geyer et al. (2017) for 2002-2014. Plastic properties and use are according to Crawford and Quinn (2017).

3.2 Detection of environmental micro- and nanoplastics in soil

Methods to detect MNPs in environmental samples have not yet been standardised due to persisting challenges related to particle recovery and interferences with organic matter. As a result, sample preparation and analytical setups for their quantification vary greatly between studies. Two approaches are commonly suggested for soil samples: spectroscopic and thermo-analytical methods. The former group of methods is based on the absorption of specific wavelengths of light by plastic polymers (Primpke et al., 2017), whereas detection by the latter is based on the characteristic degradation behaviour or degradation products of the plastic polymer when exposed to high temperatures. Thermo-analytical methods, such as pyrolysis – gas chromatography-mass spectrometry (Py–GC/MS), are destructive and yield polymer mass (Mansa and Zou, 2021). Spectroscopic methods, like micro – Fourier transform infrared spectroscopy (μ–FT-IR), operate particle-by-particle, allowing the capture of size parameters.

One major challenge in detecting MPs is that they are embedded within the complex soil matrix comprising inorganic but also organic components which cause interference. For most analytical setups, MPs are extracted from the mineral soil by density separation with a high-density solution (Thomas et al., 2020). This step is necessary in the case of spectroscopic methods that require a pure MP sample. For thermo-analytical methods it is optional and primarily serves to pre-concentrate the sample. Another common sample preparation step is the oxidative or enzymatic removal of organic matter. For Py–GC/MS, this step can be circumvented by use of an organic solvent that selectively extracts certain polymer types (Okoffo et al., 2020; Steinmetz et al., 2020). The analytical setup and detection method ultimately determine the scope of captured plastic polymers and sizes.

While often suggested as complementary (Dierkes et al., 2019), spectroscopic and thermo-analytical methods have rarely been used in conjunction, even though both particle numbers and particle mass are important for a comprehensive risk assessment. The rates of processes determining particle transport are typically proportional to particle number rather than mass (Quik et al., 2023). Mechanistic predictions of MP transport should therefore, in theory, be based on particle numbers. At the same time, particle numbers do not obey any conservation law so that many fate models still tend to utilize mass instead of particle numbers, similar to most eco-

toxicological effect studies (Kawecki and Nowack, 2019; Thornton Hampton et al., 2022). To date, however, particle-based measurements outweigh their mass-based counterparts. As a result, MP mass concentrations tend to be estimated from particle properties, such as particle sizes and density.

3.3 Micro- and nanoplastics in agricultural soils: exposure and effects

Agricultural soils are exposed to MNPs through various pathways, spanning from atmospheric deposition to their release from agricultural plastics that are used to improve crop production (Figure 2). One major pathway of MNPs to soils is through the addition of urban organic residues to agricultural land, such as composts (Porterfield et al., 2023; Weithmann et al., 2018) and municipal sewage sludge (Corradini et al., 2019; Frehland et al., 2020; Mahon et al., 2017; van den Berg et al., 2020). The role of sewage sludge as a vector for MNPs is of particular concern as its application on agricultural land is common in many European countries (Nizzetto et al., 2016). Sewage sludge contains much nitrogen, phosphorus and carbon and its reuse has thus been encouraged in some countries to achieve a more circular economy. In Sweden, the fraction of produced sewage sludge returned to agricultural land even increased from 20 % in 2010 to 46 % in 2020 (Naturvårdsverket, 2022; Appendix: Figure S1). MP concentrations found in sewage sludge-amended soils vary greatly between studies, from 600 to 48 800 particles kg^{-1} (Corradini et al., 2019; Klemmensen et al., 2024; Magnusson and Norén, 2014; Schell et al., 2022; van den Berg et al., 2020). This wide range can, in part, be explained by methodological differences that capture different plastic polymer types and sizes (section 3.2, Appendix: Table S1). In addition, MP concentrations vary with season, inlet concentrations at the wastewater treatment plant and differences in the treatment steps (Harley-Nyang et al., 2023). NPs have not been directly measured in agricultural soils to date, as most sample preparation methods include a filtration step wherein this size fraction is discarded (Pérez-Reverón et al., 2023). However, it is likely that NPs are similarly abundant in the environment given the successive fragmentation of MPs (Lambert and Wagner, 2016).

Determining the current MP concentrations in agricultural soils is important to inform environmental risk assessments. Currently reported environmental concentrations in soils tend to be below concentrations at

which effects on soil properties and crops or organisms have been observed in the laboratory (<0.05 % or 0.5 g kg^{-1}) (de Souza Machado et al., 2018; Huerta Lwanga et al., 2016; Lahive et al., 2022; Prendergast-Miller et al., 2019). Nevertheless, MNP emissions to the terrestrial environment remain a concern because of their potential persistence, continuously ongoing emissions and the successive *in-situ* fragmentation of larger particles. Negative effects of MNPs can be caused directly by the plastic or its additives (Chen et al., 2021), due to chemical or physical toxicity, or indirectly through food dilution (Thornton Hampton et al., 2022) or changes in soil properties (de Souza Machado et al., 2018). The presence of MP fibres, for instance, was shown to cause stress responses and reduced cast production for some earthworms (Lahive et al., 2022; Prendergast-Miller et al., 2019) while also affecting soil structure by decreasing water stable aggregates and decreasing soil bulk density (de Souza Machado et al., 2018). Observed effects of MPs and NPs on plants, soil biota and soil properties are often not straightforward (Ji et al., 2021), and vary with plastic polymer types, size and shape (de Souza Machado et al., 2018; Ju et al., 2019; Khalid et al., 2020; Lahive et al., 2022; Lozano and Rillig, 2020).

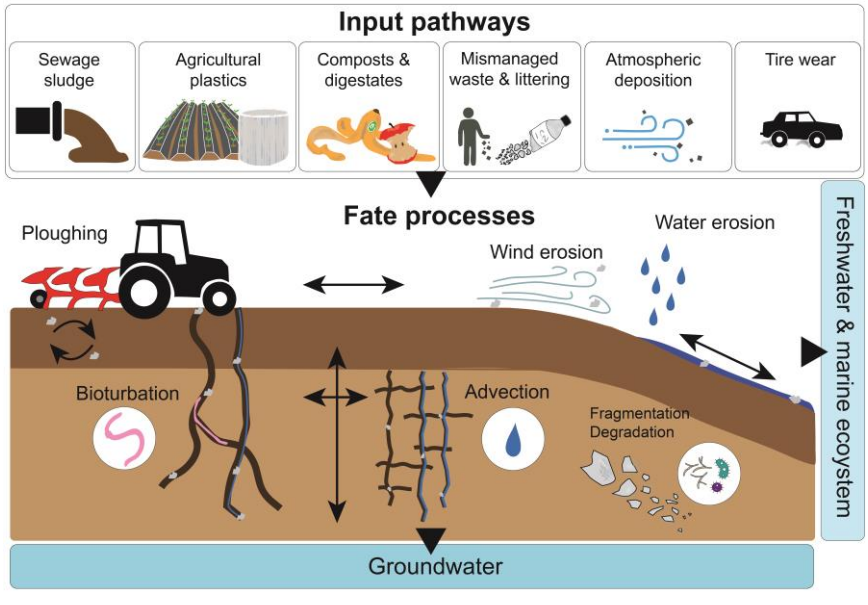

Figure 2: Overview of potential input pathways of MNPs to agricultural soils and subsequent potential fate processes.

In risk assessments, soils are often treated as a single, perfectly mixed homogeneous compartment. In reality, transport processes will alter local exposure levels spatially and temporally in the soil, resulting in a more heterogeneous exposure of different soil organisms in different parts of the soil profile. Most existing studies on agricultural soils focused on quantifying MP emissions from certain agricultural management activities (Huerta Lwanga et al., 2023), and limited themselves to the plough layer as they implicitly assume that MPs are immobile after their entry into the soil (Crossman et al., 2020). As a result, there is little knowledge on the vertical distribution and mobility of MPs in agricultural soils after long-term exposure to field conditions, the involved transport mechanisms and any factors influencing these.

3.4 Particle transport in agricultural soils

The horizontal and vertical movement of particles in soils can occur via anthropogenic and natural transport processes that are closely interlinked in agricultural management systems (Figure 2). Agricultural soils will undergo recurring events of mixing through management activities like ploughing or seedbed preparation (section 3.4.1). Particles can also be transported by water, either horizontally away from their entry site or vertically through the soil pore system (section 3.4.2). Soil biota move particles as they burrow through the soil and create larger pores (section 3.4.3). These natural transport processes are inevitably modified by soil management activities and their respective effects on soil properties. Concerning MNPs, the polymer type, size and shape may affect their respective susceptibility to these transport processes (Dong et al., 2018; Gao et al., 2021; Han et al., 2022; Ranjan et al., 2023; X. Zhang et al., 2022). However, an adequate understanding of the influence of these particle properties on their dispersal in the field in the long-term remains elusive due to a scarcity of field studies examining vertical distribution patterns (Yi et al., 2023).

3.4.1 Particle transport by ploughing

Soil particles can be redistributed in the soil by agricultural management activities. On the one hand, ploughing can lead to the incorporation of surface materials, such as organic crop residues or fertilisers, into the plough layer. On the other hand, ploughing can also lead to the lateral translocation of

particles, or tillage erosion which depends on the relief and tillage direction (Blume et al., 2016). For conventional mouldboard ploughing, the plough layer typically comprises the top 20 to 30 cm of the soil.

3.4.2 Particle transport with water

Fluvial soil erosion, i.e. the horizontal transport of soil particles with surface runoff, is dependent on rainfall and runoff dynamics, which in turn are affected by soil properties, soil management and the macro-relief. Surface runoff occurs when the precipitation exceeds the infiltration capacity of the soil, enabling transport of low-density particles and even mineral soil particles when it reaches sufficient flow energy (Blume et al., 2016). Research on MP transport with surface runoff is only just emerging, but first studies suggest preferential transport of small, low-density MP fragments (Crossman et al., 2020; Han et al., 2022; Schell et al., 2022).

The vertical water-driven transport of particles through the soil pore system is often considered a function of particle size, pore system parameters and hydraulic conditions. A range of recent studies on repacked sand and, more rarely, repacked soil columns has highlighted the strong limiting effect of MP particle size and fibrous particles shapes on their transport potential (Alimi et al., 2018; Dong et al., 2018; Waldschläger and Schüttrumpf, 2020; X. Zhang et al., 2022). Soil pore structures in the field, in contrast, also include macropores that are formed during wetting-drying and freeze-thawing cycles, or by burrowing soil biota. These macropores constitute pathways for preferential water flow, which can lead to the transport of larger particles due to a lack of bottlenecks and potentially high flow velocities (Jarvis et al., 2016; Leuther and Schlüter, 2021). Initial irrigation studies with repacked columns but more complex systems included wetting-drying, freeze-thawing or bioturbation, resulting in accelerated MP transport (Koutnik et al., 2022; O'Connor et al., 2019; Yu et al., 2019).

3.4.3 Particle transport by bioturbation

Bioturbation refers to the re-working of soil by soil biota, resulting in a re-arrangement of soil constituents and soil pore structure. Earthworms are considered especially influential '*ecosystem engineers*' due to their profound impacts on soil nutrient cycling, soil structure and water movement (Taylor et al., 2018). By burrowing earthworms change the composition and properties (e.g. compactness) of the soil through which they burrow. These

changes extend into the soil surrounding the burrow, termed the drilosphere, making it a microhabitat for many other soil organisms (Vidal et al., 2023).

There are three ecological categories into which earthworms are commonly placed: epigeic, endogeic and anecic, which in a simplified manner corresponds to litter dweller, shallow bioturbators and intense tunnelers (Bottinelli et al., 2020; Bouché, 1977; Capowiez et al., 2024). Recently, Capowiez et al. (2024) suggested a more nuanced reclassification based on their bioturbating behaviour into intense tunnelers, burrowers, shallow bioturbators, deep bioturbators, litter dwellers and intermediates. Earthworms from the different ecotypes are associated with different patterns of movement and behaviour, which consequently affects soil pore structures and the transport of particles differently (Capowiez et al., 2024). Some earthworms, such as *Lumbricus terrestris* (anecic or burrower*)*, create semi-permanent burrows that can reach as deep as 2 m (van de Logt et al., 2023). Thus, bioturbation rates to the deeper soil are thought to be strongly affected by the presence of these deep-burrowing earthworms (Torppa and Taylor, 2022). The community composition and activity of earthworms are affected by climate, soil properties and management practices that can place physical constraints or cause disruptions (Capowiez et al., 2009; Ruiz et al., 2021).

Earthworms create their burrows through a combination of soil ingestion and cavity expansion as they penetrate the soil and push particles aside (Arrázola-Vásquez et al., 2022; Larsbo et al., 2024), thereby causing a horizontal and vertical translocation of particles in the soil profile (Jarvis et al., 2010). Particles can also adhere and be released from the body of the earthworm. Moreover, earthworm burrows facilitate water-driven particle transport by creating a connected macropore network that allows even large particles to pass (section 3.4.2). Despite the importance of bioturbation for particle transport, it remains a poorly investigated transport mechanism for most contaminants (Baccaro et al., 2019). Initial studies have confirmed that MNPs are indeed transported by deep-burrowing earthworms (Huerta Lwanga et al., 2017, 2016), some stipulating a size-dependency of transport dynamics (Rillig et al., 2017). However, the mode of transport, i.e. whether MNPs are transported through mechanical mixing, ingestion or adhesion to the bodies of the earthworms remained elusive.

4. Materials and methods

"Well, I must endure the presence of a few caterpillars if I wish to become acquainted with the butterflies."
The Little Prince, Antoine de Saint-Exupéry

4.1 Field study

The distribution of MPs under field conditions was measured in soil samples taken from long-term field trials that have been ongoing since 1996 at the Lanna research station (Skara, Sweden; 58.344°N, 13.104°E; **Paper I**). MP mass and number concentrations were measured in two different fertiliser treatments: soils amended with municipal sewage sludge were compared with soils receiving conventional mineral fertiliser. Particle size, shape and plastic type were characterised to assess the influence of input pathways on these MP properties and their respective impacts on particle mobility in the soil. In addition, the vertical distribution of MPs in soil was compared to that of potentially toxic metals and total organic carbon (TOC) to elucidate if transport depths were MP specific and to identify soil factors that might potentially limit vertical transport.

4.1.1 Soil properties and agricultural management

The soil at the site was classified as a *Eutric Cambisol* (FAO, 2015). The soil texture is silty clay in the plough layer (0-20 cm) and clay in the underlying subsoil. A selection of soil properties is shown in Table 1 and the arrangement of the field plots is displayed in Figure 3. In the sewage sludge treatment, digested sewage sludge was applied bi-annually at a rate of 8 tons ha^{-1} DW, corresponding to a total application of 96 tons ha^{-1}. During the same

time period, nitrogen (N), phosphorus (P) and potassium (K) were applied at rates of 80 kg ha^{-1} y^{-1}, 40 kg ha^{-1} y^{-1} and 30 kg ha^{-1} y^{-1} to the plots receiving mineral fertiliser. The soil was mouldboard-ploughed to 20 cm depth and the dominant crops were spring-sown oats and barley. Each treatment had four replicates, each 112 m² in area, except for one plot in the mineral fertiliser treatment (84 m²). The area of the field trial only showed gentle slopes (0-1.6°) derived from a 2 × 2 m digital elevation model (Lantmäteriet, 2019).

Table 1: Soil properties for plots in the Lanna field trials receiving sewage sludge or mineral fertiliser since 1996. TOC is given as average ± standard deviation.

Treatment	**Bulk density, 0-20 cm** [a]	**Bulk density, 20-40 cm** [b]	**Earthworm density** [c]	**pH** [d]	**TOC**
Sewage sludge	1.30 g cm^{-3}	1.50 g cm^{-3}	2.8 g DW m^{-2}	4.9	2.28±0.07%
Mineral fertiliser	1.36 g cm^{-3}	1.50 g cm^{-3}	2.5 g DW m^{-2}	6.7	1.9±0.1%

General	**Soil Texture, 0-20 cm**			**Soil Texture, 20-40 cm**		
	Clay	Silt	Sand	Clay	Silt	Sand
Lanna	45%	47%	8%	61%	36%	3%

[a](Kätterer et al., 2014), [b]personal communication with field station, [c](Viketoft et al., 2021), [d](Börjesson et al., 2014)

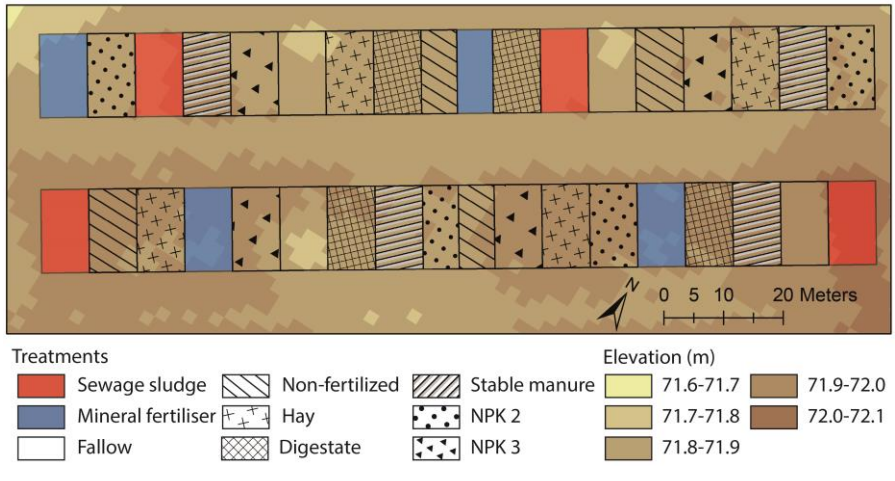

Figure 3: Setup of the long-term field study including all treatments. MP and metal concentrations were measured in each of the four replicate plots from the sewage sludge and mineral fertiliser treatments (coloured). Elevation data was used from Lantmäteriet (2019). NPK refers to different mineral fertiliser regimes with N, P and K.

4.1.2 Sampling scheme and analysis

Separate soil cores were taken down to 90 cm depth for each field plot and divided into depth segments of 10 cm. Samples from the plough layer (0-20 cm depth) were pooled together because repeated ploughing was expected to result in homogenization. The soil was air-dried, crushed, sieved (2 mm) and the fine fraction analysed. MP concentrations were determined in terms of mass and number concentrations with two separate analytical methods. Mass concentrations were measured to a depth of 90 cm for three of the most commonly produced plastic polymer types, i.e. PE, PP and PS (section 4.3.1). A particle-based method was then used to capture number concentrations of a wider range of plastic polymer types, particle sizes and shapes for samples between 0-40 cm depths (section 4.3.2). MP concentrations were not determined in archived sewage sludge samples as they were finely milled and stored in plastic containers, and the applied mineral fertiliser was not archived. TOC, total nitrogen (TN) and a selection of potentially toxic metals that are commonly associated with sewage sludge were measured to 90 cm depth (section 4.4).

4.2 Laboratory-based bioturbation studies

The MNP transport studies in **Paper II** and **III** were performed to improve the mechanistic understanding of the vertical MP and NP transport in soils. The studies consisted of two separate sets of microcosm experiments following the same general setup, but with two different kinds of plastic particles: spherical PS-NPs (**Paper II**) and fibrous PET-MPs (**Paper III**). The MNPs were provided by a collaborator and metal-doped (Mitrano et al., 2019; Schmiedgruber et al., 2019) to enable the detection of NPs (**Paper II**) and accelerate the quantification of MPs in soil samples (**Paper III**). In both studies, the top layer of repacked soil columns was spiked with either NP or MP, then exposed to bioturbation by deep-burrowing earthworms and their average vertical redistribution quantified weekly (**Paper II**) or bi-weekly (**Paper III**). In **Paper II**, the burrow system development was monitored including the potential accumulation of NPs in the drilosphere to shed light on the mode of transport. For the MP fibre study (**Paper III**), the effect of particle size (length) on transport dynamics was determined.

4.2.1 Metal-doped nanoplastics

The NPs were doped with palladium (Pd, 0.24 % m/m) as described by Mitrano et al. (2019). The metal dope was incorporated into a polyacrylonitrile core that was then coated with PS (Figure 4A). The NPs were present in suspension with diameters of 256±4 nm (average±standard deviation) as determined via dynamic light scattering (Z-average hydrodynamic diameter). The stability of the suspension was confirmed across a dilution and time series (**Paper I**: Supplementary Table S1). The detection method of metals is detailed in section 4.3.2.

4.2.2 Metal-doped microplastic fibres

The indium (In, 0.48 % m/m) dope was physically incorporated into the PET-MP fibres, which had previously shown only negligible leaching (Schmiedgruber et al., 2019). The shorter MP fibres were manually produced by cutting wound up PET filaments of 38±10 µm diameter which resulted in an average size (length) of 894±681 µm (n = 31 000, average±standard deviation). This relatively wide size range is more representative of field conditions and allowed determination of the effects of MP fibre length on transport driven by bioturbation (**Paper III**). MP fibre lengths and diameter were determined with an optical microscope as described in section 4.3.4 (see Figure 4B for an example).

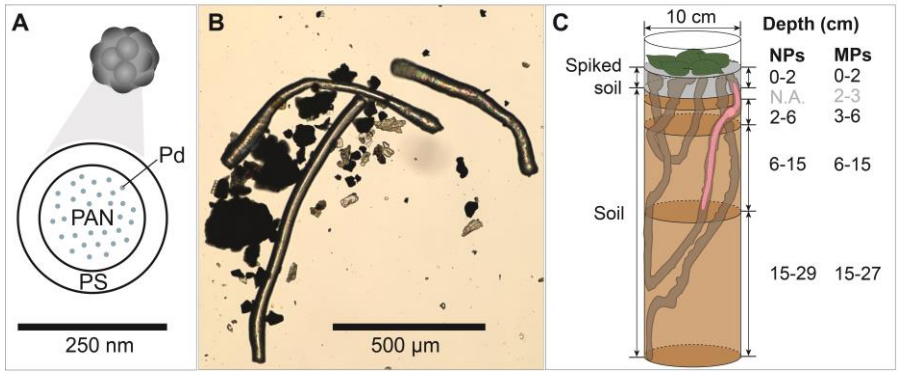

Figure 4: Metal-doped plastics used in the bioturbation transport studies: A) Schematic of metal-doped nanoplastics (NPs) inspired by SEM images by Mitrano et al. (2019), B) microplastic fibres (MPs), C) microcosm setup and sampling scheme for NPs and MP study. The grey labelled depth segment was not measured.

4.2.3 Setup, sampling scheme and analysis

The microcosm setup itself is described in detail in **Paper II** and **Paper III** and illustratively depicted in Figure 4C. The soil columns were initially packed to 30 cm depth using the same topsoil from a former agricultural site. The soil was a sandy loam (60 % sand, 28 % silt, 12 % clay) with a neutral pH around 7.2-7.6 and a relatively high organic matter content (5 m/m %). MNPs were spiked into the uppermost soil layer (0-2 cm) resulting in a concentration of 0.56 g kg^{-1} for the whole column. The anecic earthworm species *L. terrestris* was selected because of its anticipated high potential for deep-reaching vertical transport (section 3.4.3). Light, temperature and relative humidity conditions were kept constant, and soil moisture maintained by spray applications (8±1 mm $week^{-1}$). Macropore flow under these unsaturated conditions and at this low irrigation rate was unlikely.

The vertical redistribution of MNPs was determined at defined depth intervals as depicted in Figure 4C. Three microcosm replicates were destructively sampled at each sampling time point. In **Paper III**, the layer at 2-3 cm depth was added to avoid allocation of MPs to deeper soil due to sampling inaccuracies. Analysis steps and applied analytical methods for both studies are summarized in Figure 5. MNP concentrations (mg kg^{-1}) were determined for dried and homogenised subsamples using the respective

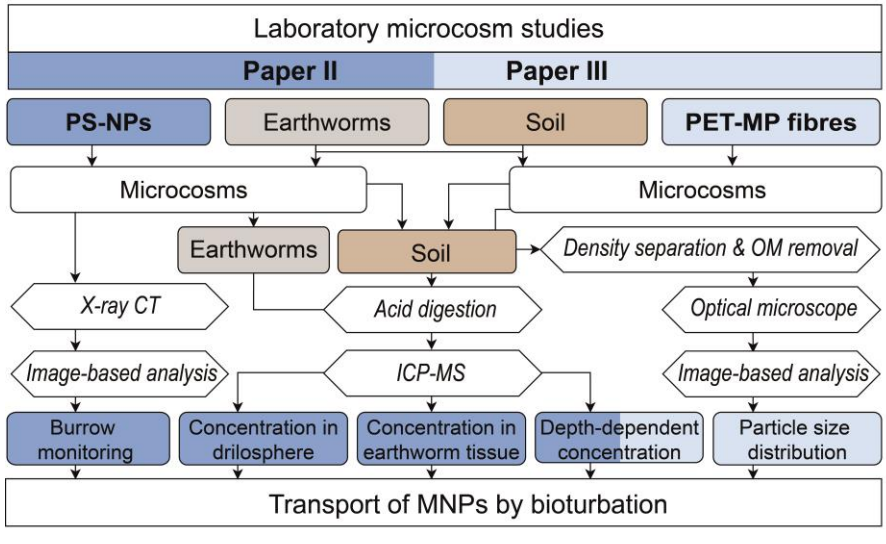

Figure 5: Workflow of microcosm transport studies with polystyrene nanoplastics (PS-NPs, **Paper II**) and polyethylene terephthalate microplastic (PET-MP, **Paper III**) fibres.

metal-dope as a proxy. MP fibres were extracted from the soil for measuring number concentrations and the depth-dependent size distribution (**Paper III**). In **Paper II**, the burrow system was analysed in more detail: the distribution of NPs in the drilosphere was compared to the undisturbed soil matrix for the different depth intervals and X-ray computed tomography (CT) was used to quantify macropores created by earthworms (i.e. bio-porosity ≥3.5 mm diameter) in soil columns with and without NPs, see **Paper II** and its supplemental material for details. Retained NPs were measured in earthworm tissue (**Paper II**).

4.3 Methods for microplastic quantification and characterisation

Different methods were applied for detecting and characterising MNPs in field and laboratory studies. For field samples, environmental plastics were quantified and characterised using Py–GC/MS for mass concentrations and µ–FT-IR imaging for number concentrations and particle morphologies (**Paper I**). The sample preparation and analysis steps differ between these approaches and are thus briefly described below (section 4.3.1 and 4.3.2).

For laboratory-based studies, metal-doped MNPs were intentionally added to the systems (**Paper II**, **III**). Therefore, these plastic particles were well-characterised prior to the experiment and quantified via their metal-dope with more standardised acid digestion methods (section 4.3.3). For the MP fibres, number-based concentrations and particle lengths were determined using an optical microscope (**Paper III**, section 4.3.4).

4.3.1 Mass-based detection of environmental microplastics via pyrolysis-gas chromatography/mass spectrometry

Mass concentrations in the field study were quantified for a selection of plastics, i.e. PE, PP and PS, using Py–GC/MS and with the aid of organic solvents as described by Steinmetz et al. (2021, 2020). Sample preparation steps are illustrated in Figure 6. MPs were pre-concentrated from soil samples (50 g) by density separation with a saturated sodium chloride (NaCl) solution. An organic solvent mixture of 1,2,4-trichlorobenzene and *p*-xylene (1:1 ratio) was then used to extract target plastics under heating. The size thresholds of the method, i.e. 12 µm to 2000 µm, were due to filtration and sieving. The internal standard, deuterated polystyrene (PS-d5), was spiked

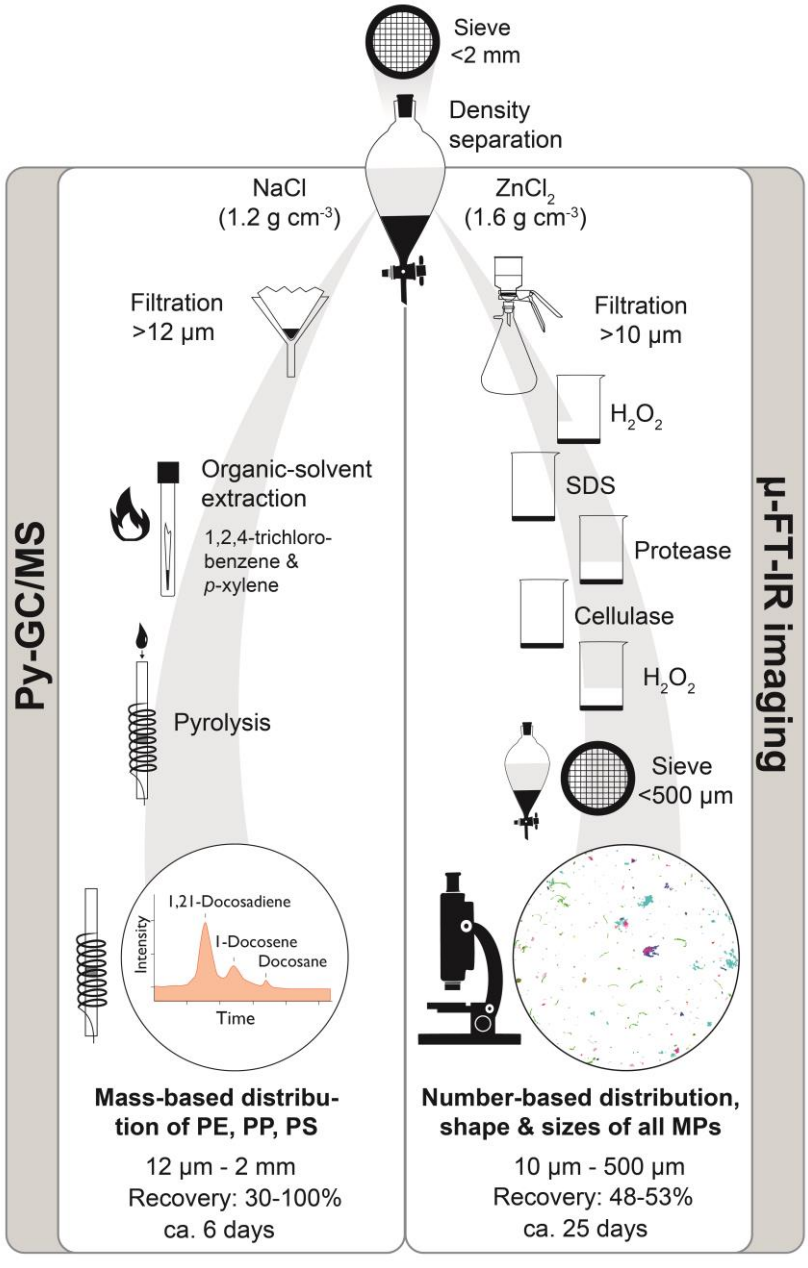

Figure 6: Applied analytical methods and required sample preparation techniques for the analysis of environmental microplastics in soil samples (**Paper I**). The time estimate refers to the completion of one pipeline from density separation to the completion of measurement.

to each sample prior to deposition on the sample carrier. The samples were flash-pyrolyzed at 700 °C, and PE, PP and PS quantified using the peaks of 1,21-docosadiene, 2,4-dimethyl-1-heptene and styrene, respectively. The methodological limits of detection in this study were 0.51 mg kg^{-1} for PE, 0.13 mg kg^{-1} for PP, and 0.02 mg kg^{-1} for PS. Detected concentrations were corrected for negative controls and using bracketing standards. Positive control (recovery) tests were done using known concentrations of the target plastics (Figure 6). For details on the analysis, including contamination control, see **Paper I** and its supplemental material.

4.3.2 Particle-based detection of environmental microplastics by imaging with micro-Fourier transform infrared spectroscopy

With µ–FT-IR imaging it was possible to capture a wider range of different plastic polymer types that were previously omitted by Py–GC/MS types (**Paper I**: Supplementary Table S8), while simultaneously recording particle size parameters and classifying MPs by their size and shape. MPs were extracted from soil samples (100 g) using a higher density solution than before (zinc chloride, $ZnCl_2$, >1.6 g cm^{-3}, three times), followed by a sequence of reagents to degrade organic material present in the soil (Figure 6), and another density separation at the end. Filtering in between the steps as well as a final sieving step determined the size thresholds (Figure 6). The extracted MPs were suspended in ethanol and a subsample analysed with a focal plane array (FPA) µ–FT-IR (pixel resolution 5.5 µm). Negative controls indicated a potential maximum error of 5.2 % for the soil sample with the lowest concentrations. If their aspect ratio was above 3, MPs were classified as fibres, otherwise they were considered a fragment (Cole, 2016; Zhang et al., 2022). For facilitating the comparison between methods, MP particle concentrations were converted to mass concentrations based on particle sizes and types (Simon et al., 2018). For details, see **Paper I** and its supplemental material.

4.3.3 Mass-based detection of metal-doped plastics in laboratory studies via inductively coupled plasma-mass spectrometry

The metal-dope was used as a proxy to track the transport of MP fibres and NPs in the soil. Subsamples of MP/NP-containing soil (0.5 g) were directly digested using microwave-assisted digestion methods with strong acids. Acid digestion protocols were optimised for each plastic type: Pd was

extracted from PS-NPs using *aqua regia* (**Paper II**) and In from PET-MPs was extracted using a mixture of H_2O_2 and concentrated nitric acid (**Paper III**). The digests were filtered and diluted prior to their analysis via inductively coupled plasma – mass spectrometry (ICP–MS). Blanks and calibration curves were matrix-matched and internal standards (i.e. In in **Paper II** and rhodium (Rh) in **Paper III**) were used for correction of detected intensities. Concentrations were then corrected for the soil background concentration of Pd (32±4 µg kg^{-1}) and In (12.1±0.3 µg kg^{-1}). For details on recovery and method optimisation see **Paper II** and **III**. For facilitating the comparison across studies, mass concentrations (mg kg^{-1}) were converted to particle masses per soil volume (mg cm^{-3}) in this thesis to account for different soil bulk densities between the microcosms due to settling of the soil.

4.3.4 Particle-based detection of metal-doped plastics in laboratory studies using the optical microscope

Particle numbers as well as size ranges of added and transported MP fibres in **Paper III** were recorded for one microcosm replicate at the end of the bioturbation experiment. MP fibres were separated from the soil matrix (50-90 g) in a similar way to the extraction procedures for the spectroscopic analysis of soil samples in section 4.3.2 (**Paper III**). Fibre length and diameter were then determined on images captured with an optical microscope and analysed using the ImageJ/FIJI software (Schindelin et al., 2012; Schneider et al., 2012). Identification of the MP fibres was possible as they were intentionally added, well-characterized and easily distinguishable from other fibrous particles owing to their distinctive surface and diameter, (Figure 4B). In the context of this thesis, mass concentrations were measured using the metal as a proxy, but also estimated from particle properties. For this purpose, a particle-to-mass conversion was implemented using polymer density (1.38 g cm^{-3}), measured individual fibre length and the average diameter, assuming a cylindrical shape (**Paper III**).

4.4 Metal, organic carbon and total nitrogen analysis

Total organic carbon (TOC), total nitrogen (TN) as well as a range of potentially toxic metals were measured in soil profiles due to their potential enrichment in sewage sludges (**Paper I**). TOC and TN were determined with

an elemental analyser. The metals included in the analysis were cadmium (Cd), chromium (Cr), copper (Cu), nickel (Ni), lead (Pb) and zinc (Zn). Soils were digested with *aqua regia* in a closed-vessel microwave system and the digest analysed on ICP sector field mass spectrometer in a similar fashion and with similar quality control measures as for ICP–MS measurements described in section 4.3.3. For further details, see Supplementary Material S2 in **Paper I**.

4.5 Data analysis

Statistical significance was tested using two-tailed t-tests (α = 0.05). Following recommendations by Wasserstein (2019), I decided to report each *p*-value above 0.001 explicitly in the two more recently published studies (**Paper I**, **Paper III**) rather than classifying *p*-values as $p>0.05$ or $p\leq0.05$ as was done in **Paper II**. Additional data analysis incorporated in this thesis was done for the contextualization of **Paper I**, including an estimation of mass concentrations for all plastics found in the plough layer of sewage sludge-amended soils (Appendix: Table S2).

5. Results and Discussion

"Everyone trusts an observation, except the [one] who made it."
Harlow Shapley

The distribution of MP refers to their spatial location in the soil in both horizontal and vertical dimensions and from the field to the smaller spatial scale. The underlying assumption in all spatial analyses is that the observed spatial patterns enable us to draw important conclusions about the underlying processes. In the context of this work, such conclusions were drawn about the potential input sources of MPs (**Paper I**), but also their behaviour after entry into the soil (**Paper I-III**). The first part of this chapter is focused on the description and interpretation of the horizontal distribution of MPs reflecting potential input sources but also transport on a field scale (**Paper I**, section 5.1), whereas the vertical distribution and underlying transport mechanisms of MNPs will be discussed in more detail in the subsequent section 5.2 (**Paper I-III**). Finally, the range of analytical methods used to characterize and quantify MNPs will be compared in order to outline future research needs for the reliable characterisation of soil exposure (**Paper I-III**, section 5.3).

5.1 Horizontal distribution of microplastics in soil in response to different fertiliser types

The horizontal distribution of MPs in the field study reflected different input sources of MPs to soils, reaffirming that sewage sludge-amended soils are more exposed to MPs than soils with conventional mineral fertilisation (**Paper I**, Figure 7). Organic residues, such as municipal sewage sludge, are

widely applied to soils with the aim to re-use and recycle nutrients, whilst simultaneously increasing organic carbon in soils. This intended increase of TN and TOC was achieved in field soils where sewage sludge was applied, but it was also accompanied by an unintentional release of potentially toxic metals and MPs (**Paper I**).

As much as half of the detected MPs were detected below the plough layer in the sewage sludge-amended soils (Figure 7, section 5.2). Vertically transported fractions are thus relevant for field and larger scale mass balances that assess the input pathways to and distribution of MPs in soils. Sampling schemes in agricultural soils are often limited to the plough layer, which comes at the cost of incomplete recoveries of the total MP load that was initially added with sewage sludge as illustrated in Figure 7 and observed elsewhere (Crossman et al., 2020; Klemmensen et al., 2024). Accordingly, when comparing detected concentrations in this work with other studies, concentrations found in the plough layer are used as reference. For general trends about MP type, size and shape in response to different input sources, all detected MPs across all measured depths are considered (Figure 8).

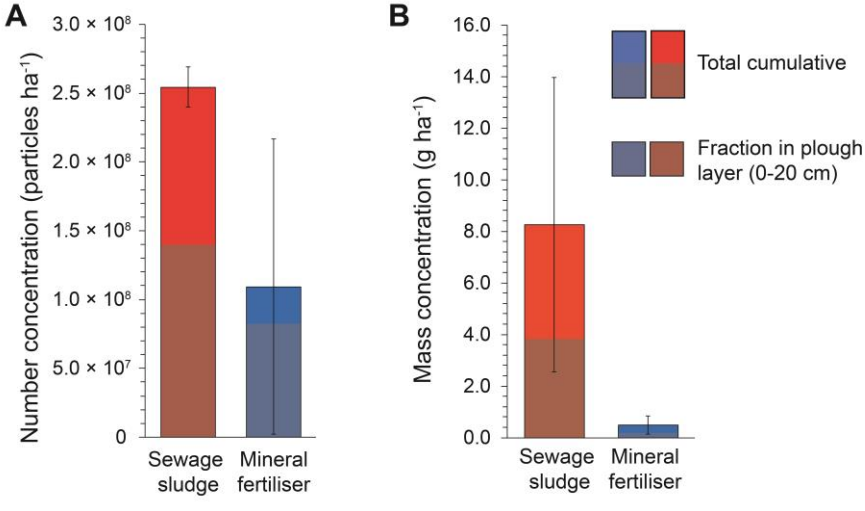

Figure 7: MP number (A) and mass concentrations (B) cumulative for all measured depths (0-40 cm for number and 0-90 cm for mass concentration). Shaded areas indicate MPs present in 0-20 cm depth. Concentrations are given as averages including standard deviations as error bars.

MP concentrations and characteristics in sewage sludge-amended soils

The detected mass and number concentrations in **Paper I** were substantially higher than in other studies on sewage sludge-amended soils, even when considering differences in application rates (Appendix: Table S1). Average MP concentrations in the plough layer of sewage sludge-amended soils were 53 700±5 900 particles kg^{-1} and 1.47±0.66 mg kg^{-1}. Notably, the measured metal concentrations remained below Swedish national thresholds (Naturvårdsverket, 2009), whereas MP concentrations in the plough layer reached currently observed effect concentrations for some soil properties and soil biota (section 3.3). The highest potential exposure level combining all detected MPs was estimated at 0.07±0.01 % (m/m) based on a conversion of particle numbers to mass (Appendix: Table S2). However, mass estimates based on conversion methods are uncertain (section 5.3) and directly measured mass concentrations for single plastic polymers, i.e. PE, PP and PS, were orders of magnitude lower (**Paper I**). Effects can vary between MP polymer types and shapes, so that a final assessment of the current risk remains challenging. Monitoring of MP concentrations in soils thus remains crucial to assess whether potential adverse effects of MP pollution outweigh the benefits of sewage sludge reuse on the long-term, given the anticipated continuation of emissions, the increasing re-use of sewage sludge in Sweden and the increasing use of plastics in general (Geyer et al., 2017; Appendix: Figure S1).

The fact that detected MP concentrations in sewage sludge-amended soils span across a wide range between different studies is not surprising *per se*. Different analytical methodologies inevitably capture different plastic polymer types and size ranges, and thus recover different fractions of the total MP load. For sewage sludge-amended soils in **Paper I** as much as 42 % of MPs were below 50 µm in size (Figure 8A). Previous studies often had a larger size cut-off in their analysis omitting MPs below 50 µm (van den Berg et al., 2020; Zhang et al., 2020), suggesting that a substantial fraction of the MPs quite literally slipped through their net. Besides methodological reasons, MP loads in sewage sludge also vary widely depending on the specific treatment steps at the wastewater treatment plant where the sludge originated and the original input to the wastewater stream (Harley-Nyang et al., 2023). As a result, MPs found in soils are intrinsically dependent on the MP composition in the original sewage sludge. Thus, it is not surprising that textile-related plastic types constituted the largest fraction in sewage sludge-

amended soils, i.e. polyester, followed by acrylic and polyamides (**Paper I**, Figure 8B). MPs are released from textiles during the washing process, often resulting in their enrichment in sewage sludge-amended soils (Klemmensen et al., 2024; Schell et al., 2022) in the shape of fibres (Corradini et al., 2019). Of the polyester MPs, 43 % were indeed classified as fibres, even if fragmental shapes dominated in general (Figure 8C). Acrylic MPs, in contrast, were mostly fragmental (93 %) which might hint at other sources than textiles, such as paints (Fang et al., 2024). PE, PP and PS are three of the most widely used plastic polymers and, thus, also present in sewage sludge-amended soils (Figure 8B). However, tracking potential sources for these plastic polymers is more challenging due to their ubiquitous use in a range of products.

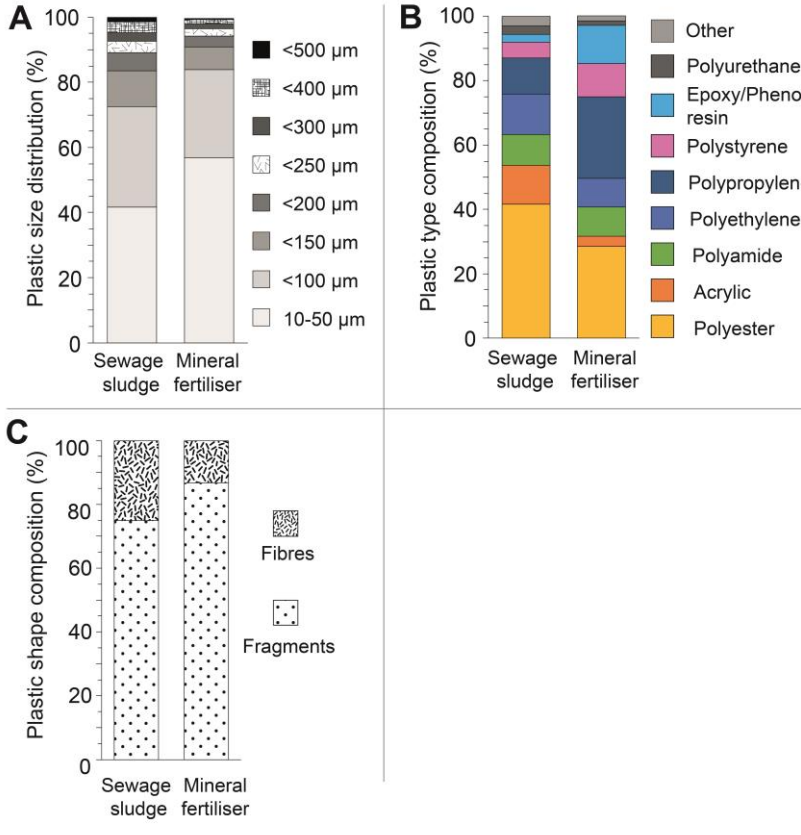

Figure 8: Microplastic (MP) sizes (A), polymer types (B) and shapes (C) in soils after long-term treatment with sewage sludge in comparison to soils receiving mineral fertiliser for 0-40 cm depth.

MP input to fields receiving mineral fertiliser

The input pathway of MPs in sewage sludge-amended soils seems straightforward, but was less clear for soils treated with conventional mineral fertiliser which contained unexpectedly high amounts of MPs (Figure 7, **Paper I**). Especially PP, PS and epoxy/phenoxy resins were relatively more abundant (Figure 8B). These MPs may, in part, originate from storage bags for fertiliser that are commonly made of PP. Another possibility is that MPs were moved horizontally from field plots with high MP inputs, such as sewage sludge-amended soils, through a combination of surface runoff or wind action and tillage. Low-density plastic types were more predominant than in sewage sludge-amended soils, in conjunction with overall smaller MP sizes (Figure 8A) and a higher share of fragments (Figure 8C) that are considered more prone to transport via runoff and wind (Han et al., 2022; Rezaei et al., 2019; Schell et al., 2022). MP transport with runoff is more pronounced on surfaces of finer-textured soils (Laermanns et al., 2021). Soils with high clay contents, such as at this field site, may thus experience MP transport with runoff at periods of low soil cover and low infiltration, e.g. in late winter during snowmelt or rainfall when the underlying soil is frozen (Larsbo et al., 2016).

Transfers from sewage sludge-amended soils would also explain the presence of textile-related plastics that are otherwise not expected in conventionally-managed soils (Figure 8B). Some of these are relatively high density plastics, such as polyester (1.37-1.46 g cm^{-3}), making transport with tillage more likely than with wind or water (Figure 2). Recently, Weber et al. (2022) observed the spread of MPs from sewage sludge-amended soils over distances of up to 40 m, with ploughing identified as the major dispersal mechanism. Distances to plots investigated in **Paper I** that received sewage sludge and also other treatments with potentially larger MP concentrations were reasonably short, making tillage a likely horizontal transport pathway. Other fertiliser practices in the field trial, such as the amendment of soils with compost and digestates of organic waste, might have represented additional sources of MPs (Weithmann et al., 2018). Even though there are indications that horizontal transfers occurred in this and other field studies, more systematic analyses are necessary to provide direct evidence for horizontal MP dispersal in the field.

5.2 Vertical distribution and transport of microplastics and nanoplastics in soil

Determining the spread of MPs in the environment is an essential step towards source apportionment and an assessment of potential risks. The field study provided evidence of MP dispersal after long-term field exposure (**Paper I**), while the microcosm studies confirmed that bioturbation can indeed lead to a substantial vertical transport of MNPs in the soil (**Paper II, III**). Both the field and microcosm studies provided insights into the factors that potentially control the rate of these transport processes.

Distribution and transport of MPs in the field

After 24 years of continuous sewage sludge applications under field conditions, MPs were evidently dispersed into the deeper soil profile (**Paper I**). MP mass and number concentrations generally decreased with increasing depth in the soil profile (Figure 9A). The largest fraction of MPs was retained in the upper part of the soil profile, but a substantial fraction of MPs was found below the plough layer (52 % by mass, 42 % by numbers), reaching maximum depths of 60-70 cm. Smaller and fragmental MPs were more susceptible to transport out of the plough layer, whereas plastic polymer type did not appear to affect MP mobility (**Paper I**: Figure 2). The

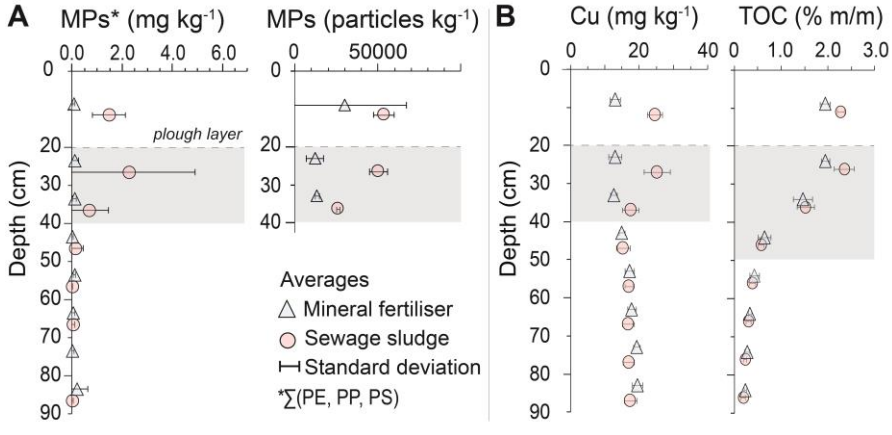

Figure 9: Depth-dependent distribution of MPs (A) and copper and TOC (B) in field soils. Mass concentrations for MPs only comprise PE, PP and PS. Particle concentrations refer to all detected plastic types. The strongest decline in detected concentrations in the soil profile is shaded in grey. Modified from Figure 1, Figure 2 and Figure 5 in **Paper I**.

transport of MPs from the plough layer will likely continue, given their longevity. However, there were also indications that the maximum transport depth was limited because MPs were not detected below 70 cm depth. The strong decrease of MPs, TOC and metals between 20-40 cm depth indicates that soil properties might affect transport rates and limit maximum transport distances at the site (Figure 9B).

The observed depth distribution of MPs in the field is a combined result of anthropogenic and natural transport processes, which in turn are moderated by the prevailing soil properties. The accumulation of MPs in the top 30 cm has been similarly observed in other soils. After sludge is added to the top of the soil, ploughing likely distributes MPs and other sludge constituents over a relatively homogeneous plough layer (Tagg et al., 2022; Weber et al., 2021). Ploughing depths in conventional agriculture are typically between 20-30 cm depending on equipment and management practices, with local variations of up to a few centimetres. MPs, metals and TOC found at 20-30 cm depth are therefore at least in part attributable to ploughing (**Paper I**). However, MPs detected deeper in the soil, as found here (Figure 9) and elsewhere (Tagg et al., 2022; Weber et al., 2021), suggest that MPs are also subjected to natural transport processes. Bioturbation is likely a contributing mechanism for the observed MP dispersal because deep reaching biopores (1 m) (Jarvis et al., 1991) and high earthworm densities of 150 individuals m^{-2} were previously reported for the soils investigated in **Paper I** (Viketoft et al., 2021). The predominant earthworm ecotypes likely determine the depth to which bioturbation occurs. Thus, MPs of larger sizes found in the subsoil (Figure 10) either hint at the presence of anecic

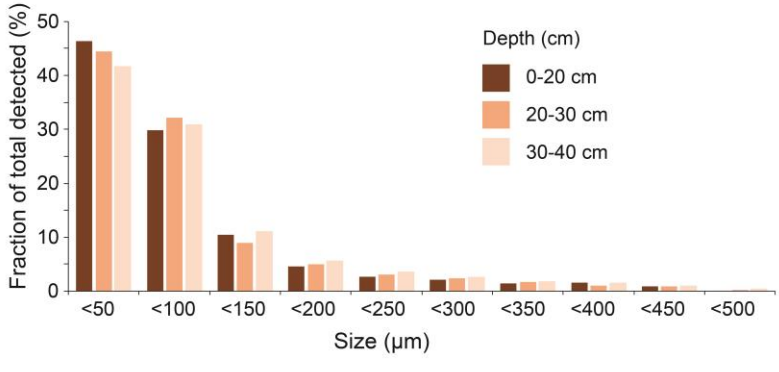

Figure 10: Depth-dependent size distribution of MPs in sewage sludge-amended field soil from 10-500 µm. Note that the bin size increases after 200 µm

earthworms or that large macropores present in this structured soil have facilitated water-driven transport, or both.

Effect of MP shape and size on transport dynamics

Results from both field and laboratory measurements suggested that MP size affects transport dynamics (**Paper I-III**). Field evidence indicated that smaller MPs are more susceptible to transport (**Paper I**). A similar effect of size was confirmed for bioturbation-driven transport in the laboratory studies: NPs were transported faster than MP fibres (Figure 12A below), and smaller MP fibres were preferentially transported in comparison to larger MP fibres (**Paper III**). A previous study observed a similar trend for spherical MPs (Rillig et al., 2017). Taken together, these studies suggest that size-dependency occurs within the different MP shape categories. It is quite intuitive that smaller sized particles are more easily ingested together with other soil constituents as earthworms burrow through the soil. However, the overall transport potential of MPs by bioturbation may not be a simple function of the major diameter of the particle, but rather a combination of aspect ratio and volume. The largest MP fibres transported by earthworms were up to several millimetres long (**Paper III**), which emphasizes that larger sized MPs are not excluded from this transport process. Seed burial studies have found that seed length but also diameter played a decisive role for their ingestion by earthworms (McTavish and Murphy, 2021). Most of the larger transported MPs in the field were classified as fibres (Figure 11 and Appendix: Table S3). Thus, fibres might be more susceptible

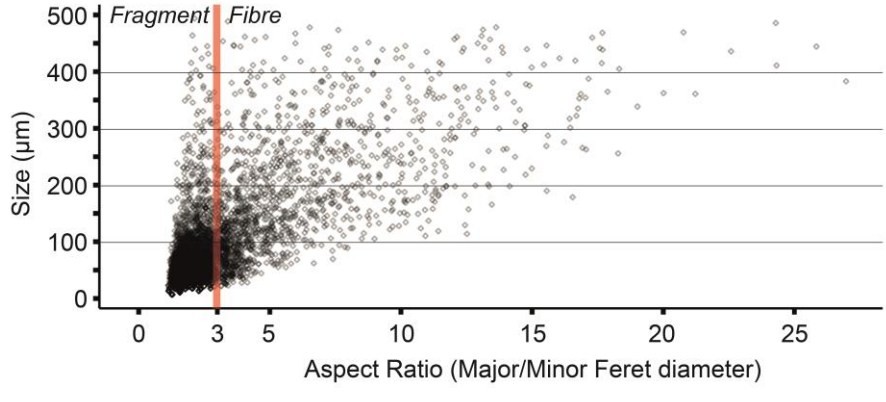

Figure 11: Size versus aspect ratio (major divided by the minor Feret diameter) of MPs transported to 20-40 cm depth in sewage sludge-amended soils from **Paper I**.

to transport by bioturbation than their spherical or fragmental counterparts with the same major diameter. It is important to highlight that even relatively large MPs were transported in the studies (**Paper I** and **Paper III**) in contrast to what many laboratory studies report. These studies repeatedly emphasized the constraining effect of particle size on MP transport in soils, postulating a low mobility of large and fibrous MPs (Keller et al., 2020; Waldschläger and Schüttrumpf, 2020). However, most of these studies did not account for transport of MPs by bioturbation or in macropores which appears to be size-dependent, but not size-exclusive.

Transport of MP fibres and NP by bioturbation

Disentangling the contribution of bioturbation and water-driven transport to the recorded MP distribution in the field is challenging, as they generally occur simultaneously. The laboratory-scale microcosm studies provided complementary evidence that deep-burrowing earthworms can cause substantial vertical translocation of MP fibres and NPs (**Paper II**, **III**; Figure 12A). *L. terrestris* characteristically creates semi-permanent burrows, as confirmed by X-ray CT (**Paper II**), so that mechanical mixing of the soil was limited after establishment of the burrow system. NP concentrations were distinctively enriched in the drilosphere (Figure 12B) and even detected in earthworm tissue after gut clearance (**Paper II**), suggesting that ingestion and subsurface egestion plays a prominent role for NP transport. Near-surface ingestion also seems the likely cause for the observed translocation of the wide size range of MP fibres (0.06-4.8 mm, **Paper III**), as previous studies have observed the ingestion of seeds of similar lengths (5 mm) (McTavish and Murphy, 2021).

As MNPs are increasingly incorporated into the drilosphere, they may become highly spatially concentrated around and in macropores, even if average concentrations in the soil are comparatively small (Figure 12B, 3-28 cm). Earthworm activity seemed unaffected by the presence of NPs, despite their enrichment in the drilosphere. The bioporosity, indicative of the burrow volume created by the earthworm, was similar in the presence of NPs as under control conditions (**Paper II**). Over the relatively short exposure time of the microcosm experiments, earthworms showed no avoidance behaviour or weight change (**Paper II, III**). However, the drilosphere as a potential small scale hotspot can have implications for the chronic exposure of earthworms and burrow-inhabiting soil organisms, the effects of which

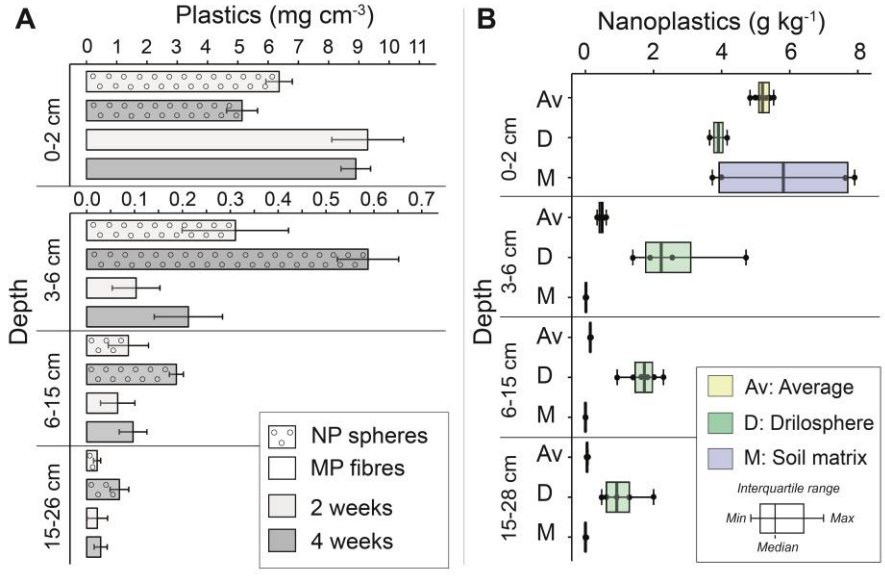

Figure 12: Micro- (MP) and nanoplastic (NP) transport by *L. terrestris*. (A) Depth-distribution of NP spheres and MP fibres after 4 weeks, bars represent averages and error bars standard deviation. Note differences in scales and that plastics in 0-2 cm is the initially spiked soil with residual plastics. (B) Depth-dependent distribution of NPs on average, in the drilosphere and in the un-borrowed soil matrix in g kg^{-1}.

are to date little explored. The accumulation of MNPs in the drilosphere can also affect their subsequent mobilization by fast flowing water in macropores during high-intensity rainfall events. Yu et al. (2019), for instance, observed accelerated MP transport with rainfall after earthworm burrowing led to the establishment of biopores. Under heavy rainfall conditions, MNPs present in the drilosphere might therefore be mobilized and transported by on average longer distances with preferential flow compared to particles that were not first transported by bioturbation.

Transferability of microcosm studies to the field

The microcosm studies served as proof-of-principle, but it is challenging to infer realistic bioturbation transport rates and depths for field conditions from these experiments. In the context of bioturbation, the distinction between transport depth and transport rates is of importance because these are dependent on the earthworm ecotypes present in the soils.

Overall transport rates in **Paper II** and **III** are undoubtedly higher than would be expected in the field due to the very high densities of deep-burrowing earthworms and the spatial constraints of the experimental setup. In the microcosm, earthworm densities were more than twice as high as those reported from the field (382 *versus* 150 individuals m^{-2}). In addition, microcosms were kept at constant favourable conditions for earthworms, whereas earthworm activity in the field will undergo temporal variations, e.g. with seasons. In the microcosms, 9 % of the MP fibres (**Paper III**) and 22% of the NPs (**Paper II**: Supplementary Table S6) were transported away from the initially spiked soil layer within just 4 weeks. In contrast, 51% of the MP mass and 41% of the particle numbers were moved out of the plough layer after 24 years of exposure in the field (**Paper I**), suggesting slower transport rates. At the same time, possible maximum transport depths were constrained to 30 cm by the experimental setup in the microcosms (**Paper II**, **III**). Anecic earthworms, such as *L. terrestris*, are generally associated with relatively longer bioturbation depths. Deeper burrowing of such earthworms under field conditions can therefore result in the longer transport distances observed in the field soil profiles in **Paper I**. Ultimately, the interactions between multiple abiotic and biotic drivers will affect MNP transport in the field, including but not limited to climate, the dominating earthworm ecotypes, soil chemistry and texture.

Transport inhibiting factors related to soil properties and management

Even though MPs were transported below the plough layer, there were indications that the maximum MP transport depth was limited at the field site (**Paper I**). Firstly, MP concentrations declined strongly at 20-40 cm depth which concurrently coincided with the decrease of TOC and metal concentrations (Figure 9). TOC and metals, in particular Cu, were closely-linked to sewage sludge applications, but both can be present in dissolved and particulate or particle-adsorbed form. Their limited depth penetration thus reinforces the impression of limited possible transport depths at the prevalent field conditions. Secondly, MPs were detected only to a depth of 60-70 cm (**Paper I**), even though some of the earthworm species found at the field site (Viketoft et al., 2021), in theory, burrow to much greater depths (van de Logt et al., 2023). Lastly, MPs have been found at greater depth, i.e. down to 2 m in studies on grassland soils (Weber et al., 2021; Weber and Opp, 2020). It thus appears that MPs are transported deeper under extensive

agricultural use (Weber et al., 2021; Weber and Opp, 2020) than under intensively used agricultural soils (**Paper I**, Tagg et al., 2022).

Differences in MP transport depths can be related to the local earthworm community composition, which is intrinsically dependent on soil management practices. Anecic earthworms are important for particle transport to the deeper soil in semi-permanent burrow systems. In contrast, endogeic (or shallow bioturbators) tend to cause faster soil turnover as they continuously create new burrows within a preferred depth of the soil (Capowiez et al., 2011). Such burrowing behaviour would lead to more intense mixing within a limited depth as particles are continuously ingested and moved by cavity expansion (Capowiez et al., 2011). The accumulation of MPs within the upper 40 cm of the soil might thus be related to the presence of endogeic earthworms. A more detailed species identification would be necessary to assess bioturbation rates and depths of MPs.

Bioturbation and water-driven transport alike are affected by agricultural management practices that can cause mechanical disruptions and increase subsoil bulk density. Annual tillage, for instance, reduces the continuity and connectivity of deep-reaching biopores whilst also potentially increasing subsoil compaction (Mossadeghi-Björklund et al., 2016). This would result in decreasing hydraulic conductivities at the lower boundary of the plough layer as was observed for soils at 0.15-0.30 m depth near the site of **Paper I** by Jarvis et al. (1991). Tillage and soil compaction also affect earthworm community composition, activity and their spatial distribution (Arrázola-Vásquez et al., 2022; Chan and Barchia, 2007; Jégou et al., 2002). Anecic earthworm species, including *L. terrestris*, are particularly susceptible to tillage-induced disruption (Torppa and Taylor, 2022). A low density and activity of deep-burrowing earthworms would affect the amount of MPs directly transported to the deeper soil by ingestion and excretion, but it would also affect the abundance of deep-reaching biopores that can serve as conduits for accelerated MP transport with macropore flow. I therefore propose that soil properties, including the interactions between predominant earthworm ecotypes and agricultural soil management practices may explain the observed depth distribution and maximum transport depth.

5.3 A comparison of detection techniques of microplastics and conversion methods

A range of different analytical techniques were used in this study to identify and quantify environmental (**Paper I**) and metal-doped MPs (**Paper II**, **III**). Hence, it was possible to more systematically compare the different methods, determine their advantages and potential limitations and discern any remaining challenges in their application.

The relative importance of specific plastic polymer types was dependent on the reported metric, since large particle numbers do not necessarily translate into large masses (**Paper I**). The conversion of particle to mass concentrations can facilitate comparisons between mass- and number-based detection methods, but it led to a considerable overestimation of the total MP mass present in the soil as demonstrated in **Paper I** (Figure 13A). Other studies have observed similar discrepancies (Primpke et al., 2020; Viitala et al., 2022), which highlights weaknesses of commonly applied conversion methods. To begin with, conversion methods are intrinsically dependent on

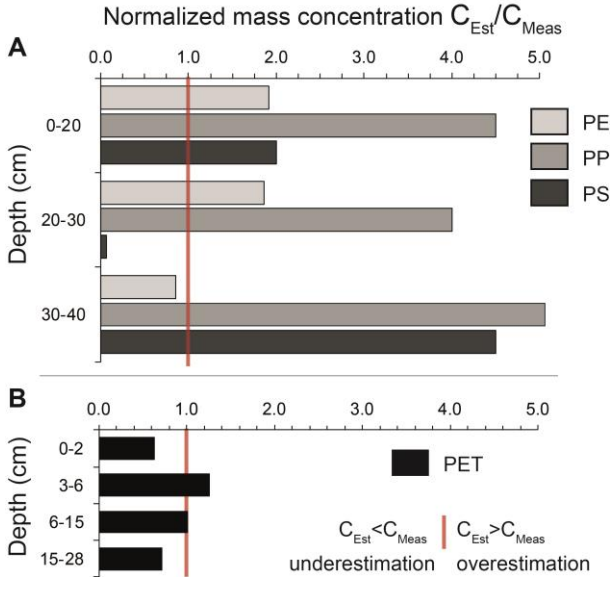

Figure 13: Comparison of estimated to measured mass concentrations for (A) MPs in sewage sludge-amended soils in the field study (**Paper I**) and (B) PET-MP fibres in the bioturbation study (**Paper III**). Measured MP mass (C_{Meas}) are directly measured masses. Estimated MP masses (C_{Est}) are based on detected MP particles, their sizes and polymer densities according to Simon et al. (2018).

the detection accuracy of MPs, or recovery. For both detection methods in **Paper I**, recoveries were incomplete thereby increasing the uncertainty of measured and subsequently converted values.

Besides these recovery challenges, assumptions underlying the conversion approach likely contributed to the observed discrepancies. Particle-based methods tend to provide a two-dimensional image of a three-dimensional object, meaning that the third dimension needs to be deduced from the available information. This unavoidably leads to simplifications of shapes and approximations of particle thickness that substantially affect the estimated weight of a particle, especially in cases of very thin, irregular or weathered particles. In the field study (**Paper I**), particle-to-mass conversions of the (on average) larger PE particles gave a better estimate of measured mass concentrations than for the smaller-sized PS and PP particles (Figure 13A). This may indicate that the smaller the particle, the more sensitive the mass estimate becomes to approximations concerning the particle thickness. To illustrate the role of particle characterisation for mass estimation, a particle-to-mass conversion was done for the metal-doped MP fibres in **Paper III**, for which number and mass concentrations were directly measured. There was a relatively good agreement with directly measured mass concentrations when masses were estimated based on the measured particle parameters (Figure 13B). In contrast to field MPs (Figure 13A), the MP fibres were well-characterised with relatively homogeneous diameters, smooth surfaces and distinct cylindrical shapes. Thus, reliable conversion from number to mass concentrations is, in principle, possible as long as the particle properties, i.e. MP shape and size in all three dimensions, are reasonably well known. However, the agreement between measured and estimated mass for MP fibres was strongly dependent on the assumed particle diameter even for the fibres, highlighting the importance of accurate size characterization (Appendix: Table S4).

Moreover, some method-specific challenges in the correct identification and quantification of specific plastic polymers arose. While PP remained below the detection limit in most cases for Py–GC/MS, μ–FT-IR imaging suggested a prominent role of this plastic polymer (**Paper I**). At this point, it remains unresolved whether low sensitivity or incomplete extraction in the case of the thermo-analytical approach led to an underestimation, or whether interferences and misclassification with the spectroscopic method caused an overestimation of PP (**Paper I**: Supplementary Figure S3).

These remaining challenges highlight the need for further development of sample treatments to increase recovery, reduce artefacts, but also for comparative analyses of particle-based and mass-based MP detection methods. The selection of a specific analytical method for MP detection is often based on multiple factors, including measurement quality but also applicability and feasibility. The MP detection via Py–GC/MS outcompeted µ–FT-IR imaging in terms of sample preparation and measurement time (Figure 6). However, the current approach supported by organic solvents has only been developed for a limited set of plastics (Steinmetz et al., 2020). Depending on prevalent input sources, such as sewage sludge, polyester and other plastic types might be more relevant (section 5.1). Current detection limits for polyester are high for established methods (0.07-1.72 m/m %) (David et al., 2018), and method validation for sewage sludge-amended soils is still ongoing (Dümichen et al., 2017). In contrast, µ–FT-IR imaging allowed a wider range of plastic types to be captured, which may help in identifying potential input sources as well as particle sizes and shapes. Using Py–GC/MS for an initial screening allowed the selection of a smaller number of samples for in-depth investigation by the more time-consuming µ–FT-IR method. Thus, although most studies exclusively apply only one analytical approach, this thesis demonstrated the advantages resulting from the complementary use of thermo-analytical and spectroscopic methods (**Paper I**).

6. Conclusions and Future Perspectives

"Don't adventures ever have an end?
I suppose not, someone else always has to carry on the story."
Bilbo in Lord of the Rings, J.R.R. Tolkien

The distribution of MNPs in the soil ecosystem is poorly understood due to persisting uncertainties about input sources on the one hand and their potential redistribution through transport processes after their entry into soils on the other hand. This thesis addressed this knowledge gap by investigating the dispersal of MPs in field soils after long-term inputs with sewage sludge and exposure to field conditions (**Paper I**). Additional laboratory-based microcosm studies contributed to a mechanistic understanding of MNP transport, illustrating the potential of bioturbation for incorporating MNPs deeper into the soil profile (**Paper II**, **III**). The combination of field and laboratory studies further highlighted potential transport limiting factors related to soil and MP properties.

6.1 Microplastic analysis in environmental samples

In **Paper I**, two analytical methods providing different metrics were applied to investigate the spread of MPs in field soils. The relative importance of plastic polymer types found in agricultural soil was strongly dependent on the reported metric, in other words whether their particle or mass concentration was considered. A conversion of particle concentrations to mass concentrations facilitated the comparison of the different metrics, but concurrently illustrated the tendency of particle-to-mass conversions to overestimate MP mass in soils.

The correct identification of plastic polymer types, persisting detection limits in terms of particle sizes and mass as well as incomplete recoveries are some of the remaining but pivotal analytical challenges that need to be solved for reliably assessing the scope of plastic pollution in soils. Systematic comparisons of spectroscopic and thermo-analytical methods are needed, not only to determine their applicability to certain research and monitoring questions, but also to support the development of appropriate conversion factors. In this context, I suggest that close attention should be paid to the approximation of the third particle dimension (thickness) as mass estimations react particularly sensitively to this parameter. Both analytical techniques encountered challenges in either the quantification or correct identification of MPs in soils, highlighting the need to systematically investigate potential background contaminations or interferences from organic matter.

The increasing awareness about MP pollution of the environment has recently cumulated in new regulations on products and efforts to include MPs into assessments of soil pollution. Detection methods for MPs in soil samples are continuously developing and still require improvements. Available techniques can, nevertheless, already provide first insights into the current state of plastic pollution, if applied methods and limitations are sufficiently documented. For larger scale applicability and monitoring purposes, it is a reasonable option to start with the major plastic polymers as indicators of plastic pollution. Owing to its relatively fast nature, I propose Py–GC/MS as a suitable method for an initial screening to identify samples for more in-depth investigations by more time-consuming spectroscopic methods, although the specific applicability depends on analytical setup and expected plastic types.

6.2 Microplastic abundance in the soil

The horizontal distribution of MPs as determined in **Paper I** reflected local input sources, but also horizontal transport dynamics of MPs at the field scale. Sewage sludge application led to larger MP mass and number concentrations in soils than when mineral fertiliser was applied, with a greater abundance of larger and textile-related plastics. MP concentrations detected in **Paper I** for single plastic polymer types were smaller than currently reported effect concentrations for soil properties and soil biota. However, knowledge gaps on potential chronic or mixture effects of MPs on

soil biota and soil properties still persist, making future monitoring of MP concentrations necessary. MNPs can be highly spatially concentrated at small scales (**Paper II**, **III**), so that exposure for some organisms may be greater than would be expected based on average concentrations in the bulk soil. Moreover, measured field concentrations were likely an underestimation of actual MP concentrations as analytical recoveries were incomplete, and size fractions below 10 µm were not captured due to filtration. Particle abundance was inversely proportional to particle size in **Paper I**. Consequently, the lower size cut-off at 10 µm makes it likely that a substantial fraction of the total number of particles was not captured in this study. Developing sample preparation methods that allow capturing these currently omitted sizes will be important to complete the picture of MNP emissions to and their fate in the environment.

The presence of MPs in soils treated with mineral fertiliser sheds light on some remaining challenges when it comes to source apportionment and determining agricultural management practices that alleviate or aggravate the contamination of soils with MPs. Investigated field sites are not decoupled from their surroundings but detected MP concentrations are closely interlinked and affected by management practices of and transport processes between neighbouring soils. Disentangling direct inputs related to the use of different fertilisers from horizontally transported MPs will require more systematic measurements, including measurements of the fertilisers prior to their application and a more targeted analysis of horizontal transfers of MPs in field conditions.

There has been an ongoing discussion about the use of sewage sludge on agricultural land, with MPs being mentioned as a potential risk factor. Despite overlapping observations between **Paper I** and other field studies, it is evident that MP emissions to soil as well as their specific properties, such as particle type, shape and size, are context-dependent. It is thus challenging to extrapolate the concentrations measured at the single site in **Paper I** to a larger scale. In Sweden, sewage sludge applications to agricultural land have been steadily increasing, so that emissions of MPs to the soil are anticipated to increase in the foreseeable future. Notably, sewage sludge is not the only source of MNPs to agricultural soils, but it needs to be considered as one factor in the wider context of an agricultural landscape. Given the persistence of MPs, a more systematic monitoring of MPs in sewage sludge and soils from different localities in Sweden is required to assess large scale mass

flows and to ensure that effect levels are not reached. MPs are only one of many stressors that soils are exposed to. Thus, potential adverse effect of MNPs need to be considered simultaneously with other persistent pollutants and other stressors.

6.3 Microplastic mobility in the soil

The distribution of MPs in the soil ecosystem is neither homogeneous nor static, but can change over time in response to transport processes, as was shown in both field and laboratory studies (**Paper I-III**). MPs were dispersed to deeper parts of the soil profile after long-term application of sewage sludge and exposure to field conditions (**Paper I**). Thus, monitoring schemes should be designed with this potential for vertical translocation of MNPs in mind, in order to gain a comprehensive picture of present and future MP loads and their distribution in the soil system, thereby avoiding a systematic underestimation of exposure. Agricultural management practices apparently affect the MP distribution in the field according to **Paper I** and other studies on the vertical distribution of MPs in field soils. Investigations of the vertical distribution of MPs across different soil types and management systems would therefore contribute to an improved understanding of the factors limiting or enhancing transport in the field.

Bioturbation is a relevant transport mechanism for the vertical displacement of MPs, as substantial transport of MNPs was confirmed in the microcosm studies (**Paper II** and **III)**. Bioturbation should, thus, be considered as a relevant transport mechanism for future fate modelling of MNPs in soils. Transport by earthworms can also have important implications for smaller scale exposure levels. Near-surface ingestion of MNPs and subsurface excretion can cause a successive enrichment of MNPs in deeper soil and a spatial concentration in the drilosphere (**Paper II**). Burrow-dwelling organisms might therefore be relatively more exposed to MNPs in soils, calling for further investigations on potential chronic exposure effects. Transport potential in **Paper II** and **III** was only assessed for a single anecic earthworm species and under favourable conditions. Transport rates and resulting spatial distribution patterns likely differ between earthworm ecotypes due to differing burrowing and feeding behaviours. Endogeic or shallow burrowing earthworms could, for instance, cause more intense mixing, but within a more restricted depth in the

shallower soil (Capowiez et al., 2024). Thus, potential transport depths and rates in the field cannot be readily inferred from a single observation with a single species, but require further investigations of earthworms with different burrowing behaviours.

Bioturbation activity, associated biopores and consequently MNP transport rates and depths by bioturbation are dependent on local soil properties, climatic conditions and different soil management factors. To add to the complexity, interactions between different soil organisms, even between different earthworm species, might affect their burrowing behaviour. Investigating MNP transport by the different earthworm ecotypes and in mixed community studies would allow to gain insights into potential interactive or even synergistic effects possibly resulting in different vertical transport dynamics and small scale spatial patterns. In the field, the effects of bioturbation and water-driven transport are difficult to distinguish as they occur simultaneously. I therefore propose to investigate MNP transport in more complex laboratory experiments, combining irrigation treatments with the presence or absence of earthworms to assess both individual and potentially synergistic effects of these biological and physical transport processes.

While field and laboratory bioturbation studies both suggested that MNPs might be more mobile in soils than often expected, they also revealed potential transport limiting factors. Particle size and shape influenced transport dynamics in **Paper I-III**. In the field, smaller and fragmental particles were more mobile and transported away from the plough layer (**Paper I**). Transport by bioturbation proved to be size-dependent as well: NPs in **Paper II** were transported faster than MP fibres in **Paper III**, and smaller MP fibres were more mobile than larger MP fibres. A remaining challenge is to disentangle the effect of different physical particle parameters. It remains unclear if the observed size effects on MP transport are transferable across the range of shapes that MPs can occur in in the field. Larger fibrous particles seemed more mobile in the field study (**Paper I**) than their fragmental counterparts of the same major diameter. Moreover, even relatively large MP fibres of several millimetres that are otherwise often considered immobile in soils were transported by earthworms (**Paper III**). Thus, I propose to further investigate the effect of particle volume and shape on bioturbation-driven transport.

Often, the question arises whether environmental compartments act as sources or sinks of MPs. The enrichment of MPs in sewage sludge-amended soils suggests that MP inputs are exceeding MP transfers to other compartments under the current land management, making soils a temporary sink (**Paper I**). Whether accumulated MPs can be transported away, vertically to the groundwater or laterally to aquatic environments, is likely location-specific due to the multitude of influencing factors that determine their mobility. Some transport processes can have synergistic effects, whereas others can counter each other. For instance, the incorporation of MNPs into the drilosphere by earthworms facilitates their remobilization and transport with preferential flow. As MNPs are moving deeper into the soil, the risk for groundwater contamination increases, but it concurrently reduces the potential horizontal transport at the soil surface. Ultimately, it is likely an intertwined effect of land use, climatic conditions, soil management activities, MP and soil properties that determines the mobility of specific MPs in soils.

References

Alimi, O.S., Farner Budarz, J., Hernandez, L.M., Tufenkji, N. (2018). Microplastics and nanoplastics in aquatic environments: aggregation, deposition, and enhanced contaminant transport. *Environmental Science & Technology*. 52, 1704–1724. https://doi.org/10.1021/acs.est.7b05559

Allen, S., Allen, D., Phoenix, V.R., Le Roux, G., Durántez Jiménez, P., Simonneau, A., Binet, S., Galop, D. (2019). Atmospheric transport and deposition of microplastics in a remote mountain catchment. *Nature Geoscience*. 12, 339–344. https://doi.org/10.1038/s41561-019-0335-5

Arkatkar, A., Arutchelvi, J., Bhaduri, S., Uppara, P.V., Doble, M. (2009). Degradation of unpretreated and thermally pretreated polypropylene by soil consortia. *International Biodeterioration & Biodegradation*. 63, 106–111. https://doi.org/10.1016/j.ibiod.2008.06.005

Arrázola-Vásquez, E., Larsbo, M., Capowiez, Y., Taylor, A., Sandin, M., Iseskog, D., Keller, T. (2022). Earthworm burrowing modes and rates depend on earthworm species and soil mechanical resistance. *Applied Soil Ecology*. 178, 104568. https://doi.org/10.1016/j.apsoil.2022.104568

Baccaro, M., Harrison, S., Berg, H. van den, Sloot, L., Hermans, D., Cornelis, G., Gestel, C.A.M. van, Brink, N.W. van den (2019). Bioturbation of Ag2S-NPs in soil columns by earthworms. *Environmental Pollution*. 252, 155–162. https://doi.org/10.1016/j.envpol.2019.05.106

Bergmann, M., Mützel, S., Primpke, S., Tekman, M.B., Trachsel, J., Gerdts, G. (2019). White and wonderful? Microplastics prevail in snow from the Alps to the Arctic. *Science Advances*. 5, 8. https://doi.org/10.1126/sciadv.aax1157

Blume, H.-P., Brümmer, G.W., Fleige, H., Horn, R., Kandeler, E., Kögel-Knabner, I., Kretzschmar, R., Stahr, K., Wilke, B.-M. (2016). Threats to the soil functions, in: Blume, H.-P., Brümmer, G.W., Fleige, H., Horn, R., Kandeler, E., Kögel-Knabner, I., Kretzschmar, R., Stahr, K., Wilke, B.-M. (Eds.), *Scheffer/Schachtschabel Soil Science*. Springer Berlin Heidelberg, Berlin, Heidelberg, pp. 485–559. https://doi.org/10.1007/978-3-642-30942-7_10

Börjesson, G., Kirchmann, H., Kätterer, T. (2014). Four Swedish long-term field experiments with sewage sludge reveal a limited effect on soil microbes and on metal uptake by crops. *Journal of Soils and Sediments*. 14, 164–177. https://doi.org/10.1007/s11368-013-0800-5

Bottinelli, N., Hedde, M., Jouquet, P., Capowiez, Y. (2020). An explicit definition of earthworm ecological categories – Marcel Bouché's triangle revisited. *Geoderma*. 372, 114361. https://doi.org/10.1016/j.geoderma.2020.114361

Bouché, M.B. (1977). Strategies lombriciennes. *Ecological Bulletins*. 25, 122–132. https://www.jstor.org/stable/20112572

Capowiez, Y., Marchán, D., Decaëns, T., Hedde, M., Bottinelli, N. (2024). Let earthworms be functional - Definition of new functional groups based on their bioturbation behavior. *Soil Biology and Biochemistry*. 188, 109209. https://doi.org/10.1016/j.soilbio.2023.109209

Capowiez, Y., Sammartino, S., Michel, E. (2011). Using X-ray tomography to quantify earthworm bioturbation non-destructively in repacked soil cores. *Geoderma*. 162, 124–131. https://doi.org/10.1016/j.geoderma.2011.01.011

Capowiez, Y., Cadoux, S., Bouchant, P., Ruy, S., Roger-Estrade, J., Richard, G., Boizard, H. (2009). The effect of tillage type and cropping system on earthworm communities, macroporosity and water infiltration. *Soil and Tillage Research*. 105, 209–216. https://doi.org/10.1016/j.still.2009.09.002

Chamas, A., Moon, H., Zheng, J., Qiu, Y., Tabassum, T., Jang, J.H., Abu-Omar, M., Scott, S.L., Suh, S. (2020). Degradation rates of plastics in the environment. *ACS Sustainable Chemistry & Engineering*. 8, 3494–3511. https://doi.org/10.1021/acssuschemeng.9b06635

Chan, K.Y., Barchia, I. (2007). Soil compaction controls the abundance, biomass and distribution of earthworms in a single dairy farm in south-eastern Australia. *Soil and Tillage Research*. 94, 75–82. https://doi.org/10.1016/j.still.2006.07.006

Chen, Y., Awasthi, A.K., Wei, F., Tan, Q., Li, J. (2021). Single-use plastics: Production, usage, disposal, and adverse impacts. *Science of The Total Environment*. 752, 141772. https://doi.org/10.1016/j.scitotenv.2020.141772

Cole, M. (2016). A novel method for preparing microplastic fibers. *Scientific Reports*. 6, 34519. https://doi.org/10.1038/srep34519

Corradini, F., Meza, P., Eguiluz, R., Casado, F., Huerta-Lwanga, E., Geissen, V. (2019). Evidence of microplastic accumulation in agricultural soils from sewage sludge disposal. *Science of The Total Environment*. 671, 411–420. https://doi.org/10.1016/j.scitotenv.2019.03.368

Crawford, C.B., Quinn, B. (2017). *Microplastic Pollutants*. Elsevier, 315 p. https://doi.org/10.1016/C2015-0-04315-5

Crossman, J., Hurley, R.R., Futter, M., Nizzetto, L. (2020). Transfer and transport of microplastics from biosolids to agricultural soils and the wider environment. *Science of The Total Environment*. 724, 138334. https://doi.org/10.1016/j.scitotenv.2020.138334

David, J., Steinmetz, Z., Kučerík, J., Schaumann, G.E. (2018). Quantitative analysis of poly(ethylene terephthalate) microplastics in soil via thermogravimetry–

mass spectrometry. *Analytical Chemistry*. 90, 8793–8799. https://doi.org/10.1021/acs.analchem.8b00355

de Souza Machado, A.A., Lau, C.W., Till, J., Kloas, W., Lehmann, A., Becker, R., Rillig, M.C. (2018). Impacts of microplastics on the soil biophysical environment. *Environmental Science & Technology*. 52, 9656–9665. https://doi.org/10.1021/acs.est.8b02212

Dierkes, G., Lauschke, T., Becher, S., Schumacher, H., Földi, C., Ternes, T. (2019). Quantification of microplastics in environmental samples via pressurized liquid extraction and pyrolysis-gas chromatography. *Analytical and Bioanalytical Chemistry*. 411, 6959–6968. https://doi.org/10.1007/s00216-019-02066-9

Dong, Z., Qiu, Y., Zhang, W., Yang, Z., Wei, L. (2018). Size-dependent transport and retention of micron-sized plastic spheres in natural sand saturated with seawater. *Water Research*. 143, 518–526. https://doi.org/10.1016/j.watres.2018.07.007

Dümichen, E., Eisentraut, P., Bannick, C.G., Barthel, A.-K., Senz, R., Braun, U. (2017). Fast identification of microplastics in complex environmental samples by a thermal degradation method. *Chemosphere*. 174, 572–584. https://doi.org/10.1016/j.chemosphere.2017.02.010

Fang, C., Zhou, W., Hu, J., Wu, C., Niu, J., Naidu, R. (2024). Paint has the potential to release microplastics, nanoplastics, inorganic nanoparticles, and hybrid materials. *Environmental Sciences Europe*. 36, 17. https://doi.org/10.1186/s12302-024-00844-6

FAO (2015). World reference base for soil resources 2014. International soil classification system for naming soils and creating legends for soil maps. *World soil resources reports 106*. ISBN 978-92-5-108369-7

Frehland, S., Kaegi, R., Hufenus, R., Mitrano, D.M. (2020). Long-term assessment of nanoplastic particle and microplastic fiber flux through a pilot wastewater treatment plant using metal-doped plastics. *Water Research*. 182, 115860. https://doi.org/10.1016/j.watres.2020.115860

Gao, J., Pan, S., Li, P., Wang, L., Hou, R., Wu, W.-M., Luo, J., Hou, D. (2021). Vertical migration of microplastics in porous media: Multiple controlling factors under wet-dry cycling. *Journal of Hazardous Materials*. 419, 126413. https://doi.org/10.1016/j.jhazmat.2021.126413

Geyer, R., Jambeck, J., Law, K. (2017). Production, use, and fate of all plastics ever made. *Science Advances*. 3, e1700782. https://doi.org/10.1126/sciadv.1700782

Gigault, J., El Hadri, H., Nguyen, B., Grassl, B., Rowenczyk, L., Tufenkji, N., Feng, S., Wiesner, M. (2021). Nanoplastics are neither microplastics nor engineered nanoparticles. *Nature Nanotechnology*. 16, 501-507. https://doi.org/10.1038/s41565-021-00886-4

Gigault, J., Halle, A. ter, Baudrimont, M., Pascal, P.-Y., Gauffre, F., Phi, T.-L., El Hadri, H., Grassl, B., Reynaud, S. (2018). Current opinion: What is a nanoplastic? *Environmental Pollution*. 235, 1030–1034. https://doi.org/10.1016/j.envpol.2018.01.024

Han, N., Zhao, Q., Ao, H., Hu, H., Wu, C. (2022). Horizontal transport of macro- and microplastics on soil surface by rainfall induced surface runoff as affected by vegetations. *Science of The Total Environment*. 831, 154989. https://doi.org/10.1016/j.scitotenv.2022.154989

Harley-Nyang, D., Memon, F.A., Osorio Baquero, A., Galloway, T. (2023). Variation in microplastic concentration, characteristics and distribution in sewage sludge & biosolids around the world. *Science of The Total Environment*. 891, 164068. https://doi.org/10.1016/j.scitotenv.2023.164068

Hartmann, N.B., Hüffer, T., Thompson, R.C., Hassellöv, M., Verschoor, A., Daugaard, A.E., Rist, S., Karlsson, T., Brennholt, N., Cole, M., Herrling, M.P., Hess, M.C., Ivleva, N.P., Lusher, A.L., Wagner, M. (2019). Are we speaking the same language? Recommendations for a definition and categorization framework for plastic debris. *Environmental Science & Technology*. 53, 1039–1047. https://doi.org/10.1021/acs.est.8b05297

Horton, A.A., Walton, A., Spurgeon, D.J., Lahive, E., Svendsen, C. (2017). Microplastics in freshwater and terrestrial environments: Evaluating the current understanding to identify the knowledge gaps and future research priorities. *Science of The Total Environment*. 586, 127–141. https://doi.org/10.1016/j.scitotenv.2017.01.190

Huerta Lwanga, E., van Roshum, I., Munhoz, D.R., Meng, K., Rezaei, M., Goossens, D., Bijsterbosch, J., Alexandre, N., Oosterwijk, J., Krol, M., Peters, P., Geissen, V., Ritsema, C. (2023). Microplastic appraisal of soil, water, ditch sediment and airborne dust: The case of agricultural systems. *Environmental Pollution*. 316, 120513. https://doi.org/10.1016/j.envpol.2022.120513

Huerta Lwanga, E., Gertsen, H., Gooren, H., Peters, P., Salánki, T., Ploeg, M. van der, Besseling, E., Koelmans, A.A., Geissen, V. (2017). Incorporation of microplastics from litter into burrows of Lumbricus terrestris. *Environmental Pollution*. 220, 523–531. https://doi.org/10.1016/j.envpol.2016.09.096

Huerta Lwanga, E., Gertsen, H., Gooren, H., Peters, P., Salánki, T., van der Ploeg, M., Besseling, E., Koelmans, A.A., Geissen, V. (2016). Microplastics in the terrestrial ecosystem: implications for Lumbricus terrestris (Oligochaeta, Lumbricidae). *Environmental Science & Technology*. 50, 2685–2691. https://doi.org/10.1021/acs.est.5b05478

Jarvis, N., Bergström, L., Dik, P.E. (1991). Modelling water and solute transport in macroporous soil. II. Chloride breakthrough under non-steady flow. *Journal*

of Soil Science. 42, 71–81. https://doi.org/10.1111/j.1365-2389.1991.tb00092.x

Jarvis, N., Koestel, J., Larsbo, M. (2016). Understanding preferential flow in the vadose zone: Recent advances and future prospects. *Vadose Zone Journal*. 15 (12), 1-11. vzj2016.09.0075. https://doi.org/10.2136/vzj2016.09.0075

Jarvis, N.J., Taylor, A., Larsbo, M., Etana, A., Rosén, K. (2010). Modelling the effects of bioturbation on the re-distribution of 137Cs in an undisturbed grassland soil. *European Journal of Soil Science*. 61, 24–34. https://doi.org/10.1111/j.1365-2389.2009.01209.x

Jégou, D., Brunotte, J., Rogasik, H., Capowiez, Y., Diestel, H., Schrader, S., Cluzeau, D. (2002). Impact of soil compaction on earthworm burrow systems using X-ray computed tomography: preliminary study. *European Journal of Soil Biology*. 38, 329–336. https://doi.org/10.1016/S1164-5563(02)01148-2

Ji, Z., Huang, Y., Feng, Y., Johansen, A., Xue, J., Tremblay, L.A., Li, Z. (2021). Effects of pristine microplastics and nanoplastics on soil invertebrates: A systematic review and meta-analysis of available data. *Science of The Total Environment*. 788, 147784. https://doi.org/10.1016/j.scitotenv.2021.147784

Ju, H., Zhu, D., Qiao, M. (2019). Effects of polyethylene microplastics on the gut microbial community, reproduction and avoidance behaviors of the soil springtail, Folsomia candida. *Environmental Pollution*. 247, 890–897. https://doi.org/10.1016/j.envpol.2019.01.097

Kätterer, T., Börjesson, G., Kirchmann, H. (2014). Changes in organic carbon in topsoil and subsoil and microbial community composition caused by repeated additions of organic amendments and N fertilisation in a long-term field experiment in Sweden. *Agriculture, Ecosystems & Environment*. 189, 110–118. https://doi.org/10.1016/j.agee.2014.03.025

Kawecki, D., Nowack, B. (2019). Polymer-specific modeling of the environmental emissions of seven commodity plastics as macro- and microplastics. *Environmental Science & Technology*. 53, 9664–9676. https://doi.org/10.1021/acs.est.9b02900

Keller, A.S., Jimenez-Martinez, J., Mitrano, D.M. (2020). Transport of nano- and microplastic through unsaturated porous media from sewage sludge application. *Environmental Science & Technology*. 54, 911–920. https://doi.org/10.1021/acs.est.9b06483

Khalid, N., Aqeel, M., Noman, A. (2020). Microplastics could be a threat to plants in terrestrial systems directly or indirectly. *Environmental Pollution*. 267, 115653. https://doi.org/10.1016/j.envpol.2020.115653

Klemmensen, N.D.R., Chand, R., Blanco, M.S., Vollertsen, J. (2024). Microplastic abundance in sludge-treated fields: Variance and estimated half-life.

Science of The Total Environment. 922, 171394. https://doi.org/10.1016/j.scitotenv.2024.171394

Koutnik, V.S., Leonard, J., Brar, J., Cao, S., Glasman, J.B., Cowger, W., Ravi, S., Mohanty, S.K. (2022). Transport of microplastics in stormwater treatment systems under freeze-thaw cycles: Critical role of plastic density. *Water Research*. 222, 118950. https://doi.org/10.1016/j.watres.2022.118950

Laermanns, H., Lehmann, M., Klee, M., Löder, M., Gekle, S., Bogner, C. (2021). Tracing the horizontal transport of microplastics on rough surfaces. *Microplastics and Nanoplastics*. 1, 11. https://doi.org/10.1186/s43591-021-00010-2

Lahive, E., Cross, R., Saarloos, A.I., Horton, A.A., Svendsen, C., Hufenus, R., Mitrano, D.M. (2022). Earthworms ingest microplastic fibres and nanoplastics with effects on egestion rate and long-term retention. *Science of The Total Environment*. 807, 151022. https://doi.org/10.1016/j.scitotenv.2021.151022

Lambert, S., Wagner, M. (2016). Characterisation of nanoplastics during the degradation of polystyrene. *Chemosphere*. 145, 265–268. https://doi.org/10.1016/j.chemosphere.2015.11.078

Lantmäteriet (2019). Höjddata, Grid 2+ 2019, Elevation data, Grid 2+. Accessed: 2024-07-07.

Larsbo, M., Koestel, J., Krab, E.J., Klaminder, J. (2024). Quantifying earthworm soil ingestion from changes in vertical bulk density profiles. *European Journal of Soil Biology*. 120, 103574. https://doi.org/10.1016/j.ejsobi.2023.103574

Larsbo, M., Sandin, M., Jarvis, N., Etana, A., Kreuger, J. (2016). Surface runoff of pesticides from a clay loam field in Sweden. *Journal of Environment Quality*. 45 (4), 1367-1374. https://doi.org/10.2134/jeq2015.10.0528

Leuther, F., Schlüter, S. (2021). Impact of freeze–thaw cycles on soil structure and soil hydraulic properties. *SOIL* 7, 179–191. https://doi.org/10.5194/soil-7-179-2021

Liu, F., Rasmussen, L., Klemmensen, N., Zhao, G., Nielsen, R., Vianello, A., Rist, S., Vollertsen, J. (2023). Shapes of hyperspectral imaged microplastics. *Environmental Science & Technology*. 57, 12431–12441. https://doi.org/10.1021/acs.est.3c03517

Ljung, E., Borg Olesen, K., Andersson, P.-G., Fältström, E., Vollertsen, J., Wittgren, H.B., Hagman, M. (2018). Mikroplaster i kretsloppet (No. 2018–13). Svenskt Vatten Utveckling.

Lozano, Y.M., Rillig, M.C. (2020). Effects of microplastic fibers and drought on Plant Communities. *Environmental Science & Technology*. 54, 6166–6173. https://doi.org/10.1021/acs.est.0c01051

Magnusson, K., Norén, F. (2014). Screening of microplastic particles in and down-stream a wastewater treatment plant, IVL Report C.

Mahon, A.M., O'Connell, B., Healy, M.G., O'Connor, I., Officer, R., Nash, R., Morrison, L. (2017). Microplastics in sewage sludge: Effects of treatment. *Environmental Science & Technology*. 51, 810–818. https://doi.org/10.1021/acs.est.6b04048

Mansa, R., Zou, S. (2021). Thermogravimetric analysis of microplastics: A mini review. *Environmental Advances*. 5, 100117. https://doi.org/10.1016/j.envadv.2021.100117

McTavish, M.J., Murphy, S.D. (2021). Three-dimensional mapping of earthworm (Lumbricus terrestris) seed transport. *Pedobiologia*. 87–88, 150752. https://doi.org/10.1016/j.pedobi.2021.150752

Mitrano, D.M., Beltzung, A., Frehland, S., Schmiedgruber, M., Cingolani, A., Schmidt, F. (2019). Synthesis of metal-doped nanoplastics and their utility to investigate fate and behaviour in complex environmental systems. *Nature Nanotechnology*. 14, 362–368. https://doi.org/10.1038/s41565-018-0360-3

Mossadeghi-Björklund, M., Arvidsson, J., Keller, T., Koestel, J., Lamandé, M., Larsbo, M., Jarvis, N. (2016). Effects of subsoil compaction on hydraulic properties and preferential flow in a Swedish clay soil. *Soil and Tillage Research*. 156, 91–98. https://doi.org/10.1016/j.still.2015.09.013

Naturvårdsverket (2022). Utsläpp till vatten och slamproduktion 2020. Kommunala avloppsreningsverk, massa- och papersindustri samt viss övrig industri. Statistiska meddelanden MI 22, 35.

Naturvårdsverket (2009). Riktvärden för förorenad mark – modellbeskrivning och vägledning. Naturvårdsverket, Stockholm.

Ng, E.-L., Huerta Lwanga, E., Eldridge, S.M., Johnston, P., Hu, H.-W., Geissen, V., Chen, D. (2018). An overview of microplastic and nanoplastic pollution in agroecosystems. *Science of the Total Environment*. 627, 1377–1388. https://doi.org/10.1016/j.scitotenv.2018.01.341

Nizzetto, L., Futter, M., Langaas, S. (2016). Are agricultural soils dumps for microplastics of urban origin? *Environmental Science & Technology*. 50 (20), 10777–10779. https://doi.org/10.1021/acs.est.6b04140

O'Connor, D., Pan, S., Shen, Z., Song, Y., Jin, Y., Wu, W.-M., Hou, D. (2019). Microplastics undergo accelerated vertical migration in sand soil due to small size and wet-dry cycles. *Environmental Pollution*. 249, 527–534. https://doi.org/10.1016/j.envpol.2019.03.092

Okoffo, E.D., Ribeiro, F., O'Brien, J.W., O'Brien, S., Tscharke, B.J., Gallen, M., Samanipour, S., Mueller, J.F., Thomas, K.V. (2020). Identification and quantification of selected plastics in biosolids by pressurized liquid extraction combined with double-shot pyrolysis gas chromatography–mass spectrometry. *Science of The Total Environment*. 715, 136924. https://doi.org/10.1016/j.scitotenv.2020.136924

Pérez-Reverón, R., Álvarez-Méndez, S.J., González-Sálamo, J., Socas-Hernández, C., Díaz-Peña, F.J., Hernández-Sánchez, C., Hernández-Borges, J. (2023).

Nanoplastics in the soil environment: Analytical methods, occurrence, fate and ecological implications. *Environmental Pollution*. 317, 120788. https://doi.org/10.1016/j.envpol.2022.120788

Porterfield, K.K., Hobson, S.A., Neher, D.A., Niles, M.T., Roy, E.D. (2023). Microplastics in composts, digestates, and food wastes: A review. *Journal of Environmental Quality*. 52, 225–240. https://doi.org/10.1002/jeq2.20450

Prendergast-Miller, M.T., Katsiamides, A., Abbass, M., Sturzenbaum, S.R., Thorpe, K.L., Hodson, M.E. (2019). Polyester-derived microfibre impacts on the soil-dwelling earthworm Lumbricus terrestris. *Environmental Pollution*. 251, 453–459. https://doi.org/10.1016/j.envpol.2019.05.037

Primpke, S., Fischer, M., Lorenz, C., Gerdts, G., Scholz-Böttcher, B.M. (2020). Comparison of pyrolysis gas chromatography/mass spectrometry and hyperspectral FTIR imaging spectroscopy for the analysis of microplastics. *Analytical and Bioanalytical Chemistry*. 412, 8283–8298. https://doi.org/10.1007/s00216-020-02979-w

Primpke, S., Lorenz, C., Rascher-Friesenhausen, R., Gerdts, G. (2017). An automated approach for microplastics analysis using focal plane array (FPA) FTIR microscopy and image analysis. *Analytical Methods*. 9, 1499–1511. https://doi.org/10.1039/C6AY02476A

Quik, J.T.K., Meesters, J.A.J., Koelmans, A.A. (2023). A multimedia model to estimate the environmental fate of microplastic particles. *Science of The Total Environment*. 882, 163437. https://doi.org/10.1016/j.scitotenv.2023.163437

Ranjan, V.P., Joseph, A., Sharma, H.B., Goel, S. (2023). Preliminary investigation on effects of size, polymer type, and surface behaviour on the vertical mobility of microplastics in a porous media. *Science of The Total Environment*. 864, 161148. https://doi.org/10.1016/j.scitotenv.2022.161148

Redondo-Hasselerharm, P.E., Vink, G., Mitrano, D.M., Koelmans, A.A. (2021). Metal-doping of nanoplastics enables accurate assessment of uptake and effects on Gammarus pulex. *Environmental Science: Nano*. 8, 1761–1770. https://doi.org/10.1039/D1EN00068C

Rezaei, M., Riksen, M.J.P.M., Sirjani, E., Sameni, A., Geissen, V. (2019). Wind erosion as a driver for transport of light density microplastics. *Science of The Total Environment*. 669, 273–281. https://doi.org/10.1016/j.scitotenv.2019.02.382

Rillig, M.C., Ziersch, L., Hempel, S. (2017). Microplastic transport in soil by earthworms. *Scientific Reports*. 7, 1362. https://doi.org/10.1038/s41598-017-01594-7

Ruiz, S.A., Bickel, S., Or, D. (2021). Global earthworm distribution and activity windows based on soil hydromechanical constraints. *Communications Biology*. 4, 612. https://doi.org/10.1038/s42003-021-02139-5

Schell, T., Hurley, R., Buenaventura, N.T., Mauri, P.V., Nizzetto, L., Rico, A., Vighi, M. (2022). Fate of microplastics in agricultural soils amended with sewage sludge: Is surface water runoff a relevant environmental pathway? *Environmental Pollution*. 293, 118520. https://doi.org/10.1016/j.envpol.2021.118520

Schindelin, J., Arganda-Carreras, I., Frise, E., Kaynig, V., Longair, M., Pietzsch, T., Preibisch, S., Rueden, C., Saalfeld, S., Schmid, B., Tinevez, J.-Y., White, D.J., Hartenstein, V., Eliceiri, K., Tomancak, P., Cardona, A. (2012). Fiji: an open-source platform for biological-image analysis. *Nature Methods*. 9, 676–682. https://doi.org/10.1038/nmeth.2019

Schmiedgruber, M., Hufenus, R., Mitrano, D.M. (2019). Mechanistic understanding of microplastic fiber fate and sampling strategies: Synthesis and utility of metal doped polyester fibers. *Water Research*. 155, 423–430. https://doi.org/10.1016/j.watres.2019.02.044

Schneider, C.A., Rasband, W.S., Eliceiri, K.W. (2012). NIH Image to ImageJ: 25 years of image analysis. *Nature Methods*. 9, 671–675. https://doi.org/10.1038/nmeth.2089

Shafea, L., Yap, J., Beriot, N., Felde, V.J.M.N.L., Okoffo, E.D., Enyoh, C.E., Peth, S. (2023). Microplastics in agroecosystems: A review of effects on soil biota and key soil functions. *Journal of Plant Nutrition and Soil Science*. 186, 5–22. https://doi.org/10.1002/jpln.202200136

Simon, M., Alst, N. van, Vollertsen, J. (2018). Quantification of microplastic mass and removal rates at wastewater treatment plants applying Focal Plane Array (FPA)-based Fourier Transform Infrared (FT-IR) imaging. *Water Research*. 142, 1–9. https://doi.org/10.1016/j.watres.2018.05.019

Sintim, H.Y., Bary, A.I., Hayes, D.G., English, M.E., Schaeffer, S.M., Miles, C.A., Zelenyuk, A., Suski, K., Flury, M. (2019). Release of micro- and nanoparticles from biodegradable plastic during in situ composting. *Science of The Total Environment*. 675, 686–693. https://doi.org/10.1016/j.scitotenv.2019.04.179

Steinmetz, Z., Löffler, P., Eichhöfer, S., David, J., Muñoz, K., Schaumann, G.E. (2021). Are agricultural plastic covers a source of plastic debris in soil? A first screening study. *SOIL*. 8, 31-47. https://doi.org/10.5194/soil-8-31-2022

Steinmetz, Z., Kintzi, A., Muñoz, K., Schaumann, G.E. (2020). A simple method for the selective quantification of polyethylene, polypropylene, and polystyrene plastic debris in soil by pyrolysis-gas chromatography/mass spectrometry. *Journal of Analytical and Applied Pyrolysis*. 147, 104803. https://doi.org/10.1016/j.jaap.2020.104803

Tagg, A.S., Brandes, E., Fischer, F., Fischer, D., Brandt, J., Labrenz, M. (2022). Agricultural application of microplastic-rich sewage sludge leads to further

uncontrolled contamination. *Science of The Total Environment*. 806, 150611. https://doi.org/10.1016/j.scitotenv.2021.150611

Tatsii, D., Bucci, S., Bhowmick, T., Guettler, J., Bakels, L., Bagheri, G., Stohl, A. (2024). Shape Matters: Long-Range Transport of Microplastic Fibers in the Atmosphere. *Environmental Science & Technology*. 58, 671–682. https://doi.org/10.1021/acs.est.3c08209

Taylor, A.R., Lenoir, L., Vegerfors, B., Persson, T. (2018). Ant and earthworm bioturbation in cold-temperate ecosystems. *Ecosystems*. 22, 981–994. https://doi.org/10.1007/s10021-018-0317-2

Thomas, D., Schütze, B., Heinze, W.M., Steinmetz, Z. (2020). Sample preparation techniques for the analysis of microplastics in soil - A review. *Sustainability*. 12, 9074. https://doi.org/10.3390/su12219074

Thornton Hampton, L.M., Brander, S.M., Coffin, S., Cole, M., Hermabessiere, L., Koelmans, A.A., Rochman, C.M. (2022). Characterizing microplastic hazards: which concentration metrics and particle characteristics are most informative for understanding toxicity in aquatic organisms? *Microplastics and Nanoplastics*. 2, 20. https://doi.org/10.1186/s43591-022-00040-4

Torppa, K.A., Taylor, A.R. (2022). Alternative combinations of tillage practices and crop rotations can foster earthworm density and bioturbation. *Applied Soil Ecology*. 175, 104460. https://doi.org/10.1016/j.apsoil.2022.104460

van de Logt, R., van der Sluijs, T., van Eekeren, N. (2023). Lumbricus terrestris abundance in grasslands on sandy soils in relation to soil texture, hydrology and earthworm community. *European Journal of Soil Biology*. 119, 103545. https://doi.org/10.1016/j.ejsobi.2023.103545

van den Berg, P., Huerta-Lwanga, E., Corradini, F., Geissen, V. (2020). Sewage sludge application as a vehicle for microplastics in eastern Spanish agricultural soils. *Environmental Pollution*. 261, 114198. https://doi.org/10.1016/j.envpol.2020.114198

Vidal, A., Blouin, M., Lubbers, I., Capowiez, Y., Sanchez-Hernandez, J.C., Calogiuri, T., van Groenigen, J.W. (2023). Chapter One - The role of earthworms in agronomy: Consensus, novel insights and remaining challenges, in: Sparks, D.L. (Ed.), *Advances in Agronomy*. Academic Press, pp. 1–78. https://doi.org/10.1016/bs.agron.2023.05.001

Viitala, M., Steinmetz, Z., Sillanpää, Mika, Mänttäri, M., Sillanpää, M. (2022). Historical and current occurrence of microplastics in water and sediment of a Finnish lake affected by WWTP effluents. *Environmental Pollution*. 314, 120298. https://doi.org/10.1016/j.envpol.2022.120298

Viketoft, M., Riggi, L.G.A., Bommarco, R., Hallin, S., Taylor, A.R. (2021). Type of organic fertilizer rather than organic amendment per se increases abundance of soil biota. *PeerJ*. 9, e11204. https://doi.org/10.7717/peerj.11204

Waldschläger, K., Schüttrumpf, H. (2020). Infiltration behavior of microplastic particles with different densities, sizes, and shapes - From glass spheres to

natural sediments. *Environmental Science & Technology*. 54, 9366–9373. https://doi.org/10.1021/acs.est.0c01722

Wasserstein, R.L., Schirm, A.L., Lazar, N.A. (2019). Moving to a world beyond "p < 0.05." *The American Statistician*. 73, 1–19. https://doi.org/10.1080/00031305.2019.1583913

Weber, C.J., Santowski, A., Chifflard, P. (2022). Investigating the dispersal of macro- and microplastics on agricultural fields 30 years after sewage sludge application. *Scientific Reports*. 12, 6401. https://doi.org/10.1038/s41598-022-10294-w

Weber, C.J., Opp, C., Prume, J.A., Koch, M., Andersen, T.J., Chifflard, P. (2021). Deposition and in-situ translocation of microplastics in floodplain soils. *Science of The Total Environment*. 819, 152039. https://doi.org/10.1016/j.scitotenv.2021.152039

Weber, C.J., Opp, C. (2020). Spatial patterns of mesoplastics and coarse microplastics in floodplain soils as resulting from land use and fluvial processes. *Environmental Pollution*. 267, 115390. https://doi.org/10.1016/j.envpol.2020.115390

Weithmann, N., Möller, J.N., Löder, M.G.J., Piehl, S., Laforsch, C., Freitag, R. (2018). Organic fertilizer as a vehicle for the entry of microplastic into the environment. *Science Advances*. 4, 4. https://doi.org/10.1126/sciadv.aap8060

Yi, S., Zuo, W., Xu, L., Wang, Y., Gu, C., Shan, Y., Bai, Y. (2023). Accumulation and migration of microplastics and its influencing factors in coastal saline-alkali soils amended with sewage sludge. *Ecotoxicology and Environmental Safety*. 266, 115597. https://doi.org/10.1016/j.ecoenv.2023.115597

Yu, M., van der Ploeg, M., Lwanga, E.H., Yang, X., Zhang, S., Ma, X., Ritsema, C.J., Geissen, V. (2019). Leaching of microplastics by preferential flow in earthworm (Lumbricus terrestris) burrows. *Environmental Chemistry*. 16, 31–40. https://doi.org/10.1071/EN18161

Zhang, L., Xie, Y., Liu, J., Zhong, S., Qian, Y., Gao, P. (2020). An overlooked entry pathway of microplastics into agricultural soils from application of sludge-based fertilizers. *Environmental Science & Technology*. 54, 4248–4255. https://doi.org/10.1021/acs.est.9b07905

Zhang, X., Chen, Y., Li, X., Zhang, Y., Gao, W., Jiang, J., Mo, A., He, D. (2022). Size/shape-dependent migration of microplastics in agricultural soil under simulative and natural rainfall. *Science of The Total Environment*. 815, 152507. https://doi.org/10.1016/j.scitotenv.2021.152507

Zhang, Y.-Q., Lykaki, M., Markiewicz, M., Alrajoula, M.T., Kraas, C., Stolte, S. (2022). Environmental contamination by microplastics originating from textiles: Emission, transport, fate and toxicity. *Journal of Hazardous Materials*. 430, 128453. https://doi.org/10.1016/j.jhazmat.2022.128453

Popular science summary

Global plastic production and consumption are steadily increasing leading to unintentional emissions of plastics to the environment. Plastic products are part of everyday life and designed to be very durable in various conditions. While these characteristics are desirable for their intended use, it also makes them persistent pollutants when they enter the environment. In particular the smaller-sized particles below 5 mm in size, commonly called microplastics and the even smaller nanoplastics, are considered problematic because they are expected to move through the food chain. These plastic particles can be directly produced in this size range, as pellets for instance, but they can also be released from larger plastics as they become brittle and fragment. Much attention has initially been on marine environments, but the majority of microplastics it thought to be emitted to the environment on land.

Microplastics can end up in soils as they fragment from agricultural plastics, such as mulching films, but they can also be unintentionally added with urban organic residues like composts and sewage sludge. Once micro- and nanoplastics enter the soil, they can have adverse effects on the soil ecosystem. The local impact depends on whether they remain in the soil, are transported on the soil surface to rivers and oceans or incorporated deeper into the soil. Particles, including micro- and nanoplastics, can be transported deeper into the soil with the movement of water or by burrowing soil organisms, also called bioturbation. The spatial distribution of microplastics is determined by input sources but can be changed by transport processes, both of which are only poorly understood for these synthetic particles. The main focus of this thesis was to improve our understanding of input pathways of microplastics to the soil environment on the one hand, and to investigate their further spread to the deeper soil on the other hand.

In a first step, potential input pathways of microplastics to the soil environment were investigated by measuring current concentrations in soils that received different fertiliser types for a period of 24 years. Sewage sludge applications led to higher microplastic concentrations in agricultural soils than mineral fertiliser applications. Textile-related plastic types were most abundant in soils treated with sewage sludge, likely because of their release from textiles when they are washed. Approximately half of the microplastics in sewage sludge-amended soils were found in deeper soil layers. A range of microplastic measurement techniques were applied for measuring microplastics in these field soils illustrating remaining analytical challenges. Standardisation of detection methods is still ongoing for microplastics in soils, but necessary to assess potential risks and develop reliable monitoring programs. Further optimisation and comparisons of detection methods is therefore necessary for a reliable and comprehensive assessment of plastic pollution of terrestrial ecosystems.

In order to shed light on the contribution of earthworms to the transport of plastics in soils, I conducted two laboratory experiments with soil and earthworms kept in soil cylinders under controlled conditions. One of the experiments was done with microplastic fibres, the other with nanoplastics. Deep-burrowing earthworms were found to transport both nano- and microplastics downwards in the soil. The smaller nanoplastics and smaller fibres were transported faster, probably because earthworms tend to eat them together with the surrounding soil. But even relatively long microplastic fibres were transported by the earthworms owing to the relatively narrow width of microplastic fibres. Earthworms can therefore be considered drivers of microplastic transport in the soil. Thereby, they also run the risk of being negatively affected themselves by the plastics because they incorporate micro- and nanoplastics into their burrows.

Collectively, these findings emphasize the need to consider micro- and nanoplastic transport in soils when estimating the overall plastic pollution of soil ecosystems and setting up monitoring schemes and in future predictions of their spread in the environment.

Populärvetenskaplig sammanfattning

Utsläppen av plast till miljön ökar i takt med den globala produktionen och konsumtionen av plast. Plastprodukter är en del av vardagen och materialen är utformade för att motstå slitage och nedbrytning under olika förhållanden. Även om produkternas motståndskraft är önskvärd medan de används, blir de samtidigt långlivade föroreningar när de kommer ut i miljön. I synnerhet de mindre partiklarna under 5 mm i storlek, vanligen kallade mikroplaster, och de ännu mindre nanoplasterna, anses vara problematiska, för att de kan röra sig och tas upp av olika organismer i näringskedjorna. Plastpartiklarna kan ha sin lilla storlek genom tillverkningen, som pellets till exempel, men de kan också frigöras från större plaster då de blir spröda och faller sönder i mindre fragment. Marina miljöer har varit föremål för mycket uppmärksamhet, men majoriteten av mikroplasterna släpps antagligen ut till ekosystemen på land.

I jordbruksmark kan mikroplaster hamna genom fragmentisering av plaster använda i just jordbruket, såsom marktäckningsdukar, men de kan också komma från urbana källor genom tillförsel av kompost och avloppsslam. När mikro- och nanoplaster väl hamnar i marken kan de ha negativa effekter på markens ekosystem. Den lokala påverkan beror på om de finns kvar i marken, transporteras på markytan till floder och hav eller förs djupare i marken. Transport ned i marken sker när vatten strömmar genom jorden eller med hjälp av grävande markorganismer, så kallad bioturbation. Både källorna till mikroplaster och deras transportprocesser i marken är dåligt kända; båda är viktiga för deras spridning i miljön. I den här avhandlingen ville jag framförallt förbättra vår förståelse av hur mikroplaster hamnar i vår markmiljö och undersöka deras vidare spridning till den djupare delen av marken.

I en första studie undersökte jag plasternas koncentration på olika djup i jordbruksjordar som under 24 år fått olika typer av gödsel. Tillförsel av avloppsslam ledde till högre mikroplastkoncentrationer i jorden än tillförsel av mineralgödsel. Textilrelaterade plasttyper förekom mest i jordar som behandlats med avloppsslam, troligen på grund av att plaster släppt från textilier under tvätt. Ungefär hälften av mikroplasterna återfanns i djupare jordlager. Metodstandardisering fortfarande pågår inom mikroplastforskningen och i avhandlingsarbetet använde jag en rad olika tekniker för att mäta koncentrationen av olika mikroplaster i dessa åkermarker. Analytiska utmaningar kvarstår, och ytterligare optimering och jämförelser av detektionsmetoder är nödvändiga för en tillförlitlig och heltäckande bedömning av plastföroreningar i terrestra ekosystem.

För att belysa hur daggmaskar bidrar till att transportera plast i åkermark genomförde jag sedan två laboratorieförsök, ett med mikroplastfibrer och ett med nanoplaster. Under kontrollerade förhållanden med jord och maskar i cylindrar på labbet övervakade jag den vertikala spridningen av mikro- och nanoplaster genom bioturbation. De djupgrävande daggmaskarna visade sig påskynda transporten av nano- och mikroplasttransport mot djupet. De mindre nanoplasterna och de mindre fibrerna transporterades snabbare, förmodligen för att daggmaskar tenderade att äta upp dem när de åt av den omgivande jorden. Men även relativt långa mikroplastfibrer transporterades, troligen på samma sätt och tack vare att fibrerna var så pass tunna. Daggmaskar kan därför betraktas som drivkrafter för mikroplasttransport i marken. Därmed kan de också själva påverkas negativt av plasten eftersom de tar in mikro- och nanoplaster i sina hålor.

Sammantaget understryker resultaten att transporten av mikro- och nanoplast i jordar måste tas i beaktande när man försöker mäta den totala plastföroreningen av markekosystemen, när man utvecklar övervakningssystem och i framtida förutsägelser om deras spridning i miljön.

Acknowledgements

Firstly, I would like to thank my main supervisor *Geert Cornelis* for giving me the opportunity to pursue a PhD in Soil Science, for your guidance, trust and support throughout the journey. Thank you for always supporting new ideas, for the countless critical discussions and for reminding me to sometimes take a step back. Thank you also to my co-supervisors, *Denise Mitrano* and *Elma Lahive* for your academic and personal support throughout this time, for always being there to give insights, discuss new ideas and for checking in even during busy times. Thank you to *Nick Jarvis* and *Anke Herrmann* – even though not everything worked out as we had planned, I greatly appreciated the opportunity to discuss new ideas and work together. It has been a privilege to have had you all as mentors.

Thanks *to all my current and former colleagues at the Department of Soil and Environment at SLU, to the Soil Chemistry research group*, and those that work behind the scenes. Especially *Sara Wassén, Mina Spångberg, Sofia Delin, David Törling* – thank you for all your patience whenever I needed help with field, administrative or laboratory questions. Thanks also to the internal committee *Eva Krab* and *Magnus Simonsson* for critical feedback on this thesis and *Hanna Sjulgård* for proof-reading.

The last four and a half years, I have not only been working (even though that was a pretty good proportion of what I did). Especially thanks to the usual suspects *Elsa, Erica, Lukas, Viki, Eduardo, Frederic, Evelin, Hanna, Maarten, Nithya, Rebecca, Tobias, Tino, Tove, Tamlyn, Vide, Yaana* and to all others current and former young researchers at the department *Florian, Getch, Hugo, Jelena, Jumpei, Karolina, Layla, Leti, Louis, Louise, Marie-Cecile, Miyanda, Péter, Sabina, Sara, Ylva*. Thanks for countless lunches, fikas, heart-to-heart talks and/or heated and critical discussions, hikes,

dinners, board game nights, crayfish parties, weekend trips and other adventures – you are what made Uppsala my home.

To all the fellow scientists I met at conferences and workshops, *to all my collaborators* from other institutes, especially to *Zacharias Steinmetz, Nanna Dyg Ratje Klemmensen, Asta Hooge, Jes Vollertsen* and *John Koestel:* Thank you for the productive exchange and opportunity to do science together. Working with you has changed my view of how we should do research, and opened my eyes to how much more can be achieved through true collaboration, critical discussions and open science. Thanks also to *Nora* and *Kathrin* for your contributions within my project. Thanks also to my remote support network at ETH Zürich – especially *Roman* and *Francesco*.

Now I'm taking a journey back in time and would also like to thank all the other people that guided or accompanied me along the way – knowingly and unknowingly, directly and indirectly, starting from the very beginning of my soil science journey. *Stefan Hecht* from the Institute of Geography, thank you for sparking my passion for soil science. It all started in a small, inconspicuous, windowless lecture hall in Heidelberg University. After just one lecture you fully convinced that soil is the most amazing subject to study in this world – something that is inspiring me to this day. Special thanks to *Gerd Schukraft*: many of the lab working habits I have today are a result of my years in your research lab (especially the meticulous cleaning habits). Thanks to the other research assistants in the *Geomorphology and Geoecology* lab during my time in Heidelberg – there is nothing bonds like digging a soil pit together.

To my friends from my geography bachelor studies in Heidelberg (das *Rudel*) – thanks for dragging me along into that soil geography lecture, and for each of you being as passionate about your own topics and the world as you are to this day. Thanks also to my *JTW friends from my time abroad at Kyushu University* in Fukuoka, Japan. As most people know, I probably wouldn't have moved to Sweden without this wonderful year of cultural exchange, intense Japanese studying and new friendships. *My EnvEuro friends from my master studies* in Copenhagen and Uppsala – there is nothing that can push you like curiosity blended with a good portion of academic ambition, spiked with strong competition and topped off with friendship.

My deepest gratitude also goes to *my family and all my friends at home*. Especially *to my mum*: thank you for always supporting me and encouraging me to pursue whatever field I'm interested in and making every of my international journeys and adventures possible. *Jens*, *Anka* and *Marcel* for always cheering me on along the way. *To my dad* – I wished you would have witnessed this day in other circumstances. *To Soso*, thanks for always insisting that I'm smart enough for this endeavour, and *to Ylvi* for taking my mind off work. Thanks *to my grandpa and grandma*, *Helmut Kiewitt* and *Madame*, whom I have to thank for being able to pursue my dreams without worrying.

I would also (quite unconventionally) like to thank myself, for the perseverance and determination I kept throughout these years. Finally, I would like to thank *Karl Dyrhage*. No one has experienced the different phases of my PhD journey as closely as you have, the successes but also the struggles, and no one supported me more during this time. Thank you for always being there and believing in me, even at times I didn't believe in myself.

Appendix

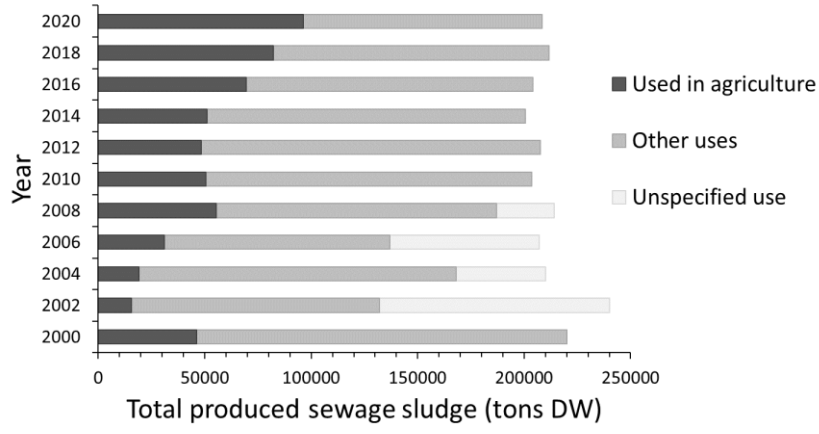

Figure S1: Total produced sewage sludge (tons dry weight, DW) in Sweden for the years 2000-2020 including the respective fractions returned to agricultural soils and other uses (including landfill, incineration and storage). Data was collected from bi-annual reports by Naturvårdsverket (Naturvårdsverket, 2022, 2018, 2016, 2014, 2014, 2012, 2010, 2008, 2006, 2004, 2002, 2000).

Table S1: Overview of reported MP concentrations in sewage sludge-amended soils.

Concentrations			
Reference	**Sample**	**Reported concentration (particles kg^{-1})**	**(mg kg^{-1})**
(Corradini et al., 2019)	1-5 times applications 40 tons/ha per application (0-25 cm)	Median: 1100, 1600, 1700, 2300, 3500 Total range: 600-10 400	Estimated median: 1.37, 2.03, 2.22, 2.88, 4.38 Total range: 0.73-12.9
(van den Berg et al., 2020)	w/o sewage sludge (0-10, 10-30 cm)	930 (±740) (light density); 1100 (±570) (heavy density)	NA
	1-8 applications 20-22 tons/ha per application (0-10, 10-30 cm)	2130 (±950) (light density); 3060 (±1680) (heavy density) Per application: 710 particles kg^{-1}	NA
(Ljung et al., 2018)	w/o sewage sludge:	NA	0.3
	1 application (1 t/ha/yr)	NA	0.32
	1 application (3 t/ha/yr)	NA	3.4
(Zhang et al., 2020)	w/o sewage sludge (0-5, 5-15, 15-25 cm)	5±0.4 4.0±0.4 0-5 cm 1.0±0.4 5-15 cm 0.0 15-25 cm	NA
	Composted sewage sludge (15 t/ha) (0-5, 5-15, 15-25 cm)	88±9 28±4 0-5 cm 45±8 5-15 cm 15±2 15-25 cm	NA
	Composted sewage sludge (30 t/ha)	546±46 36±5 0-5 cm 330±22 5-15 cm 180±28 15-25 cm	NA
(Klemmensen et al., 2024)	Sewage sludge-amended soils (0-20 cm)	Total range 2392-48 791 Mean 12 896±923	Estimated: 0.17-8.51
(Schell et al., 2022)	w/o sewage sludge start/end of 1 year (0-5, 5-10. 10-15 cm)	Mean: 57/99 Total range: 31-120	NA
	historical sewage sludge application, 5 years ago (0-5, 5-10. 10-15 cm)	Mean: 330/204 Total range: 226-412/177-235	NA
	recent sewage sludge application (0-5, 5-10. 10-15 cm)	Mean: 215/211 Total range: 183-231/138-288	NA

Table S1 (continued). Size, shape and plastic polymer type distribution.

Size, shape and plastic polymer type distribution					
	Sample	**Size (%)**	**Shape (%)**	**Polymer type (%)**	**Method specifics**
(Corradini et al., 2019)	1-5 times applications 40 tons/ha per application (0-25 cm)	Median: 0.97 mm length, 20 µm diameter Most <50 µm	Fibres: 97%	NA	Density separation: NaCl & $ZnCl_2$ (1.55 g cm^{-3}) Detection: Microscope
(van den Berg et al., 2020)	w/o sewage sludge (0-10, 10-30 cm)	ca. 60 % 150-500 µm	Fragments*: 92 Fibres*: 2 Films*: 6	PP: 60 PVC: 40	Density separation: water, NaI (>1.7 g cm^{-3}) Size: 50 µm – 1 mm Detection: Microscope
	1-8 applications 20-22 tons/ha per application (0-10, 10-30 cm)		Fragments*: 82 Fibres*: 8 Films*: 10		
(Ljung et al., 2018)	w/o sewage sludge:	NA	NA	polyester : 40 PE: 36 PP: 15 PS: 1-2 PA	Density separation: $ZnCl_2$ Organic matter removal: H_2O_2, enzymes Size: 10-500 µm Detection: µ-FT-IR
	1 application (1 t/ha/yr)			PP: 55 PE: 10 PS: 7 polyester: 6 Alkyd: 5 PA: 3 other: 12	
	1 application (3 t/ha/yr)			polyester: 93 PU: 3 PP: 2 PE: 1 other: 0.4	

*estimated from Figures

Table S1 (continued). Size, shape and plastic polymer type distribution.

	Sample	Size (%)	Shape (%)	Polymer type (%)	Method specifics
(Zhang et al., 2020)	w/o sewage sludge (0-5, 5-15, 15-25 cm)	0.5-5.0 mm: 50 0.2-0.5 mm: 50	Flakes: 29 Fibres: 71	PE: 18 PP: 59 PET: 18	Density separation: NaCl, $ZnCl_2$ (saturated) Organic matter removal: H_2O_2 Size: 100-5000 µm Detection: stereomicroscope, random subsample µ–FT-IR
	Composted sewage sludge (15 t/ha) (0-5, 5-15, 15-25 cm)	0.5-5.0 mm: 83-94 0.2-0.5 mm: 6-17	Films: 50 Fibres: 31 Flakes: 19		
	Composted sewage sludge (30 t/ha)	0.5-5.0 mm: 84-93 0.2-0.5 mm: 7-16	Films: 2 Fibres: 13 Flakes: 86		
(Klemmensen et al., 2024)	Sewage sludge-amended soils (0-20 cm)	10-75 µm: 59±2 75-150 µm*: 30 150-500 µm*: 8-15	NA	polyester: 39±9 acrylic: 20±2 PU*: 15 PP*: 10 PS*: 5 PE*: 5 PA*: 4	Density separation: $ZnCl_2$ Organic matter removal: H_2O_2, SDS, enzymes Size: 10-500 µm Detection: µ–FT-IR
(Schell et al., 2022)	w/o sewage sludge start/end of 1 year (0-5, 5-10. 10-15 cm) historical sewage sludge application, 5 years ago start/end of 1 year (0-5, 5-10. 10-15 cm)	Fragments*: 90 Films*: 10 Fragments*: 60 Fibres*: 30 Beads*: 10	Fibres: 44-91 Fragments: 4-44 Most fibres >1000 µm in size	polyester: 22-53 acrylic: 22-37 PE*: 3-10 PP*: 5-10 Viscose*: 2-5 PA*: 2-7	Density separation: water (2x), NaI (>1.75 g cm^{-3}) Organic matter removal: H_2O_2 Size: 50-500 µm Detection: stereomicroscope, MPs > 300 µm with ATR-FTIR, 50-300 µm µ–FT-IR
	recent sewage sludge application (0-5, 5-10. 10-15 cm)	Fragments*: 80 Fibres*: 10 Films*: 5 Granules*: 5			

*estimated from Figures

Table S2: Conversion of MP particles to mass for MPs detected in the plough layer of sewage sludge-amended field soils (**Paper I**, all plastic polymer types) based on detected particle sizes and polymer type-specific density (Simon et al., 2018).

	Estimated mass concentration (mg kg^{-1})	Estimated concentration (% DW m/m)
Average±Standard deviation	721±137	0.07±0.01

Table S3: Shape classification and aspect ratio of different size fractions of MPs detected in sewage sludge-amended field soils (**Paper I**). Minimum and maximum size thresholds in this study were 10-500 µm based on sieving and filtration steps.

	Fraction of total (%)							
	All depths 0-40 cm		0-20 cm		20-30 cm		30-40 cm	
Size fraction	Fragment	Fibre	Fragment	Fibre	Fragment	Fibre	Fragment	Fibre
<50	96%	4%	95%	5%	98%	2%	5%	95%
<100	83%	17%	84%	16%	82%	18%	83%	17%
<150	50%	50%	52%	48%	46%	54%	52%	48%
<200	27%	73%	28%	73%	25%	75%	31%	69%
<300	22%	78%	24%	76%	20%	80%	20%	80%
<400	14%	86%	18%	82%	13%	88%	9%	91%
<500	12%	88%	14%	86%	12%	88%	7%	93%
Total	75%	25%	72%	28%	77%	23%	77%	23%
	Aspect ratio (average ± standard deviation)							
Size fraction	All depths 0-40 cm		0-20 cm		20-30 cm		30-40 cm	
<50	1.9±0.5		1.9±0.5		1.8±0.5		2.0±0.5	
<100	2.3±0.9		2.3±0.9		2.3±0.9		2.3±0.9	
<150	3.5±1.8		3.4±1.6		3.6±1.9		3.6±2.3	
<200	5.2±2.9		5.3±3.0		5.2±2.9		4.8±2.7	
<300	6.1±3.4		5.9±3.3		6.3±3.6		6.3±3.5	
<400	8.1±4.5		7.9±4.8		8.1±4.2		8.3±4.7	
<500	10.5±6.8		9.4±5.7		12.0±8.8		11.1±5.7	
Total	2.9±2.5		3.1±2.6		2.8±2.5		2.9±2.4	

Table S4: Conversion of MP fibre lengths and numbers to mass concentrations for the respective depth layers. The relative comparison refers to the ratio of estimated mass concentration to measured mass concentration ($C_{estimated}/C_{measured}$). The *Average* refers to the average fibre diameter including the standard deviation (Stdev) measured for MP fibres (38±10 µm, n = 142).

Absolute comparison		0-2 cm	3-6 cm	6-15 cm	15-26 cm
Measured	Mass concentration (mg kg^{-1})	6414	149	75	25
Estimated (mg kg^{-1})	Average	3646	169	68	17
	Average+10%	2954	137	55	13
	Average-10%	4412	204	83	20
	Average-Stdev	1980	92	37	9
	Average+Stdev	5818	269	109	27
Relative comparison		0-2 cm	3-6 cm	6-15 cm	15-26 cm
$C_{estimated}/C_{measured}$	Average	0.57	1.13	0.91	0.68
	Average+10%	0.46	0.92	0.73	0.55
	Average-10%	0.69	1.37	1.10	0.82
	Average-Stdev	0.31	0.61	0.49	0.37
	Average+Stdev	0.91	1.80	1.44	1.08

Additional references used in Appendices:

Naturvårdsverket, 2022. Utsläpp till vatten och slamproduktion 2020. Kommunala avloppsreningsverk, massa- och pappersindustri samt viss övrig industri. Statistiska meddelanden MI 22 (35).

Naturvårdsverket, 2018. Utsläpp till vatten och slamproduktion 2018. Kommunala reningsverk, skogsindustri samt viss övrig industri. Statistiska meddelanden MI 22 (SM 2001).

Naturvårdsverket, 2016. Utsläpp till vatten och slamproduktion 2016. Kommunala reningsverk, skogsindustri samt viss övrig industri. Statistiska meddelanden MI 22 (SM 1801).

Naturvårdsverket, 2014. Utsläpp till vatten och slamproduktion 2014. Kommunala reningsverk, skogsindustri samt viss övrig industri. Statistiska meddelanden MI 22 (SM 1601).

Naturvårdsverket, 2012. Utsläpp till vatten och slamproduktion 2012. Kommunala reningsverk, skogsindustri samt viss övrig industri. Statistiska meddelanden MI 22 (SM 1401).

Naturvårdsverket, 2010. Utsläpp till vatten och slamproduktion 2010. Kommunala reningsverk, skogsindustri samt viss övrig industri. Statistiska meddelanden MI 22 (SM 1201).

Naturvårdsverket, 2008. Utsläpp till vatten och slamproduktion 2008. Kommunala reningsverk, skogsindustri samt viss övrig industri, korrigerad version 2012-06-15. Statistiska meddelanden MI 22 (SM 1001).

Naturvårdsverket, 2006. Utsläpp till vatten och slamproduktion 2006. Kommunala reningsverk, skogsindustri samt viss övrig industri. Statistiska meddelanden MI 22 (SM 0801).

Naturvårdsverket, 2004. Utsläpp till vatten och slamproduktion 2004. Kommunala reningsverk, skogsindustri samt viss övrig industri, korrigerad 2007-11-20. Statistiska meddelanden MI 22 (SM 0701).

Naturvårdsverket, 2002. Utsläpp till vatten och slamproduktion 2002. Kommunala reningsverk, skogsindustri samt viss övrig industri. Statistiska meddelanden MI 22 (SM 0401).

Naturvårdsverket, 2000. Utsläpp till vatten och slamproduktion 2000. Kommunala reningsverk, skogsindustri samt viss övrig industri. Statistiska meddelanden MI 22 (SM 0101).

I

Environmental Pollution 356 (2024) 124343

Contents lists available at ScienceDirect

Environmental Pollution

journal homepage: www.elsevier.com/locate/envpol

Vertical distribution of microplastics in an agricultural soil after long-term treatment with sewage sludge and mineral fertiliser☆

Wiebke Mareile Heinze [a], Zacharias Steinmetz [b], Nanna Dyg Rathje Klemmensen [c], Jes Vollertsen [c], Geert Cornelis [a,*]

[a] Swedish University of Agricultural Sciences, Department of Soil and Environment, Box 7014, 75007, Uppsala, Sweden
[b] RPTU Kaiserslautern-Landau, iES Landau, Institute for Environmental Sciences, Environmental and Soil Chemistry Lab, Fortstraße 7, 76829, Landau, Germany
[c] Aalborg University, Department of the Built Environment, Division of Civil and Environmental Engineering, Thomas Manns Vej 23, 9220, Aalborg, Denmark

ARTICLE INFO

Keywords:
Spatial distribution
Field scale
Transport
μ-FT-IR
Py-GC/MS
Metals
Organic carbon

ABSTRACT

Sewage sludge applications release contaminants to agricultural soils, such as potentially toxic metals and microplastics (MPs). However, factors determining the subsequent mobility of MPs in long-term field conditions are poorly understood. This study aimed to understand the vertical distribution of MPs in soils amended with sewage sludge in comparison to conventional mineral fertiliser for 24 years. The depth-dependent MP mass and number concentrations, plastic types, sizes and shapes were compared with the distribution of organic carbon and metals to provide insights into potentially transport-limiting factors. Polyethylene, polypropylene and polystyrene mass concentrations were screened down to 90 cm depth via pyrolysis-gas chromatography/mass spectrometry. MP number concentrations, additional plastic types, sizes, and shapes were analysed down to 40 cm depth using micro-Fourier transform-infrared imaging. Across all depths, MP numbers were twice and mass concentrations 8 times higher when sewage sludge was applied, with a higher share of textile-related plastics, more fibres and on average larger particles than in soil receiving mineral fertiliser. Transport of MPs beyond the plough layer (0–20 cm) is often assumed negligible, but substantial MP numbers (42 %) and mass (52 %) were detected down to 70 cm in sewage sludge-amended soils. The initial mobilization of MPs was shape- and size-dependent, because the fractions of fragmental-shaped and relatively small MPs increased directly below the plough layer, but not at greater depths. The sharp decline of total MP concentrations between 20 and 40 cm depth resembled that of metals and organic matter suggesting similar transport limitations. We hypothesize that the effect of soil management, such as ploughing, on soil compactness and subsequent transport by bioturbation and via macropores drives vertical MP distribution over long time scales. Risk assessment in soils should therefore account for considerable MP displacement to avoid underestimating soil exposure.

1. Introduction

Organic residues such as sewage sludge are typically applied to agricultural land to recycle nutrients. Other than a more efficient use of resources, sewage sludge also increases the carbon content of soils in contrast to conventional mineral fertilisers. However, sewage sludge may also release a range of potentially toxic metals (Chu and He, 2021; van Straalen et al., 1989) and, as recently highlighted, microplastics (MPs, ≤5 mm) to soils (Hurley and Nizzetto, 2018). Frequently occurring plastic types are polyesters (including polyethylene terephthalate, PET) and polyamides (PA), both commonly used in textiles, but also polyethylene (PE), polypropylene (PP) and polystyrene (PS) (Klemmensen et al., 2024). Most of these polymer types are resistant to biodegradation (Chamas et al., 2020) and may cause adverse effects in

Abbreviations: μ-FT-IR, micro-Fourier transform-infrared; DW, dry weight; K_d, partitioning coefficient; MP, microplastic; MPs, microplastics; Py-GC/MS, Pyrolysis-Gas Chromatography/Mass Spectrometry; PA, polyamides; PE, polyethylene; PET, polyethylene terephthalate; PP, polypropylene; PS, polystyrene; PTFE, polytetrafluoroethylene; WWTP, wastewater treatment plant.

☆ This paper has been recommended for acceptance by Eddy Y. Zeng.

* Corresponding author.
E-mail addresses: wiebkemareile.heinze@slu.se (W.M. Heinze), steinmetz-z@uni-landau.de (Z. Steinmetz), ndrk@build.aau.dk (N.D.R. Klemmensen), jesvollertsen@build.aau.dk (J. Vollertsen), geert.cornelis@slu.se (G. Cornelis).

https://doi.org/10.1016/j.envpol.2024.124343
Received 22 March 2024; Received in revised form 5 June 2024; Accepted 6 June 2024
Available online 7 June 2024

the long term either emerging from the plastics themselves or by releasing potentially toxic additives (Bucci et al., 2020; de Souza Machado et al., 2018). Transport processes may alter the distribution of both, MPs and metals, in the soil profile and thereby determine the local exposure concentrations of crops or terrestrial biota.

While it has been established that agricultural soils become enriched in MPs following sewage sludge applications (Corradini et al., 2019; Crossman et al., 2020; Ljung et al., 2018; Schell et al., 2022; Tagg et al., 2022; van den Berg et al., 2020; Zhang et al., 2020), there are still uncertainties about the subsequent mobility and further vertical distribution of MPs in agricultural soils, especially under long-term field conditions. Most of the existing field investigations on sewage sludge-amended soils have focused on the uppermost few centimetres of the soil assuming a limited mobility of MPs beyond the plough layer (Crossman et al., 2020; Ljung et al., 2018; Schell et al., 2022; Zhang et al., 2020). MPs may, however, be incorporated deeper into the soil by burrowing soil biota (Heinze et al., 2021; Huerta Lwanga et al., 2017; Rillig et al., 2017) and by transport with penetrating rainfall or irrigation water (Ren et al., 2021; X. Zhang et al., 2022; Zhao et al., 2022) or because of soil management, such as ploughing (Weber et al., 2022). MP properties, such as the polymer type (Gao et al., 2021; Koutnik et al., 2022), size (Dong et al., 2018; Qi et al., 2022; Ranjan et al., 2023) and shape (Han et al., 2022; X. Zhang et al., 2022), are thought to determine the magnitude of these transport processes and whether MPs are retained in the uppermost layers of the soils. Most of these aforementioned MP studies were laboratory-based and focused on isolated transport processes and thus, the obtained transport depths are not readily transferable to soils in the field. Factors facilitating or limiting MP transport in agricultural soils under long-term field conditions are still evasive. Transport of other soil constituents, such as metals and organic matter, is comparably better understood. While some metals can be transported in dissolved form, other metals are predominantly transported with preferential flow while bound to organic matter or mineral colloids (Moreira et al., 2022; Zheljazkov and Warman, 2004). Hence, comparing the distribution pattern of different metals or organic matter with that of MPs could facilitate the identification of factors that similarly control MP transport.

The overarching aim of this study was to understand the long-term vertical distribution of MPs in soil amended with sewage sludge in comparison to soil receiving conventional mineral fertiliser. MP analyses are often limited to either particle-based or mass-based methods, though both metrics are necessary for a comprehensive exposure assessment (Thomas et al., 2020; Thornton Hampton et al., 2022). We therefore measured MP mass and numbers directly by applying both a thermo-analytical and a spectroscopic method. We sampled soils from long-term field trials with these two fertiliser regimes and examined the mass-based distribution of MPs along the soil profile to 90 cm depth. For improving our understanding of potentially transport-limiting factors under long-term field conditions, we subsequently examined MP numbers and particle characteristics in the most enriched depth layers. Lastly, we compared the depth-distribution of MPs with that of organic matter and potentially toxic metals commonly associated with sewage sludge applications to provide insights into potentially soil-specific factors of transport dynamics. Our hypothesis was that MPs are redistributed in the soil profile by anthropogenic and natural transport processes, with transport distances decreasing with increasing MP size and elongated shapes.

2. Materials & methods

2.1. Field trials and soil properties

Soils were sampled at the Lanna long-term field trials, Skara, Sweden (N58.344, E13.104), in January 2021. Soils with two common agricultural fertilisation practices were compared: field plots with bi-annual application of municipal sewage sludge at rates of 8 tons dry weight (DW) ha^{-1} since 1996 (4 tons DW ha^{-1} $year^{-1}$, total 96 tons ha^{-1}), and annual application of conventional mineral fertiliser during the same period (80 kg ha^{-1} N as calcium nitrate, 40 kg ha^{-1} P, 30 kg ha^{-1} K). Each treatment comprised four replicate field plots with areas of 112 m^2 (8 × 14 m) except one field plot of the mineral fertiliser treatment with a smaller area (6 × 14 m). The plots had a minimum distance of 8 m relative to each other (see Supplementary Material S1 for a field map). Based on the maximum distance (120 m) between plots, the potential background contamination from diffuse microplastic sources may be assumed similar across plots. The difference in MP concentrations between the treatments can therefore be explained by differences in fertilisation inputs. Aboveground plant material was harvested each year, after which plots were fertilised and mouldboard-ploughed to a depth of ca. 20 cm. The dewatered and digested sewage sludge was sourced from nearby municipal wastewater treatment plants (WWTPs), with suppliers changing between years. In the autumn of 2020, the applied sewage sludge had a dry matter content of 18 % and an organic matter content of 62 % (loss on ignition). The dominant cropping system was spring-sowed oats and barley.

The soil at the site was classified as a *Eutric Cambisol* according to the World Reference Base (IUSS Working Group, 2015) with clay, silt and sand contents of 45 %, 47 % and 8 % in the plough layer (0–20 cm), and 61 %, 36 % and 3 % in deeper soil layers (20–40 cm) respectively (Kätterer et al., 2014), making it susceptible to compaction under management (Jarvis et al., 1991). The bulk density in the plough layer was lower for the sewage sludge-amended soil compared to the mineral fertiliser treated soil (1.30 g cm^{-3} versus 1.36 g cm^{-3}). For the soil below the plough layer, a bulk density of 1.5 g cm^{-3} was assumed for both treatments according to personal communication with the field station. The sewage sludge-amended soil was relatively acidic (pH 4.9) in comparison to the conventionally fertilised soil (pH 6.7) (Börjesson et al., 2014), and had a higher total organic carbon (TOC) content (2.28 ± 0.07 % versus 1.9 ± 0.1 %). For soils at this site, Jarvis et al. (1991) previously remarked the well-structured subsoil (0.3–0.7 m) dominated by angular aggregates, and the presence of biopores down to 1.0 m depth in their soil profile description. In 2021, an earthworm abundance of 150 individuals m^{-2} (2.8 g DW m^{-2}) was measured in the sewage sludge-amended soil, and 70 individuals m^{-2} (2.5 g DW m^{-2}) for the mineral fertiliser treatment (Viketoft et al., 2021).

2.2. Sampling and sample homogenization

Soil cores of 90 cm depth (diameter 2.5 cm) were used for determining the vertical distribution of MPs, selected metals, TOC and total nitrogen (N). In each field plot, 6–8 soil cores were taken at randomly selected positions. The cores were segmented into sections of 10 cm and mixed on-site, yielding one composite sample per depth segment for each replicate field plot (306–647 g DW, Supplementary Material S1). Samples from the uppermost 0–20 cm, corresponding to the plough layer, were pooled together given the probable homogenization of this layer ($n = 8$ per field, $n = 32$ per treatment). Samples were stored and air-dried in glass jars covered with aluminium foil. Then, approximately 200–300 g of the dried sample was homogenized with a mortar and pestle, and sieved to 2 mm.

2.3. Metal, organic carbon and total nitrogen analysis

Potentially toxic metals that are commonly associated with sewage sludge, i.e. cadmium (Cd), chromium (Cr), copper (Cu), nickel (Ni), lead (Pb) and zinc (Zn), were analysed using inductively coupled plasma sector field mass spectrometry following an acid extraction with *aqua regia* in a closed-vessel microwave system. For details on the procedure and quality control, see Supplementary Materials S2. TOC and total N were determined on 1.0 g subsamples using an elemental analyser (Leco, Tru-Mac). The mobility of metals in soils is often expressed by partitioning coefficients (K_d-values). We estimated the K_d value for Cu and Cd

from the prevalent soil conditions (pH, TOC) for the sewage sludge-amended soil based on empiric correlation equations from the literature (Sauvé et al., 2000) to compare the potential mobility of these metals.

2.4. Microplastic analysis

We used a thermo-analytical method to screen the vertical mass distribution of the most frequent MP types (PE, PP, PS) to a depth of 90 cm, followed by a more in-depth analysis using micro-Fourier Transform-Infrared (μ-FT-IR) imaging on selected samples to capture a wider range of plastic types and to assess the effect of MP size and shape on transport dynamics. The combination of the two methods further allowed us to compare the relative contribution of different plastics in terms of particle mass and numbers.

2.4.1. Py-GC/MS

The mass-based distribution of PE, PP, and PS was measured to a depth of 90 cm using Py-GC/MS (n = 32 per treatment). The MP extraction and analysis procedure was largely based on Steinmetz et al. (2022, 2020). Briefly, 50 g soil underwent density separation using a saturated sodium chloride solution (1.19 g cm^{-3}, 250 mL) to selectively extract the target plastics (0.86–1.05 g cm^{-3}) reducing possible interferences. After shaking (4 h) and at least 16 h of sedimentation, the settled material was released and the supernatant was collected with cellulose filters (pore size 4–12 μm). The filters were transferred to culture tubes and plastics extracted with 1,2,4-trichlorobenzene and *p*-xylene (1:1, 7.76 mL) at 180 °C for 1 h with intermittent vortexing (0, 20, 40 min and after cooling). Then, 200 μL of the supernatant was spiked with deuterated polystyrene as internal standard (PS-d5, 4 μL of 5 mg L^{-1}). In contrast to Steinmetz et al. (2022), MP detection limits were decreased by analysing larger sample volumes (6 μL instead of 2 μL) by sequentially transferring 3 μL with intermittent air-drying (≥24 h) onto sample carriers. The resulting methodological limits of detection were 0.51 mg kg^{-1} for PE, 0.13 mg kg^{-1} for PP, and 0.02 mg kg^{-1} for PS (Supplementary Material S3).

Samples were pyrolyzed in a Pyroprobe 6150 filament pyrolyzer (CDS Analytical) and measured with a Trace GC Ultra (DSQII mass spectrometer, Thermo Fisher Scientific). Pyrolysis steps included an initial heating to 300 °C (3 min), followed by a flash pyrolysis at 700 °C (15 s, 10 K ms^{-1}) and a vent time of 3 min at 300 °C. The peaks used for quantification of PE, PP, and PS were 1,21-docosadiene, 2,4-dimethyl-1-heptene and styrene respectively. We used the open-source software OpenChrom for data processing (Wenig and Odermatt, 2010), with an automatic peak integration based on retention indices followed by a manual control (Steinmetz et al., 2022). All Py-GC/MS based results were corrected for negative controls and corrected for the daily drift using bracketing standards. For details on the general contamination control, setup and quality control for Py-GC/MS following reporting guidelines by Cowger et al. (2020) see Supplementary Material S3.

2.4.2. FPA-μ-FT-IR imaging

Focal plane array (FPA) μ-FT-IR imaging was used on separate subsamples for capturing particle sizes and shapes, as well as covering a wider range of plastic types. We chose to focus on the particle fraction <500 μm because these MPs are expected to be more mobile than larger MPs in soils. Soil samples (100 g) were selected based on MP concentrations from Py-GC/MS analyses, i.e. only depth segments between 0 and 40 cm (n = 12 per treatment). The sample preparations followed developed methods (Hurley et al., 2018; Liu et al., 2019; Löder et al., 2017), with deviations in the order of steps and reagents used. A higher density solution of zinc chloride (≥1.6 g cm^{-3}, 500 mL) than during the previous screening with Py-GC/MS was used to extract a wider range of MP types. Density separations were repeated three times for each sample, and the supernatant was filtered through a stainless-steel mesh (mesh width 10 μm). Organic material was removed by a sequence of hydrogen peroxide (H_2O_2, 10 %), sodium dodecyl-sulphate, protease (*Bacillus licheniformis*) and cellulase (*Aspergillus* sp) treatments. Particles ≥500 μm were removed with a test sieve, and the remaining sample was treated with a final H_2O_2 step and density separation. The supernatant was collected, rinsed, dried and re-suspended in 5.00 mL ethanol. For the field samples, 500–600 μL (10–12 % of total sample volume) were measured on zinc selenide windows with FPA-μ-FT-IR (Cary 670, Agilent Technologies, 128 × 128 FPA, wavelength range 850–3750 cm^{-1}, pixel resolution 5.5 μm). Procedural blanks revealed a potential contamination of 16 ± 15 particles per sample (n = 3), corresponding to 160 ± 150 particles kg^{-1}, and therefore a potential maximum error of 5.2% for the lowest detected concentration in field soils (3100 particles kg^{-1}).

After automatic processing in the freeware siMPle (Primpke et al., 2017, 2020a), the spectra of all detected MP particles were manually checked (n = 10 087). Approximately 15 % of particles initially classified as MPs were rejected in this process due to potential interferences of other organic materials, the lack of unique peaks used for identification within the recorded IR range or a combination thereof. Plastic types with a relative frequency of less than 5 % in any sample were jointly classified as "other". The setup was limited to MP sizes of 10–500 μm, based on filter and sieve mesh width. Large but thin fibres may still bypass the sieve, so detected particles larger than 500 μm were excluded from the analysis (1.7 % of all detected MPs). Particles were distinguished into fragments and fibres based on their aspect ratio, i.e. the ratio of the largest to the smallest Feret diameter. Particles with an aspect ratio ≥3.0 were classified as fibres (Cole, 2016; Zhang et al., 2022), all other particles were classified as fragments. For more details on protocols, quality control and a comprehensive list of detected plastic types see Supplementary Material S4.

2.4.3. Recovery tests for MP extraction

Recoveries of 48–53% for PS spheres (52 μm and 106 μm) were found previously for the μ-FT-IR method (Klemmensen et al., 2024). Recovery tests for Py-GC/MS analysis were done by spiking the target plastics (PE, PP, PS) at three different concentrations (5, 20, 40 mg kg^{-1}) into two soils (50 g): a fine-textured reference soil (RefeSol06 A) and a composite sample of the deeper soil layers of the mineral fertiliser treatment (60–90 cm). Average recoveries ranged from 30 to 70% at the lowest, and 50–100% at the highest spike concentration (Supplementary Table S6). Improved recoveries at higher spike concentrations may explain the lower recovery observed here in comparison to other studies with substantially higher spike concentrations (20 g kg^{-1} to 50 g kg^{-1}) (Okoffo et al., 2020). There was only little to weak evidence that recoveries were different between the soils (PE: $p = 0.17$, PP: $p = 0.07$, PS: $p = 0.9$). However, recoveries in the reference soil were more variable, which might indicate background contamination as reference soils are typically not processed with measures to prevent plastic contamination. While our recoveries were lower than expected, we still deemed the method suitable for screening purposes of PE, PP and PS.

2.5. Data processing and statistical analysis

Further data processing of the Py-GC/MS and μ-FT-IR data was done in R (version 4.3.0), see Supplementary Material S5 for a comprehensive overview of R packages used. For testing statistical significance, we used two-tailed t-tests ($\alpha = 0.05$) and reported the p-value according to recommendations (Wasserstein et al., 2019), unless p-values were below 0.001. For a more comprehensive assessment of MP presence and mobility in the soil, we compared the mass of PE, PP and PS as directly measured by Py-GC/MS with a mass estimate based on particle metrics obtained via μ-FT-IR imaging. We illustratively applied the conversion method incorporated into the siMPle software (Liu et al., 2019; Simon et al., 2018). In brief, the particle type-specific density is combined with size metrics, with the ratio of minor to major Feret diameter used to estimate particle thickness, assuming ellipsoid shapes for all but fibrous

particles.

3. Results

3.1. Microplastic mass concentrations

Overall, the application of sewage sludge was associated with an enrichment of PE, PP, and PS in terms of mass concentration obtained by Py-GC/MS ($p = 0.003$) (Fig. 1), especially in the plough layer where concentrations ranged from 0.97 to 2.4 mg kg^{-1} (mean 1.47 ± 0.66 mg kg^{-1}). Concentrations in soils receiving mineral fertiliser overall were 8 times lower and even 25 times lower in the plough layer located at 0–20 cm depth, i.e. 0.00–0.09 mg kg^{-1} (mean 0.06 ± 0.04 mg kg^{-1}). To a large degree, this trend was caused by substantially higher PE concentrations in the sewage sludge treatment ($p = 0.001$).

MP mass concentrations generally decreased with depth, although the highest average mass concentration was found at 20–30 cm depth in sewage sludge-amended soils, largely due to high PS concentrations in one replicate field plot (Fig. 1). While MPs were detectable to depths of 60–70 cm in discrete instances, 48 % of the MP mass was detected in the plough layer, 37 % at 20–30 cm and 11 % at 30–40 cm for the sewage sludge-amended soil. Hence, only these depth segments were selected for in-depth analysis using μ-FT-IR imaging.

3.2. Microplastic number concentrations

MP number concentrations were measured via μ-FT-IR imaging for the depth segments 0–20, 20–30 and 30–40 cm as displayed in Fig. 2. Sewage sludge applications resulted in higher average particle numbers than mineral fertiliser applications (plough layer: averages 53 700 ± 5900 particles kg^{-1} versus 30 000 ± 37 000 particles kg^{-1}; $p = 0.002$). The unexpectedly high average concentrations in soils receiving mineral fertiliser were mostly due to one sample in which MP numbers were 5–12 times higher than in the other three replicate field plots (Fig. 2).

MP number concentrations were similar in the plough layer and in 20–30 cm depth sections for the sewage sludge-amended soils ($p = 0.4$), but then decreased to half at 30–40 cm depth ($p < 0.001$). Accordingly, 58 % of the total MP numbers in the sewage sludge treatment were found in the plough layer, 27 % were located in 20–30 cm and 14 % in 30–40 cm depth. Soils receiving mineral fertiliser showed a comparable distribution in terms of particle numbers with 57 %, 32 %, 11 % for 0–20 cm, 20–30 cm and 30–40 cm, when excluding the aforementioned highest value.

3.3. Depth-dependent distribution of microplastic types, shapes and sizes

The most abundant plastics found in the sewage sludge-amended soils are commonly associated with textiles (polyester, acrylic, polyamides; 63 %). While polyester was an important plastic type in both field treatments, PP, PS, and epoxy/phenoxy resins accounted for a larger proportion of all MPs when soils received mineral fertiliser (Fig. 2). There was no consistent depth-dependent pattern that would indicate preferential transport of a particular plastic type.

The majority of detected MPs were classified as fragments, but the proportion of fibres in sewage sludge-amended soil was higher (Table 1) and decreased from the plough layer to the underlying layers shown by decreasing aspect ratios ($p < 0.001$ for 20–30 cm). However, there was no evidence that shape differed at even greater depths for either treatments (sewage sludge: $p = 0.5$, mineral fertiliser $p = 0.9$).

Most of the MPs within the top 40 cm of the soil were <100 μm in size, i.e. 84 % of all particles in the mineral fertiliser, and 73 % for the sewage sludge treatment. Mean and median particle sizes were overall smaller in soils treated with mineral fertiliser than in soils treated with sewage sludge ($p < 0.001$, Table 1). MP sizes further decreased from the plough layer down to 20–30 cm for soils treated with mineral fertiliser ($p = 0.034$) and sewage sludge ($p < 0.001$). However, the size distributions within either treatment were very similar at greater depth (sewage sludge: $p = 0.8$; mineral fertiliser: $p = 0.9$). Interestingly, the size distribution showed plastic-type and treatment-dependent trends (Fig. 3). Polyester, PE and PP particles tended to be much larger than the other plastic types, but only in the sewage treated soils. PS and PA, in contrast, were much smaller with narrower size distributions.

3.4. Comparison of mass-based and number-based concentrations

Based on mass measurements of the sewage sludge-amended soil (Py-GC/MS), PE dominated and PS was primarily present in 20–30 cm depth sections, whereas PP concentrations were negligible. μ-FT-IR imaging conversely suggested that PP was as or even more important than PE in terms of particle numbers. Comparisons between mass-based and number-based methods are challenging but can be facilitated by particle-to-mass conversions based on size metrics obtained via μ-FT-IR.

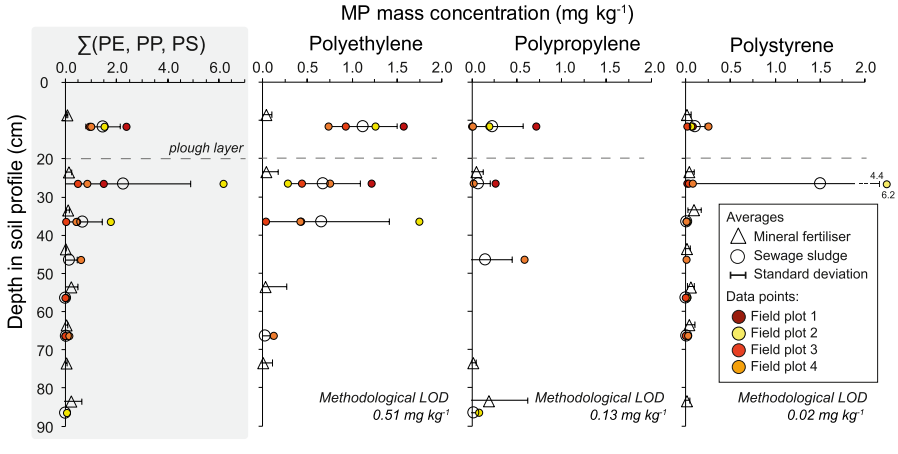

Fig. 1. Detected concentrations of polyethylene (PE), polypropylene (PP) and polystyrene (PS) according to sampling depth segments in sewage sludge and mineral fertiliser treatments in mass concentrations for Py-GC/MS (n = 4 for each treatment and depth).

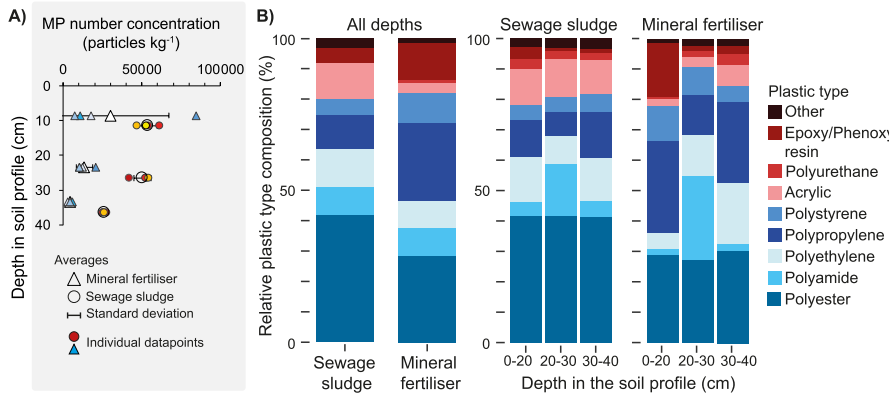

Fig. 2. MP number concentration (A) and plastic type composition (B) for sewage sludge-amended soil in comparison to soil receiving mineral fertiliser in 0–20, 20–30 and 30–40 cm depth in the soil profile.

Table 1
Treatment- and depth-dependent number based size and shape distribution of MPs in sewage sludge-amended soil and soil receiving mineral fertiliser.

	Depth (cm)	Size (μm)		Shape[a] (%)		Size classes (%) μm					
		Median	Mean	Fibre	Fragments	<50	50–100	100–200	200–300	300–400	400–500
Sewage sludge	0–20	66	101 ± 91	28.0	72.0	36	31	19.7	7.8	3.6	1.8
	20–30	54	84 ± 81	23.1	79.6	46	30	15.0	4.7	3.1	1.1
	30–40	56	85 ± 81	23.4	76.6	44	32	13.9	5.6	2.8	1.1
	All	**59**	**91 ± 86**	**25.2**	**74.8**	**42**	**31**	**16.7**	**6.1**	**3.3**	**1.4**
Mineral fertiliser	0–20	46	71 ± 71	13.5	86.5	55	28	10.9	4.3	1.2	1.0
	20–30	43	64 ± 65	14.2	85.8	62	24	9.1	3.1	1.6	0.5
	30–40	46	64 ± 60	14.0	86.0	57	28	10.8	2.7	0.9	0.5
	All	**45**	**68 ± 68**	**13.2**	**86.8**	**57**	**27**	**10.4**	**3.8**	**1.3**	**0.8**

[a] Classification based on aspect ratio (major to minor Feret diameter), <3 as fragment, >3 fibre.

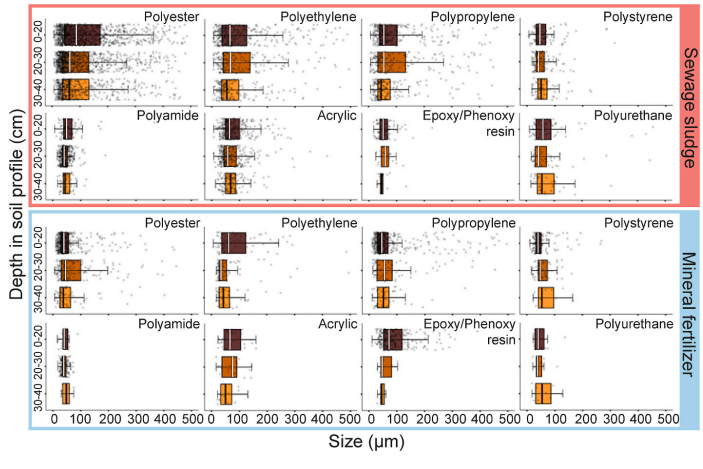

Fig. 3. Size distribution of the dominating plastic types (≥5% of all plastics in any one sample) according to depth segments (0–20, 20–30, 30–40 cm), for soils treated with sewage sludge and mineral fertiliser.

After particle-to-mass conversion, we found the relative importance of PE increased owing to on average larger particle sizes than PP (Fig. 3), whereas PS continued to play a minor role because small average particle sizes translated into small masses (Figs. 3 and 4). A lower size cut-off was used during sample preparing for the μ-FT-IR imaging method (500 μm) compared to that of the Py-GC/MS method (2 mm).

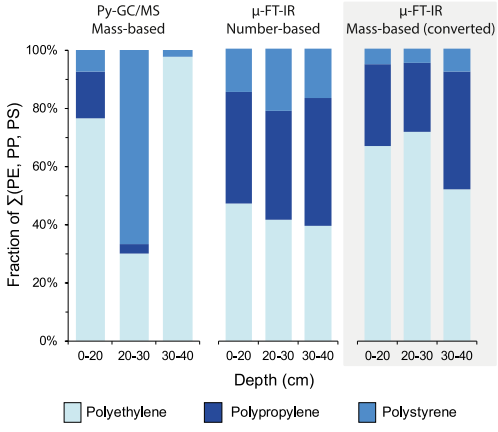

Fig. 4. Relative distribution of PE, PP and PS in sewage sludge-amended soil according to mass concentrations (mg kg^{-1}) measured using Py-GC-MS, number concentrations (particles kg^{-1}) measured using μ-FT-IR imaging and mass concentrations (mg kg^{-1}) estimated from μ-FT-IR-based size distributions by sampling depth.

Py-GC-MS was thus expected to yield higher mass concentrations than μ-FT-IR. However, mass concentrations for PE, PP, and PS estimated from particle-based size distributions generally exceeded the mass concentrations measured by Py-GC/MS, often by a factor of 2–4 (Supplementary Material S6).

3.5. Metal, organic carbon and nitrogen concentration and distribution

Unsurprisingly, sewage sludge applications increased the TOC, total N content and Cu ($p < 0.001$) and Zn ($p < 0.001$) concentrations in comparison to soils receiving mineral fertiliser, especially at 0–40 cm depth (Fig. 5). The concentrations of other metals commonly associated with sewage sludge, i.e. Cd, Cr and Ni were not noticeably affected by the different fertiliser regimes (Supplementary Material S2). The elevated Cd concentrations in the upper soil profile occurred similarly regardless of fertilisation practice ($p = 0.8$, Fig. 5).

For the sewage sludge amended soils, the concentrations of Cu, Cd, TOC, and total N concentrations were the highest between 0 and 30 cm depth, followed by a pronounced depth-dependent decline (Cu: $p < 0.001$, Cd: $p = 0.001$, TOC: $p = 0.001$, total N: $p < 0.001$). Notably, the vertical distribution of TOC, total N, Cu and Zn coincided with that of MPs (Fig. 1). K_d-values estimated based on pH and organic matter content were higher for Cu (920 L kg^{-1}) than for Cd (100 L kg^{-1}) in the sewage sludge-amended soil. Hence, a lower mobility is expected for Cu compared to Cd, mostly because of a stronger adsorption to organic matter at the prevailing soil conditions. Accordingly, the depth distribution of Cu coincided with that of TOC (Fig. 5), whereas Cd penetrated slightly deeper in the soil profile.

4. Discussion

4.1. Sewage sludge amendments caused enrichment of metals and microplastics in soil

Sewage sludge applications increased soil TOC and total N, but also led to an enrichment of potentially toxic metals and MPs when compared to conventional mineral fertiliser applications (Figs. 1, 2 and 5). Only Cu and Zn were elevated in response to sewage sludge applications (Fig. 5), but they remained below recommended maximum thresholds for Sweden (Naturvårdsverket, 2009). The total number concentrations of MPs were approximately twice and mass concentrations even 8 times higher when sewage sludge was used instead of mineral fertiliser. Although MPs found in soils treated with conventional fertiliser could originate from storage bags, we deem it more likely that they were transported from nearby field plots by ploughing, given the high MP concentrations in the sewage sludge-amended soils and the proximity between field plots (Figs. 1 and 2). Weber et al. (2022) recently attributed the spread of MPs from soils with a history of sewage sludge applications to ploughing activities with even larger transport distances of up to 40 m.

Both MP mass concentrations and number concentrations in our study were higher than previously reported for sewage sludge-amended soils. Field measurements of MP mass concentrations in soil are scarce (Steinmetz et al., 2022), and to our knowledge completely lacking for sewage sludge-amended soils. However, our measured concentrations (1.5 ± 0.6 mg kg^{-1}) exceed expected concentrations when combining previously reported MP mass concentrations for sewage sludge with the sludge application rate. For instance, based on PE concentrations in sewage sludge measured by Okoffo et al. (2020) (1.9 mg g^{-1} DW), we would expect only 0.07 mg kg^{-1} PE in our soil.

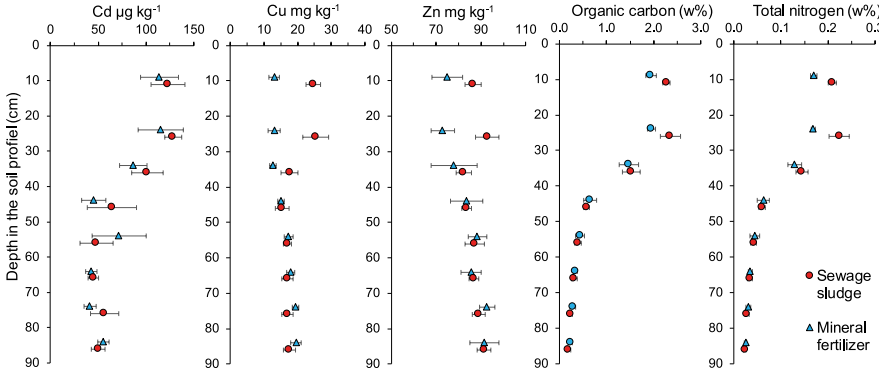

Fig. 5. Depth-dependent distribution of selected metals (cadmium, copper, and zinc), total organic carbon and total nitrogen in sewage sludge-amended soil in comparison to soil receiving mineral fertiliser.

Likewise, MP numbers were much higher than previously reported for sewage sludge-amended soils, ranging from 600 to 10 400 particles kg^{-1} (Corradini et al., 2019; Magnusson and Norén, 2014; Schell et al., 2022; van den Berg et al., 2020), and surpassed estimates based on MP numbers measured in sewage sludge and sludge application rates (Harley-Nyang et al., 2023). We infer that the lower size cut-off of our method (10 μm) partly explains the differences with other studies: 42–57 % of all MPs were below 50 μm in our study (Table 1). In comparison, Van den Berg et al. (2020) found ten times lower concentrations despite twice the amount of sewage sludge applied, but only reported numbers for particles >50 μm. Indeed, MP concentrations in our soils are within the expected range when estimating MP numbers based on recent sewage sludge measurements from Europe with a comparable lower size cut-off and quantification method (Chand et al., 2021; Horton et al., 2021). In addition, previous work on MP loads in sewage sludge has illustrated a high variability between sludge sourced from different WWTPs ranging between 644 and 5.8 × 10^6 particles kg^{-1} DW (Harley-Nyang et al., 2023). Such variability has been related to methodological differences between studies, but also different wastewater treatment steps and seasonal fluctuations of plastic inputs (Hooge et al., 2023; Li et al., 2018; Lofty et al., 2022). For instance, digested sludge, as was applied in our study, can contain higher MP numbers (Chand et al., 2021; Lares et al., 2018). Location-specific MPs loads might, for instance, explain that fragmental shaped MPs dominated in our study (Table 1), although sewage sludge is usually more associated with MP fibres (Corradini et al., 2019; Mahon et al., 2017).

4.2. Comparison of detected mass and number concentrations

In this study, we combined thermo-analytical and spectroscopic methods to directly measure MP mass and particle numbers for a more comprehensive assessment of MP concentrations in the soil. Unsurprisingly, the relative importance of the plastic types analysed with both methods (PE, PP, PS) depended on the presented metric because large quantities of small particles do not necessarily translate to large masses (Fig. 4). Conversion methods are commonly applied to translate particle sizes to particle masses for exposure assessments (Klemmensen et al., 2024). In terms of plastic mass concentrations, both analytical methods confirmed the importance of the on average larger sized PE MPs, and the minor role of the on average smaller PS MPs (Fig. 4). Discrepancies remained between the two methods concerning the role of PP, even after particle-to-mass conversion, likely related to analytical challenges of both methods: for Py-GC/MS with the quantification limit and μ-FT-IR imaging with the correct identification of PP. Weathering of PP can result in reduced signals in Py-GC/MS (Toapanta et al., 2021), though the effect on organic solvent-extracted PP detection is currently unclear. Furthermore, interferences and misclassification in μ-FT-IR imaging are potential sources for overestimating PP contents (Supplementary Material S4).

The comparison of directly measured MP mass with particle-based mass estimates also illustrated remaining challenges of conversion factors: Particle-derived MP masses greatly exceeded measured mass concentrations, a trend that was earlier reported for surface water and sediment samples (Primpke et al., 2020b; Viitala et al., 2022). While the omission of additives by Py-GC/MS can be a potential source for underestimating MP masses for some plastics, PE, PP and PS tend to contain only negligible concentrations of additives (Hahladakis et al., 2018). To address persisting uncertainties of conversion factors, further systematic comparisons of spectroscopic and thermo-analytical methods are necessary to understand the relationship between MP number, size and mass concentrations.

4.3. Microplastics are transported to soil depths below the plough layer

Sewage sludge application to agricultural soil is usually followed by ploughing that mixes sewage sludge and therefore organic matter, associated metals and MPs into the soil. Existing studies often assume a low mobility of MPs beyond this ploughed topsoil (Crossman et al., 2020). MP concentrations were indeed high in the plough layer (Figs. 1 and 2), but we were able to detect a substantial amount of MPs at greater depths in terms of mass (52 %) and number concentrations (42 %). Local variations in ploughing depth may have contributed to the presence of MPs, metals and organic matter at 20–30 cm depth. However, MPs found at greater depths up to 60–70 cm suggest continued transport in the soil profile by other transport processes.

In laboratory-based transport studies, MP mobility is often considered negligible (Alimi et al., 2018). Especially larger-sized (Dong et al., 2018; Ranjan et al., 2023) and fibrous MPs (Schell et al., 2022; X. Zhang et al., 2022) are typically considered largely immobile because of size exclusion, entanglement, straining or sedimentation. Indeed, we found a larger fraction of fragmental and smaller particles beyond 20 cm depth, but plastic type, as well as particle shape and size remained similar at greater depths (Table 1, Fig. 3). This lack of size- or shape-discrimination at greater depths can either be explained by the presence of macropores in which relatively large particles can still be transported by preferential flow or another less size-selective transport process. Burrowing soil biota play a vital role in the vertical redistribution of soil particles (Taylor et al., 2018). Earthworms, for instance, can transport particles as large as 5 mm through ingestion (McTavish and Murphy, 2021), potentially including MPs (Huerta Lwanga et al., 2017; Prendergast-Miller et al., 2019). Biopores at this site were previously found as far down as 1.0 m (Jarvis et al., 1991), making bioturbation-driven transport a likely process causing the observed transport distances of MPs. Similarly to other macropores, biopores can further facilitate the transport of relatively large particles to deeper parts of the soil profile (Jarvis et al., 2016; Leuther et al., 2023; Yu et al., 2019). MP transport in laboratory studies is accelerated and less size-restricted when processes such as bioturbation, drying-wetting or freeze-thawing cycles are included (Koutnik et al., 2022; O'Connor et al., 2019; Yu et al., 2019; X. Zhang et al., 2022; Zhao et al., 2022). These processes promote the development of connected macropores that can result in strong preferential flow, which was also observed for the clayey subsoils at the study site (Jarvis et al., 1991; Larsson and Jarvis, 1999). Consequently, bioturbation and preferential flow in macropores are likely causes for the observed translocation of even relatively large MPs in this agricultural soil.

The observed vertical MP transport in this and other field studies with soils under different management systems (Wahl et al., 2024; Weber et al., 2021) likely contributes to the reported discrepancies between estimated MP inputs, based on measurements in the initial sewage sludge in comparison to MP concentrations measured in soil plough layers (Crossman et al., 2020; Klemmensen et al., 2024). Neglecting vertical MP transport in sampling schemes can therefore result in a systematic underestimation of MP exposure of the soil ecosystem.

4.4. Microplastic and metal transport is affected by management

Although MPs were transported to the deeper soil, MP concentrations decreased considerably between 20 and 40 cm depth (Figs. 1 and 2). We suspect that this depth reflects the effect of heavy machinery and ploughing activities on the soil structure and pore connectivity below the plough layer, because similar depth distributions were found in other studies of agricultural cropland (Qiu et al., 2023; Tagg et al., 2022; Wahl et al., 2024; Weber and Opp, 2020). No-plough soils, such as grassland and riparian soils, often demonstrate more connected and deeper reaching soil pore systems (Larsbo et al., 2009; Torppa and Taylor, 2022), where indeed large MPs (2–5 mm) were found as deep as 60–90 cm in soil profiles reaching down 2 m (Weber and Opp, 2020).

Soil compactness can reduce plant rooting and the activity of earthworm burrowing (Arrázola-Vásquez et al., 2022; Capowiez et al., 2021), while annual tillage can disrupt deep-burrowing earthworm species, and the soil pore connectivity (Capowiez et al., 2009). Transport

dynamics can thus be affected directly by soil management, through decreased water movement (Schlüter et al., 2020), and indirectly through a changed behaviour of soil biota (Blanchy et al., 2023; Jégou et al., 2002; Keller et al., 2017). The previously recorded strong decrease in hydraulic conductivity in soils at our study site between 15 and 30 cm depth (Jarvis et al., 1991) may indicate such compaction. While this measurement was done ca. 30 years before samples were taken for the current study, continued agricultural activity would be expected to further increase these trends. The depth distribution of other soil constituents likewise suggested reduced transport dynamics at greater depths (Fig. 5). For instance, the sharp decrease of TOC not only coincided with the distribution of MPs (30–40 cm, Fig. 5), but is also characteristic for mouldboard-ploughing systems with compact layers below the plough layer (Martínez et al., 2016; Zhou et al., 2023). The distribution of Cu largely followed that of TOC, Cd, in contrast, is expected to transport in dissolved form both in macro- and micropores, explaining its slightly higher mobility in the soil. Hence, although agricultural management practices did not completely restrict transport dynamics of MPs, TOC and metals entering the soil via external sources, it likely explains why transport distances of MP in agricultural soils were on average lower compared to MPs in other land uses such as grassland (Weber and Opp, 2020).

5. Implications and conclusion

24 years of sewage sludge applications to agricultural soil increased soil TOC but also led to a higher exposure to MPs and potentially toxic metals as compared to soils receiving mineral fertiliser. The measured MP particle and mass concentrations exceeded previously reported values, likely because of methodological differences and variations in MP contents in applied sewage sludges. The relative contribution of different plastic types depended on the measured metric, i.e. mass or number concentration, highlighting the need for measuring both for a comprehensive assessment. Long-term exposure to field conditions facilitated the vertical transport of a substantial fraction of particularly relatively small, fragmentally shaped MPs below the plough layer, likely facilitated by burrowing soil biota and connected macropores. Neglecting vertical MP transport during long-term projections of MP exposure therefore results in a systematic underestimation of MPs present in the whole soil ecosystem. Despite the observed transport, concentrations of MPs, TOC and metals all decreased sharply between 20 and 40 cm depth; a depth that is indicative of compaction in response to agricultural soil management practices like ploughing. Hence, there is a further need to improve our understanding of the interactions between soil structure, soil management and MP properties to assess their long-term fate in agricultural soils reliably.

Funding

This work was supported by ACEnano (EU Horizon 2020; grant agreement no. 720952), the Swedish research council FORMAS (project no. 2018–01080), Horizon 2020 European Join Program (EJP) Soil (project no. 862695) - WP3 project EOM4Soil, the Swedish University of Agricultural Sciences, RPTU Kaiserslautern-Landau and Aalborg University.

CRediT authorship contribution statement

Wiebke Mareile Heinze: Writing – review & editing, Writing – original draft, Visualization, Validation, Methodology, Investigation, Formal analysis, Conceptualization. **Zacharias Steinmetz:** Writing – review & editing, Validation, Software, Methodology, Investigation, Formal analysis. **Nanna Dyg Rathje Klemmensen:** Writing – review & editing, Methodology, Investigation, Formal analysis. **Jes Vollertsen:** Writing – review & editing, Supervision, Methodology. **Geert Cornelis:** Writing – review & editing, Supervision, Funding acquisition, Conceptualization.

Declaration of competing interest

The authors declare that they have no known competing financial interests or personal relationships that could have appeared to influence the work reported in this paper.

Data availability

Data will be made available on request.

Acknowledgements

Special thanks to Nora Ottander and Silvia Eichhöfer who provided much support during the laboratory analysis, to Sofia Delin and Lanna research station, and to Tobias Klöffel, Maarten Wynants and Katrin Rychel for feedback.

Appendix A. Supplementary data

Supplementary data to this article can be found online at https://doi.org/10.1016/j.envpol.2024.124343.

References

Alimi, O.S., Farner Budarz, J., Hernandez, L.M., Tufenkji, N., 2018. Microplastics and nanoplastics in aquatic environments: aggregation, deposition, and enhanced contaminant transport. Environ. Sci. Technol. 52, 1704–1724. https://doi.org/10.1021/acs.est.7b05559.

Arrázola-Vásquez, E., Larsbo, M., Capowiez, Y., Taylor, A., Sandin, M., Iseskog, D., Keller, T., 2022. Earthworm burrowing modes and rates depend on earthworm species and soil mechanical resistance. Appl. Soil Ecol. 178, 104568 https://doi.org/10.1016/j.apsoil.2022.104568.

Blanchy, G., Bragato, G., Di Bene, C., Jarvis, N., Larsbo, M., Meurer, K., Garré, S., 2023. Soil and crop management practices and the water regulation functions of soils: a qualitative synthesis of meta-analyses relevant to European agriculture. SOIL 9, 1–20. https://doi.org/10.5194/soil-9-1-2023.

Börjesson, G., Kirchmann, H., Kätterer, T., 2014. Four Swedish long-term field experiments with sewage sludge reveal a limited effect on soil microbes and on metal uptake by crops. J. Soils Sediments 14, 164–177. https://doi.org/10.1007/s11368-013-0800-5.

Bucci, K., Tulio, M., Rochman, C.M., 2020. What is known and unknown about the effects of plastic pollution: a meta-analysis and systematic review. Ecol. Appl. 30, e02044 https://doi.org/10.1002/eap.2044.

Capowiez, Y., Cadoux, S., Bouchant, P., Ruy, S., Roger-Estrade, J., Richard, G., Boizard, H., 2009. The effect of tillage type and cropping system on earthworm communities, macroporosity and water infiltration. Soil Tillage Res. 105, 209–216. https://doi.org/10.1016/j.still.2009.09.002.

Capowiez, Y., Sammartino, S., Keller, T., Bottinelli, N., 2021. Decreased burrowing activity of endogeic earthworms and effects on water infiltration in response to an increase in soil bulk density. Pedobiologia 85–86, 150728. https://doi.org/10.1016/j.pedobi.2021.150728.

Chamas, A., Moon, H., Zheng, J., Qiu, Y., Tabassum, T., Jang, J.H., Abu-Omar, M., Scott, S.L., Suh, S., 2020. Degradation rates of plastics in the environment. ACS Sustain. Chem. Eng. 8, 3494–3511. https://doi.org/10.1021/acssuschemeng.9b06635.

Chand, R., Rasmussen, L.A., Tumlin, S., Vollertsen, J., 2021. The occurrence and fate of microplastics in a mesophilic anaerobic digester receiving sewage sludge, grease, and fatty slurries. Sci. Total Environ. 798, 149287 https://doi.org/10.1016/j.scitotenv.2021.149287.

Chu, L., He, W., 2021. Toxic metals in soil due to the land application of sewage sludge in China: Spatiotemporal variations and influencing factors. Sci. Total Environ. 757, 143813 https://doi.org/10.1016/j.scitotenv.2020.143813.

Cole, M., 2016. A novel method for preparing microplastic fibers. Sci. Rep. 6, 34519 https://doi.org/10.1038/srep34519.

Corradini, F., Meza, P., Eguiluz, R., Casado, F., Huerta-Lwanga, E., Geissen, V., 2019. Evidence of microplastic accumulation in agricultural soils from sewage sludge disposal. Sci. Total Environ. 671, 411–420. https://doi.org/10.1016/j.scitotenv.2019.03.368.

Cowger, W., Booth, A.M., Hamilton, B.M., Thaysen, C., Primpke, S., Munno, K., Lusher, A.L., Dehaut, A., Vaz, V.P., Liboiron, M., Devriese, L.I., Hermabessiere, L., Rochman, C., Athey, S.N., Lynch, J.M., De Frond, H., Gray, A., Jones, O.A.H., Brander, S., Steele, C., Moore, S., Sanchez, A., Nel, H., 2020. Reporting guidelines to increase the reproducibility and comparability of research on microplastics. Appl. Spectrosc. 74, 1066–1077. https://doi.org/10.1177/0003702820930292.

Crossman, J., Hurley, R.R., Futter, M., Nizzetto, L., 2020. Transfer and transport of microplastics from biosolids to agricultural soils and the wider environment. Sci. Total Environ. 724, 138334 https://doi.org/10.1016/j.scitotenv.2020.138334.
de Souza Machado, A.A., Lau, C.W., Till, J., Kloas, W., Lehmann, A., Becker, R., Rillig, M. C., 2018. Impacts of microplastics on the soil biophysical environment. Environ. Sci. Technol. 52, 9656–9665. https://doi.org/10.1021/acs.est.8b02212.
Dong, Z., Qiu, Y., Zhang, W., Yang, Z., Wei, L., 2018. Size-dependent transport and retention of micron-sized plastic spheres in natural sand saturated with seawater. Water Res. 143, 518–526. https://doi.org/10.1016/j.watres.2018.07.007.
Gao, J., Pan, S., Li, P., Wang, L., Hou, R., Wu, W.-M., Luo, J., Hou, D., 2021. Vertical migration of microplastics in porous media: Multiple controlling factors under wet-dry cycling. J. Hazard Mater. 419, 126413 https://doi.org/10.1016/j.jhazmat.2021.126413.
Hahladakis, J.N., Velis, C.A., Weber, R., Iacovidou, E., Purnell, P., 2018. An overview of chemical additives present in plastics: migration, release, fate and environmental impact during their use, disposal and recycling. J. Hazard Mater. 344, 179–199. https://doi.org/10.1016/j.jhazmat.2017.10.014.
Han, N., Zhao, Q., Ao, H., Hu, H., Wu, C., 2022. Horizontal transport of macro- and microplastics on soil surface by rainfall induced surface runoff as affected by vegetations. Sci. Total Environ. 831, 154989 https://doi.org/10.1016/j.scitotenv.2022.154989.
Harley-Nyang, D., Memon, F.A., Osorio Baquero, A., Galloway, T., 2023. Variation in microplastic concentration, characteristics and distribution in sewage sludge & biosolids around the world. Sci. Total Environ. 891, 164068 https://doi.org/10.1016/j.scitotenv.2023.164068.
Heinze, W.M., Mitrano, D.M., Lahive, E., Koestel, J., Cornelis, G., 2021. Nanoplastic transport in soil via bioturbation by Lumbricus terrestris. Environ. Sci. Technol. 55, 16423–16433. https://doi.org/10.1021/acs.est.1c05614.
Hooge, A., Hauggaard-Nielsen, H., Heinze, W.M., Lyngsie, G., Ramos, T.M., Sandgaard, M.H., Vollertsen, J., Syberg, K., 2023. Fate of microplastics in sewage sludge and in agricultural soils. TrAC, Trends Anal. Chem. 166, 117184 https://doi.org/10.1016/j.trac.2023.117184.
Horton, A.A., Cross, R.K., Read, D.S., Jürgens, M.D., Ball, H.L., Svendsen, C., Vollertsen, J., Johnson, A.C., 2021. Semi-automated analysis of microplastics in complex wastewater samples. Environ. Pollut. 268, 115841 https://doi.org/10.1016/j.envpol.2020.115841.
Huerta Lwanga, E., Gertsen, H., Gooren, H., Peters, P., Salánki, T., Ploeg, M. van der, Besseling, E., Koelmans, A.A., Geissen, V., 2017. Incorporation of microplastics from litter into burrows of Lumbricus terrestris. Environ. Pollut. 220, 523–531. https://doi.org/10.1016/j.envpol.2016.09.096.
Hurley, R.R., Lusher, A.L., Olsen, M., Nizzetto, L., 2018. Validation of a method for extracting microplastics from complex, organic-rich, environmental matrices. Environ. Sci. Technol. 52, 7409–7417. https://doi.org/10.1021/acs.est.8b01517.
Hurley, R.R., Nizzetto, L., 2018. Fate and occurrence of micro(nano)plastics in soils: knowledge gaps and possible risks. Curr. Opin. Environ. Sci. Health 1, 6–11. https://doi.org/10.1016/j.coesh.2017.10.006.
IUSS Working Group, 2015. World Reference Base for Soil Resources 2014, Update 2015: International Soil Classification System for Naming Soils and Creating Legends for Soil Maps. World Soil Resource Reports FAO.
Jarvis, N., Bergström, L., Dik, P.E., 1991. Modelling water and solute transport in macroporous soil. II. Chloride breakthrough under non-steady flow. J. Soil Sci. 42, 71–81. https://doi.org/10.1111/j.1365-2389.1991.tb00092.x.
Jarvis, N., Koestel, J., Larsbo, M., 2016. Understanding preferential flow in the vadose zone: recent advances and future prospects. Vadose Zone J. 15 https://doi.org/10.2136/vzj2016.09.0075 vzj2016.09.0075.
Jégou, D., Brunotte, J., Rogasik, H., Capowiez, Y., Diestel, H., Schrader, S., Cluzeau, D., 2002. Impact of soil compaction on earthworm burrow systems using X-ray computed tomography: preliminary study. Eur. J. Soil Biol. 38, 329–336. https://doi.org/10.1016/S1164-5563(02)01148-2.
Kätterer, T., Börjesson, G., Kirchmann, H., 2014. Changes in organic carbon in topsoil and subsoil and microbial community composition caused by repeated additions of organic amendments and N fertilisation in a long-term field experiment in Sweden. Agric. Ecosyst. Environ. 189, 110–118. https://doi.org/10.1016/j.agee.2014.03.025.
Keller, T., Colombi, T., Ruiz, S., Manalili, M.P., Rek, J., Stadelmann, V., Wunderli, H., Breitenstein, D., Reiser, R., Oberholzer, H., Schymanski, S., Romero-Ruiz, A., Linde, N., Weisskopf, P., Walter, A., Or, D., 2017. Long-term soil structure observatory for monitoring post-compaction evolution of soil structure. Vadose Zone J. 16 https://doi.org/10.2136/vzj2016.11.0118 vzj2016.11.0118.
Klemmensen, N.D.R., Chand, R., Blanco, M.S., Vollertsen, J., 2024. Microplastic abundance in sludge-treated fields: Variance and estimated half-life. Sci. Total Environ. 171394 https://doi.org/10.1016/j.scitotenv.2024.171394.
Koutnik, V.S., Leonard, J., Brar, J., Cao, S., Glasman, J.B., Cowger, W., Ravi, S., Mohanty, S.K., 2022. Transport of microplastics in stormwater treatment systems under freeze-thaw cycles: Critical role of plastic density. Water Res. 222, 118950 https://doi.org/10.1016/j.watres.2022.118950.
Lares, M., Ncibi, M.C., Sillanpää, Markus, Sillanpää, Mika, 2018. Occurrence, identification and removal of microplastic particles and fibers in conventional activated sludge process and advanced MBR technology. Water Res. 133, 236–246. https://doi.org/10.1016/j.watres.2018.01.049.
Larsbo, M., Stenström, J., Etana, A., Börjesson, E., Jarvis, N.J., 2009. Herbicide sorption, degradation, and leaching in three Swedish soils under long-term conventional and reduced tillage. Soil Tillage Res. 105, 200–208. https://doi.org/10.1016/j.still.2009.08.003.
Larsson, M.H., Jarvis, N.J., 1999. Evaluation of a dual-porosity model to predict field-scale solute transport in a macroporous soil. J. Hydrol. 215, 153–171. https://doi.org/10.1016/S0022-1694(98)00267-4.
Leuther, F., Mikutta, R., Wolff, M., Kaiser, K., Schlüter, S., 2023. Structure turnover times of grassland soils under different moisture regimes. Geoderma 433, 116464. https://doi.org/10.1016/j.geoderma.2023.116464.
Li, X., Chen, L., Mei, Q., Dong, B., Dai, X., Ding, G., Zeng, E.Y., 2018. Microplastics in sewage sludge from the wastewater treatment plants in China. Water Res. 142, 75–85. https://doi.org/10.1016/j.watres.2018.05.034.
Liu, F., Olesen, K.B., Borregaard, A.R., Vollertsen, J., 2019. Microplastics in urban and highway stormwater retention ponds. Sci. Total Environ. 671, 992–1000. https://doi.org/10.1016/j.scitotenv.2019.03.416.
Ljung, E., Borg Olesen, K., Andersson, P.-G., Fältström, E., Vollertsen, J., Wittgren, H.B., Hagman, M., 2018. Mikroplaster i kretsloppet (No. 2018–13). Svenskt Vatten Utveckling.
Löder, M.G.J., Imhof, H.K., Ladehoff, M., Löschel, L.A., Lorenz, C., Mintenig, S., Piehl, S., Primpke, S., Schrank, I., Laforsch, C., Gerdts, G., 2017. Enzymatic purification of microplastics in environmental samples. Environ. Sci. Technol. 51, 14283–14292. https://doi.org/10.1021/acs.est.7b03055.
Lofty, J., Muhawenimana, V., Wilson, C.A.M.E., Ouro, P., 2022. Microplastics removal from a primary settler tank in a wastewater treatment plant and estimations of contamination onto European agricultural land via sewage sludge recycling. Environ. Pollut. 304, 119198 https://doi.org/10.1016/j.envpol.2022.119198.
Magnusson, K., Norén, F., 2014. Screening of Microplastic Particles in and Down-Stream a Wastewater Treatment Plant, IVL Report C.
Mahon, A.M., O'Connell, B., Healy, M.G., O'Connor, I., Officer, R., Nash, R., Morrison, L., 2017. Microplastics in sewage sludge: effects of treatment. Environ. Sci. Technol. 51, 810–818. https://doi.org/10.1021/acs.est.6b04048.
Martínez, I., Chervet, A., Weisskopf, P., Sturny, W.G., Etana, A., Stettler, M., Forkman, J., Keller, T., 2016. Two decades of no-till in the Oberacker long-term field experiment: Part I. Crop yield, soil organic carbon and nutrient distribution in the soil profile. Soil Tillage Res. 163, 141–151. https://doi.org/10.1016/j.still.2016.05.021.
McTavish, M.J., Murphy, S.D., 2021. Three-dimensional mapping of earthworm (Lumbricus terrestris) seed transport. Pedobiologia 87–88, 150752. https://doi.org/10.1016/j.pedobi.2021.150752.
Moreira, A., Moraes, L.A.C., de Melo, T.R., Heinrichs, R., Moretti, L.G., 2022. Chapter Five - management of copper for crop production. In: Sparks, D.L. (Ed.), Advances in Agronomy. Academic Press, pp. 257–298. https://doi.org/10.1016/bs.agron.2022.02.005.
Naturvårdsverket, 2009. Riktvärden För Förorenad Mark – Modellbeskrivning Och Vägledning. Naturvårdsverket, Stockholm.
O'Connor, D., Pan, S., Shen, Z., Song, Y., Jin, Y., Wu, W.-M., Hou, D., 2019. Microplastics undergo accelerated vertical migration in sand soil due to small size and wet-dry cycles. Environ. Pollut. 249, 527–534. https://doi.org/10.1016/j.envpol.2019.03.092.
Okoffo, E.D., Ribeiro, F., O'Brien, J.W., O'Brien, S., Tscharke, B.J., Gallen, M., Samanipour, S., Mueller, J.F., Thomas, K.V., 2020. Identification and quantification of selected plastics in biosolids by pressurized liquid extraction combined with double-shot pyrolysis gas chromatography–mass spectrometry. Sci. Total Environ. 715, 136924 https://doi.org/10.1016/j.scitotenv.2020.136924.
Prendergast-Miller, M.T., Katsiamides, A., Abbass, M., Sturzenbaum, S.R., Thorpe, K.L., Hodson, M.E., 2019. Polyester-derived microfibre impacts on the soil-dwelling earthworm Lumbricus terrestris. Environ. Pollut. 251, 453–459. https://doi.org/10.1016/j.envpol.2019.05.037.
Primpke, S., Cross, R.K., Mintenig, S.M., Simon, M., Vianello, A., Gerdts, G., Vollertsen, J., 2020a. Toward the systematic identification of microplastics in the environment: evaluation of a new independent software tool (siMPle) for spectroscopic analysis. Appl. Spectrosc. https://doi.org/10.1177/0003702820917760, 0003702820917760.
Primpke, S., Fischer, M., Lorenz, C., Gerdts, G., Scholz-Böttcher, B.M., 2020b. Comparison of pyrolysis gas chromatography/mass spectrometry and hyperspectral FTIR imaging spectroscopy for the analysis of microplastics. Anal. Bioanal. Chem. 412, 8283–8298. https://doi.org/10.1007/s00216-020-02979-w.
Primpke, S., Lorenz, C., Rascher-Friesenhausen, R., Gerdts, G., 2017. An automated approach for microplastics analysis using focal plane array (FPA) FTIR microscopy and image analysis. Anal. Methods 9, 1499–1511. https://doi.org/10.1039/C6AY02476A.
Qi, S., Song, J., Shentu, J., Chen, Q., Lin, K., 2022. Attachment and detachment of large microplastics in saturated porous media and its influencing factors. Chemosphere 305, 135322. https://doi.org/10.1016/j.chemosphere.2022.135322.
Qiu, Y., Zhou, S., Zhang, C., Chen, L., Qin, W., Zhang, Q., 2023. Vertical distribution and weathering characteristic of microplastics in soil profile of different land use types. Sci. Total Environ. 905, 166902 https://doi.org/10.1016/j.scitotenv.2023.166902.
Ranjan, V.P., Joseph, A., Sharma, H.B., Goel, S., 2023. Preliminary investigation on effects of size, polymer type, and surface behaviour on the vertical mobility of microplastics in a porous media. Sci. Total Environ. https://doi.org/10.1016/j.scitotenv.2022.161148.
Ren, Z., Gui, X., Wei, Y., Chen, X., Xu, X., Zhao, L., Qiu, H., Cao, X., 2021. Chemical and photo-initiated aging enhances transport risk of microplastics in saturated soils: Key factors, mechanisms, and modeling. Water Res. 202, 117407 https://doi.org/10.1016/j.watres.2021.117407.
Rillig, M.C., Ziersch, L., Hempel, S., 2017. Microplastic transport in soil by earthworms. Sci. Rep. 7, 1362. https://doi.org/10.1038/s41598-017-01594-7.
Sauvé, S., Hendershot, W., Allen, H.E., 2000. Solid-solution partitioning of metals in contaminated soils: dependence on pH, total metal burden, and organic matter. Environ. Sci. Technol. 34, 1125–1131. https://doi.org/10.1021/es9907764.

Schell, T., Hurley, R., Buenaventura, N.T., Mauri, P.V., Nizzetto, L., Rico, A., Vighi, M., 2022. Fate of microplastics in agricultural soils amended with sewage sludge: is surface water runoff a relevant environmental pathway? Environ. Pollut. 293, 118520 https://doi.org/10.1016/j.envpol.2021.118520.

Schlüter, S., Albrecht, L., Schwärzel, K., Kreiselmeier, J., 2020. Long-term effects of conventional tillage and no-tillage on saturated and near-saturated hydraulic conductivity – can their prediction be improved by pore metrics obtained with X-ray CT? Geoderma 361, 114082. https://doi.org/10.1016/j.geoderma.2019.114082.

Simon, M., Alst, N. van, Vollertsen, J., 2018. Quantification of microplastic mass and removal rates at wastewater treatment plants applying Focal Plane Array (FPA)-based Fourier Transform Infrared (FT-IR) imaging. Water Res. 142, 1–9. https://doi.org/10.1016/j.watres.2018.05.019.

Steinmetz, Z., Kintzi, A., Muñoz, K., Schaumann, G.E., 2020. A simple method for the selective quantification of polyethylene, polypropylene, and polystyrene plastic debris in soil by pyrolysis-gas chromatography/mass spectrometry. J. Anal. Appl. Pyrolysis 104803. https://doi.org/10.1016/j.jaap.2020.104803.

Steinmetz, Z., Löffler, P., Eichhöfer, S., David, J., Muñoz, K., Schaumann, G.E., 2022. Are agricultural plastic covers a source of plastic debris in soil? A first screening study. SOIL 8, 31–47. https://doi.org/10.5194/soil-8-31-2022.

Tagg, A.S., Brandes, E., Fischer, F., Fischer, D., Brandt, J., Labrenz, M., 2022. Agricultural application of microplastic-rich sewage sludge leads to further uncontrolled contamination. Sci. Total Environ. 806, 150611 https://doi.org/10.1016/j.scitotenv.2021.150611.

Taylor, A.R., Lenoir, L., Vegerfors, B., Persson, T., 2018. Ant and earthworm bioturbation in cold-temperate ecosystems. Ecosystems 22, 981–994. https://doi.org/10.1007/s10021-018-0317-2.

Thomas, D., Schütze, B., Heinze, W.M., Steinmetz, Z., 2020. Sample preparation techniques for the analysis of microplastics in soil - a review. Sustainability 12, 9074. https://doi.org/10.3390/su12219074.

Thornton Hampton, L.M., Brander, S.M., Coffin, S., Cole, M., Hermabessiere, L., Koelmans, A.A., Rochman, C.M., 2022. Characterizing microplastic hazards: which concentration metrics and particle characteristics are most informative for understanding toxicity in aquatic organisms? Microplastics Nanoplastics 2, 20. https://doi.org/10.1186/s43591-022-00040-4.

Toapanta, T., Okoffo, E.D., Ede, S., O'Brien, S., Burrows, S.D., Ribeiro, F., Gallen, M., Colwell, J., Whittaker, A.K., Kaserzon, S., Thomas, K.V., 2021. Influence of surface oxidation on the quantification of polypropylene microplastics by pyrolysis gas chromatography mass spectrometry. Sci. Total Environ. 796, 148835 https://doi.org/10.1016/j.scitotenv.2021.148835.

Torppa, K.A., Taylor, A.R., 2022. Alternative combinations of tillage practices and crop rotations can foster earthworm density and bioturbation. Appl. Soil Ecol. 175, 104460 https://doi.org/10.1016/j.apsoil.2022.104460.

van den Berg, P., Huerta-Lwanga, E., Corradini, F., Geissen, V., 2020. Sewage sludge application as a vehicle for microplastics in eastern Spanish agricultural soils. Environ. Pollut. 261, 114198 https://doi.org/10.1016/j.envpol.2020.114198.

van Straalen, N.M., Schobben, J.H.M., de Goede, R.G.M., 1989. Population consequences of cadmium toxicity in soil microarthropods. Ecotoxicol. Environ. Saf. 17, 190–204. https://doi.org/10.1016/0147-6513(89)90038-9.

Viitala, M., Steinmetz, Z., Sillanpää, Mika, Mänttäri, M., Sillanpää, Markus, 2022. Historical and current occurrence of microplastics in water and sediment of a Finnish lake affected by WWTP effluents. Environ. Pollut. 314, 120298 https://doi.org/10.1016/j.envpol.2022.120298.

Viketoft, M., Riggi, L.G.A., Bommarco, R., Hallin, S., Taylor, A.R., 2021. Type of organic fertilizer rather than organic amendment per se increases abundance of soil biota. PeerJ 9, e11204. https://doi.org/10.7717/peerj.11204.

Wahl, A., Davranche, M., Rabiller-Baudry, M., Pédrot, M., Khatib, I., Labonne, F., Canté, M., Cuisinier, C., Gigault, J., 2024. Condition of composted microplastics after they have been buried for 30 years: vertical distribution in the soil and degree of degradation. J. Hazard Mater. 462, 132686 https://doi.org/10.1016/j.jhazmat.2023.132686.

Wasserstein, R.L., Schirm, A.L., Lazar, N.A., 2019. Moving to a world beyond "p < 0.05.". Am. Statistician 73, 1–19. https://doi.org/10.1080/00031305.2019.1583913.

Weber, C.J., Opp, C., 2020. Spatial patterns of mesoplastics and coarse microplastics in floodplain soils as resulting from land use and fluvial processes. Environ. Pollut. 267, 115390 https://doi.org/10.1016/j.envpol.2020.115390.

Weber, C.J., Opp, C., Prume, J.A., Koch, M., Andersen, T.J., Chifflard, P., 2021. Deposition and in-situ translocation of microplastics in floodplain soils. Sci. Total Environ. 152039 https://doi.org/10.1016/j.scitotenv.2021.152039.

Weber, C.J., Santowski, A., Chifflard, P., 2022. Investigating the dispersal of macro- and microplastics on agricultural fields 30 years after sewage sludge application. Sci. Rep. 12, 6401. https://doi.org/10.1038/s41598-022-10294-w.

Wenig, P., Odermatt, J., 2010. OpenChrom: a cross-platform open source software for the mass spectrometric analysis of chromatographic data. BMC Bioinf. 11, 405. https://doi.org/10.1186/1471-2105-11-405.

Yu, M., van der Ploeg, M., Lwanga, E.H., Yang, X., Zhang, S., Ma, X., Ritsema, C.J., Geissen, V., 2019. Leaching of microplastics by preferential flow in earthworm (Lumbricus terrestris) burrows. Environ. Chem. 16, 31–40. https://doi.org/10.1071/EN18161.

Zhang, L., Xie, Y., Liu, J., Zhong, S., Qian, Y., Gao, P., 2020. An overlooked entry pathway of microplastics into agricultural soils from application of sludge-based fertilizers. Environ. Sci. Technol. 54, 4248–4255. https://doi.org/10.1021/acs.est.9b07905.

Zhang, X., Chen, Y., Li, X., Zhang, Y., Gao, W., Jiang, J., Mo, A., He, D., 2022. Size/shape-dependent migration of microplastics in agricultural soil under simulative and natural rainfall. Sci. Total Environ. 815, 152507 https://doi.org/10.1016/j.scitotenv.2021.152507.

Zhang, Y.-Q., Lykaki, M., Markiewicz, M., Alrajoula, M.T., Kraas, C., Stolte, S., 2022. Environmental contamination by microplastics originating from textiles: Emission, transport, fate and toxicity. J. Hazard Mater. 430, 128453 https://doi.org/10.1016/j.jhazmat.2022.128453.

Zhao, Z., Zhao, K., Zhang, T., Xu, Y., Chen, R., Xue, S., Liu, M., Tang, D., Yang, X., Giessen, V., 2022. Irrigation-facilitated low-density polyethylene microplastic vertical transport along soil profile: an empirical model developed by column experiment. Ecotoxicol. Environ. Saf. https://doi.org/10.1016/j.ecoenv.2022.114232.

Zheljazkov, V.D., Warman, P.R., 2004. Phytoavailability and fractionation of copper, manganese, and zinc in soil following application of two composts to four crops. Environ. Pollut. 131, 187–195. https://doi.org/10.1016/j.envpol.2004.02.007.

Zhou, J., Wang, Y., Tong, Y., Sun, H., Zhao, Y., Zhang, P., 2023. Regional spatial variability of soil organic carbon in 0–5 m depth and its dominant factors. Catena 231, 107326. https://doi.org/10.1016/j.catena.2023.107326.

Supplementary information for: Vertical distribution of microplastics in an agricultural soil after long-term treatment with sewage sludge and mineral fertiliser

Note that the supporting information displayed here was reformatted for the purpose of this thesis. The content remains unchanged. The original is available free of charge at DOI:10.1016/j.envpol.2024.124343.

Wiebke Mareile Heinze[A], *Zacharias Steinmetz*[B], *Nanna Dyg Rathje Klemmensen*[C], *Jes Vollertsen*[C], *Geert Cornelis*[A]

[A]Swedish University of Agricultural Sciences, Department of Soil and Environment, Box 7014, 75007 Uppsala, Sweden
[B]RPTU Kaiserslautern-Landau, iES Landau, Institute for Environmental Sciences, Environmental and Soil Chemistry Lab, Fortstraße 7, 76829 Landau, Germany
[C]Aalborg University, Department of the Built Environment, Division of Civil and Environmental Engineering, Thomas Manns Vej 23, 9220 Aalborg, Denmark

Supplementary material S1. Overview of the field trials, treatments and Sampling

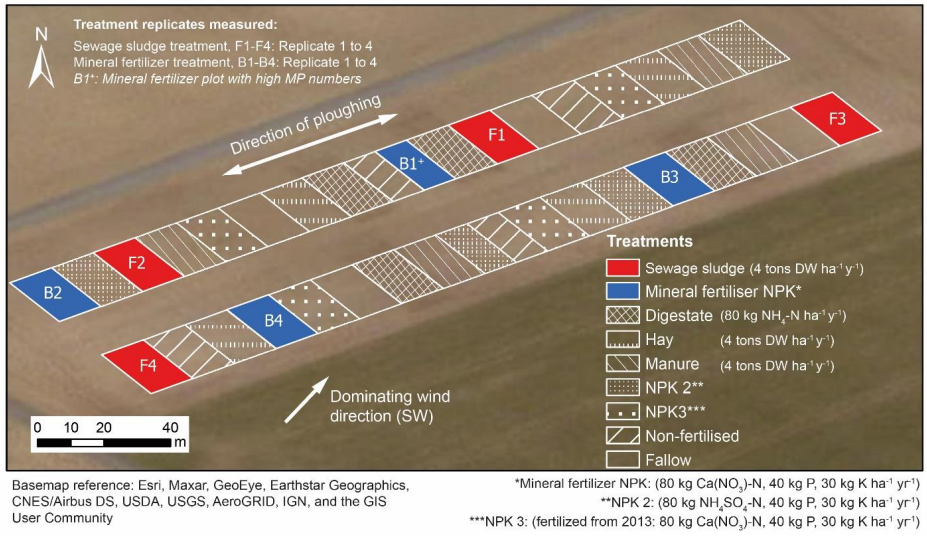

Supplementary Figure S1: Overview of the field trials and treatments, including the direction of ploughing and dominating wind direction.

Supplementary Table S1. Composite sample weight acquired per replicate field plot in dry weight (DW). Each composite sample consists of 6-8 cores directly segmented and mixed on-site, resulting in different total weights per depth and field plot.

	Replicate ID	Soil dry weight (DW) (g) 0-20 cm	20-30 cm	30-40 cm	40-50 cm	50-60 cnm	60-70 cm	70-80 cm	80-90 cm
Sewage sludge	F1	438	391	450	413	431	381	387	405
	F2	466	374	445	445	424	401	395	434
	F3	488	349	365	422	428	446	364	312
	F4	582	316	420	416	409	437	436	404
Mineral fertiliser	B1	580	NA	538	510	571	526	504	429
	B2	647	306	444	431	386	407	395	430
	B3	434	380	531	528	497	497	412	439
	B4	479	377	438	461	440	411	376	400

SUPPLEMENTARY MATERIAL S2. METAL AND ORGANIC CARBON ANALYSIS

We determined the depth-dependent concentration of copper (Cu), cadmium (Cd), chromium (Cr), lead (Pb), nickel (Ni) and zinc (Zn), and silver (Ag). Ag was below detection limit in all samples, and was thus removed from the data analysis and presentation. Soil samples (approximately 0.5 g) were treated with *aqua regia* (3.75 mL HNO3, 65 vol.%; 1.25 mL HCl, 37 vol.%). Acid digestion was done in a closed-vessel microwave-assisted system (Ethos Easy, Milestone, MAXI-44), with 20 min ramping to 180°C, where temperature remained for 10 min, followed by a cooling period until room temperature was reached. Samples were transferred to volumetric flasks, diluted to a final volume of 50 mL and sent to an external laboratory (ALS Scandinavia AB Luleå) for analysis via inductively coupled sector field mass spectrometry (ICP-SFMS). The reported limits of detection were 0.1 µg L^{-1} for Cd, 0.5 µg L^{-1} for Cr, 5 µg L^{-1} for Cu, 0.5 for Pb, 3 µg L^{-1} for Ni, 10 µg L^{-1} for Zn and 3 µg L^{-1} for Ag. For quality assurance, the analysis included procedural blanks, i.e. negative controls (n=3), spike recoveries in negative controls (n=3) for each metal in each digestion batch (A-F). Spike recoveries for each respective batch are shown in Supplementary Table S2. All samples were corrected for the procedural blanks (n=3) in their respective digestion batch before conversion to mass per kilogram soil. Measured concentrations in soils are shown in Supplementary Table S3.

Supplementary Table S2. Recovery of spiked solutions of the different metals, expressed as percentage of the measured versus expected concentration.

	Recovery (%)						
Digestion batch	**Cd (%)**	**Cr (%)**	**Cu (%)**	**Pb (%)**	**Ni (%)**	**Zn (%)**	**Ag (%)**
Batch A	NA	111±7	105±5	86±1	NA	NA	102±1
Batch B	102±1	115±2	109±3	96±1	116±3	96±2	112±1
Batch C	98±3	118±6	106±9	96±4	106±11	95±1	113±7
Batch D	102±2	117±2	112±2	96±2	112±2	96±2	111±1
Batch E	98±6	125±5	113±2	96±2	117±6	99±2	114±3
Batch F	104±2	121±1	112±3	99±3	115±2	106±3	117±3
Overall	101±3	118±5	110±3	95±5	113±4	98±5	112±5

Supplementary Table S3. Mean concentrations of selected metals (cadmium, chromium, copper, lead, nickel and zinc) in different depth segments in soil treated with mineral fertilizer and sewage sludge, including standard deviation (Stdev), relative standard deviation (RSD) and number of digested replicate samples (n).

	Depth (cm)	Cd µg kg^{-1}		Cr mg kg^{-1}		Cu mg kg^{-1}		Pb mg kg^{-1}		Ni mg kg^{-1}		Zn mg kg^{-1}		
		Mean± Stdev	RSD (%)	Mean± Stdev	RSD (%)	Mean± Stdev	RSD (%)	Mean± Stdev	RSD (%)	Mean± Stdev	RSD (%)	Mean± Stdev	RSD (%)	n
Sewage sludge	0-20	123±18	14	32±2	5	25±2	9	13±0	3	15±1	8	87±4	4	9
	20-30	128±9	7	32±2	6	25±4	15	13±1	5	15±1	9	93±5	6	8
	30-40	101±16	16	34±3	8	18±2	14	13±1	6	18±3	18	82±4	4	8
	40-50	64±26	40	37±4	10	15±2	13	13±1	6	25±5	20	84±2	3	8
	50-60	48±17	36	39±3	7	17±1	7	13±0	3	24±3	12	87±4	5	8
	60-70	45±6	13	37±3	8	17±2	10	13±1	6	23±3	12	87±2	2	8
	70-80	56±15	26	36±3	8	17±2	9	12±0	2	24±3	12	89±3	3	8
	80-90	50±7	14	37±3	8	17±2	10	13±1	4	24±2	10	91±3	3	8
Mineral fertilizer	0-20	114±20	17	35±2	6	13±2	12	13±1	6	17±1	6	75±7	9	8
	20-30	116±24	21	36±1	4	13±2	15	12±1	9	18±3	14	73±5	7	7
	30-40	86±14	17	38±3	8	13±1	8	12±0	3	19±2	9	78±10	13	4
	40-50	45±13	28	42±2	5	15±1	6	12±1	10	24±2	10	84±7	9	4
	50-60	72±29	40	44±3	7	17±1	8	12±1	5	28±2	6	88±4	5	4
	60-70	43±6	13	44±3	6	18±1	7	12±1	7	27±2	9	86±5	5	4
	70-80	41±6	15	44±3	7	19±1	5	12±1	9	27±0	2	93±4	4	4
	80-90	55±6	11	43±3	6	20±2	8	12±1	6	28±3	9	92±6	7	4

Supplementary Table S4: Organic carbon and total nitrogen in depth profiles (0-90 cm) of sewage sludge-amended soil and soil receiving mineral fertilizer based on four replicates each (one per replicate field plot).

	Depth (cm)	Organic carbon %		Total nitrogen %	
Sewage sludge	0-20	2.28	±0.07	0.21	±0.01
	20-30	2.35	±0.21	0.22	±0.02
	30-40	1.52	±0.18	0.14	±0.01
	40-50	0.58	±0.07	0.06	±0.01
	50-60	0.39	±0.07	0.04	±0.01
	60-70	0.31	±0.05	0.03	±0.01
	70-80	0.23	±0.04	0.03	±0.00
	80-90	0.19	±0.05	0.02	±0.00
Mineral fertilizer	0-20	1.94	±0.11	0.17	±0.01
	20-30	1.95	±0.09	0.17	±0.00
	30-40	1.47	±0.20	0.13	±0.01
	40-50	0.65	±0.13	0.06	±0.01
	50-60	0.44	±0.10	0.04	±0.01
	60-70	0.34	±0.04	0.03	±0.00
	70-80	0.28	±0.05	0.03	±0.01
	80-90	0.24	±0.03	0.03	±0.00

SUPPLEMENTARY MATERIAL S3. DETAILS ON MP SAMPLE PREPARATION, ANALYSIS, QA/QC AND DATA PROCESSING FOR PY-GC/MS MEASUREMENTS

Supplementary Table S5. Details on materials used (A), the setup of the pyrolysis gas chromatography mass spectrometry (Py-GC/MS) and details on polymer quantification (B), and quality control measures (C).

A) Materials	
Microplastics for recovery tests	The same plastic materials were used as by Steinmetz *et al*. (2020): • Polystyrene beads, 250 µm: CAS 9003-53-6,; Goodfellow, Huntingdon, United Kingdom • Polypropylene fragments, 1000 µm: CAS 9003-07-0, Aldrich Chemistry, Taufkirchen, Germany • Polyethylene beads, 500 µm: CAS 9002-88-4,; Alfa Aesar, Kandel, Germany Target concentrations: 5 µg g^{-1}, 10 µg g^{-1}, 20 µg g^{-1}
Soil for recovery test	Two soils were used: • Reference soil: RefeSol-06A • Field soil: mixture of subsoil samples from the field sites with the anticipated lowest background contamination (mineral fertilizer treatment, 60-90 cm)
Salt	• NaCl, 1.19 g cm^{-3} • Density separation at solid:liquid ratio of 1:6.8
Organic solvents	1,2,4-trichlorobenzene and *p*-xylene (ratio 1:1, 7.76 mL)
Cellulose filter	Whatman-Pleat filter 589/2 ½, cellulose, nominal pore size 4-12 µm
Sample carrier and sample transfer	See setup by Steinmetz *et al.* (2020): • Quartz tube • SiO_2-filter as carrier material inside (Whatman QM-A microfiber filter disks) • Syringe with PTFE plunger (Hamilton 1701 N, 26s gauge) for pipetting
B) Setup of and polymer quantification with Py-GC/MS	
Calibration*	External calibration standards: • 5, 10, 15, 20, 50, 100, 150, 200 µg mL^{-1} PE, PP, PS dissolved in xylene/TCB at 150°C • at beginning of each measurement series
Instruments (Pyrolyzer, GC, MS)	Pyroprobe 6150 filament pyrolyzer (CDS Analytical) Trace GC Ultra (DSQII mass spectrometer, Thermo Fisher Scientific)
Temperature; duration (s or min)	Sequence: • initial heating: 300°C 3 min (interface), • flash pyrolysis at 700°C for 15 seconds (coil, 10 K ms^{-1}) • vent time: 300°C for 3 min (interface); Transfer line (passive) temperature: 350°C
Sample size and sample transfer	• 2 µL of aliquots for recovery samples according to spiked concentrations • 6 µL (2 x 3 µL) for field samples with intermittent air-drying
Temperatures for interface and transfer line	• sample change only if temperatures were <100°C; • interface always >50°C; • transfer line always 350°C;
GC oven program, carrier gas	• Oven program: 40 °C (2 min hold), 8 K/min ramp to 300 °C (5 min hold) • Carrier gas: 1.3 mL/min He
MS ionization voltage, scanning frequency, temperature	• MS ionization voltage: 70 eV • Scanning frequency: 0.24 s

	• Temperature: 230 °C
Pyrolysates used for quantification	• PS pyrolysate: styrene • PP pyrolysate: 2,4-dimethyl-1- heptane • PE pyrolysate: n-alkadienes, i.e. 1,21-docosadiene
Py-GC/MS matching criteria	MS selective monitoring (SIM mode): • PP pyrolysate: 2,4-dimethyl-1-heptene (2,4Me9:1(1), RI 841) = 70 and 126 m/zs • PS pyrolysate: styrene (Sty, RI 895) and methylstyrene (MeSty, RI 140 981) = 104 m/zs and 118 m/zs • PE pyrolysates: n-alkadienes like 1,21-docosadiene (22:2(1,21), RI 2187) = 82 m/zs and 95 m/zs • internal standard: styrene-d5 (Sty-d5, RI 892) = 109 m/z
C) Quality control measures	
Bracketing standards*	• PE, PP and PS concentrations of 100 µg mL^{-1}: • inter-day variation, at least 2 bracketing standards each day • daily correction of integrated areas based on daily bracketing factor according to Steinmetz *et al*. (2020)
Internal standard	• deuterated polystyrene, Sty-d5 • manual quality control • 4 µL added to each sample (200 µL) directly after organic solvent extraction
Negative control	• blank sample, including all sample treatment steps • samples were corrected for the respective batch of NaCl salt used (total number of negative controls included, n=7)
Limit of detection:	• LOD calculated from SDs of signal intensities of blank measurement (DIN 32645)
Recovery (positive control) *†*	• Spike concentrations: 5 mg kg^{-1}, 20 mg kg^{-1} and 40 mg kg^{-1} • Samples without soil, but otherwise treated the exact same (i.e. addition of NaCl, shaking, sedimentation, release, filtration, organic solvent extraction, addition of deuterated PS, pipetting)
General contamination control measures	• Sample preparation was mostly done inside a fume hood. • Synthetic materials and clothing was avoided as much as possible, no make-up used. • Surfaces were carefully and repeatedly cleaned with paper towels and de-ionized water. • All hardware used for analysis was cleaned and thoroughly rinsed with ultrapure water (Milli-Q). • Containers were covered with Al-foil, glass beakers or glass petri dishes during passive times, such as sedimentation and sample release during density separation, treatment, or filtration. • Samples were stored in non-coated paper bags and cleaned glass jars.

**Relevant calibration curves and internal standards are presented in Supplementary Figure S2.*
†See Supplementary Table S6 for results of recovery tests.

Supplementary Table S6: Recovery of PE, PP and PS via Py-GC/MS after density separation and organic solvent extraction of two spiked soils: 1) field soil, i.e. subsoil from soils of the mineral fertiliser treatment (n=3), and 2) a fine-textured reference soil (n=3).

Soils	Plastic type	Spike recovery (%)		
		5 mg kg^{-1}	20 mg kg^{-1}	40 mg kg^{-1}
Field soil	PE	51±3	80±10	100±30
	PP	51±7	80±10	90±10
	PS	50±10	60±10	68±6
RefeSol-06A	PE	50±20	70±20	70±30
	PP	30±10	60±20	70±20
	PS	70±20	71±1	50±30

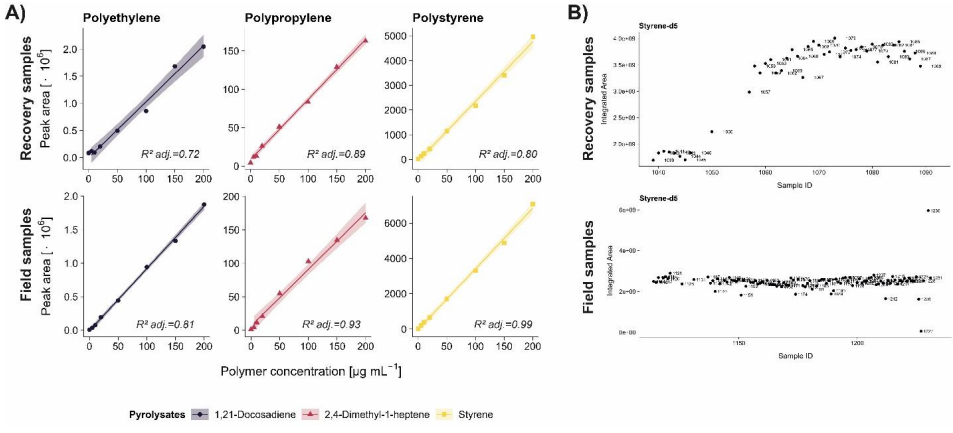

Supplementary Figure S2: Calibration curve for recovery samples and field samples for pyrolysates used for quantification of polyethylene, polypropylene and polystyrene (A), and overview of integrated areas obtained for internal standard (deuterated polystyrene) (B).

SUPPLEMENTARY MATERIAL S4. DETAILS ON MP SAMPLE PREPARATION, ANALYSIS, QA/QC AND DATA PROCESSING FOR µ-FT-IR IMAGING

Supplementary Table S7. Overview of A) the sample treatment steps, conditions and materials used for microplastic extraction and B) setup specific for analysis via µ-FT-IR imaging and C) quality control measures.

A) Microplastic extraction		
Sample treatment step	**Materials used (volumes and masses are per sample)**	**Treatment conditions and duration**
Filtration	Stainless steel filter, 10 µm nominal mesh width	Intermittent step in between each treatment below
Density separation	$ZnCl_2$ (≥1.6 g cm^{-3}, 500 mL) separatory funnel (glass, 1 L, glass lid, PTFE stopcock) Soil sample (ca. 100 g)	4 h shaking, settling for >24 h, release and settling for >24h repeated 3 times
Oxidation I	H_2O_2 (10 vol.%, 80 mL) water bath	24 h reaction under heating (50°C), 48 h at room temperature
SDS	SDS (5 weight%, 80 mL) water bath	48 h at 50°C
Enzyme treatment I	1.67 mL Protease enzyme solution (*Bacillus licheniformis*, ≥2.4 U g^{-1}) TRIS buffer solution (1 mol L^{-1}, pH 8.2, 80 mL) water bath	48 h at 50°C
Enzyme treatment II	1 mL of Cellulase enzyme solution (*Aspergillus* sp.) Na-acetate buffer (1 M, pH 4.8, 80 mL) water bath	48 h at 50°C
Oxidation II	H_2O_2 (10 vol.%, 80 mL) water bath	24 h reaction under heating (50°C), 48 h at room temperature
Density separation II	$ZnCl_2$ (≥1.6 g cm^{-3}, 150 mL) separatory funnel (glass, 250 mL, glass lid, PTFE stopcock)	24 h settling, release, filtration and rinsing
Storage in ethanol	Ethanol (50-70 vol.%) water bath with nitrogen flow	Evaporation until sample is dry, then suspension in 5 mL

B) Setup of and identification with µ-FT-IR imaging	
Microscope	Cary 670, Agilent Technologies, 15× Cassegrain objective
Detector	Mercury-cadmium-telluride detector
Captured wavelength range	850-3750 cm^{-1}
Measurement mode	Transmission mode, beam attenuation throughput 50%
FPA and pixel resolution	128×128 FPA, pixel resolution 5.5 µm, 8 cm^{-1} instrumental resolution
Background scans	120
Sample carrier	ZnSe window, 13mm diameter, 2 mm thickness
Sample volume	200-300 µL per window, 2 replicates per sample (sample volume 5.0 mL)

Supplementary Table S7 (continued)

C) Quality control measures	
General contamination control measures	See Supplementary Table S5 for general contamination control measures.
Additional contamination control measures	• Repeated filtration of all solutions used for sample treatment ($ZnCl_2$, H_2O_2, SDS, Na-acetate buffer solution, TRIS buffer solution, ethanol) through quartz fibre filters (glass microfiber filter, Whatman, GF/B grade, nominal mesh width 3 µm). • Thorough rinsing of all containers (glassware, filters, etc) with ultrapure water (Milli-Q) prior to use. • For transport of suspended particles, samples were transferred to glass culture tubes (rinsed with ultrapure water) with PTB lids and PTFE inlets, and an additional Al-foil to avoid contamination.
Negative control	Blank samples (n=3), including all sample treatment steps were not used for correction, but to determine potential contamination during sample treatment: • Analyzed volumes of total sample (5 mL), detected number of MPs: o 1.0 mL (20%), 4 MPs o 0.7 mL (14%), 4 MPs o 0.8 mL (16%), 0 MPs • Upscaled number of MPs in total sample: 20, 29, 0 MPs • Theoretical error expected for a soil sample (100 g): 200, 286, 0 particles kg^{-1}, mean 160±150 particles kg^{-1}
Methodological limitations	• Only plastic types with densities below 1.6 g cm^{-3} (density of the prepared $ZnCl_2$ solution) • Theoretical size limitations: 10-500 µm (mesh and sieve width respectively) and resulting exclusion of all particles >500 µm o 1.8 % of all detected MPs in sewage sludge amended soil o Polyester 50 %, PP 25 %, PE 24 %; mostly fibrous (89 %)

Supplementary Table S8. List of all plastic types detected by µ-FT-IR imaging in filed soil samples and the respective classification or exclusion criteria.

Plastic type		**Total detected (nbr)**	**(%)**	**Comment**	**Total rejected (nbr)**	**(%)**	**Exclusion criteria**
polyester (includes PET)		3269	32	*NA*	21	1.32	*NA*
polypropylene	PP	2180	22	*NA*	868	54.70	peaks for identification ambiguous
polyethylene	PE	1059	11	*NA*	70	4.41	*NA*
acrylic		810	8.0	*NA*	4	0.25	*NA*
polyamides	PA	786	7.8	*NA*	9	0.57	*NA*
polystyrene	PS	563	5.6	*NA*	30	1.89	*NA*
epoxy/phenoxy resins		425	4.2	*NA*	4	0.25	*NA*
polyurethane	PU	198	2.0	*NA*	3	0.19	*NA*
cellulose ester		154	1.53	excluded	154	9.70	peaks for identification ambiguous
silicone		133	1.32	excluded	133	8.38	peaks for identification ambiguous
anti-fouling paint		111	1.1	excluded	111	6.99	peaks for identification ambiguous

Supplementary Table S8 (continued)

Plastic type		Total detected (nbr)	(%)	Comment	Total rejected (nbr)	(%)	Exclusion criteria
poly(vinylpyrrolidone co-vinyl acetate)		96	0.95	<5% in any sample, 'other'	66	4.16	
polyvinylchloride	PVC	91	0.9	<5% in any sample, 'other'	6	0.38	
vinyl chloride copolymer		42	0.42	<5% in any sample, 'other'	0		
acrylonitrile butadiene styrene	ABS	31	0.31	<5% in any sample, 'other'	4	0.25	
ethylene-vinyl acetate	EVA	29	0.29	<5% in any sample, 'other'	27	1.70	
polyetherimide	PEI	21	0.21	<5% in any sample, 'other'	20	1.26	
polyvinyl alcohol	PVOH	20	0.2	<5% in any sample, 'other'	4	0.25	
polyvinylidene fluoride	PVDF	16	0.16	excluded	16	1.01	poor spectral fit
modified cellulose		14	0.14	excluded	14	0.88	peaks for identification ambiguous
polyoxymethylene	POM	13	0.13	<5% in any sample, 'other'	13	0.82	
alkyd		10	0.10	<5% in any sample, 'other'	1	0.06	
polycarbonate	PC	5	0.05	<5% in any sample, 'other'	2	0.13	
polytetrafluoro-ethylene	PTFE	5	0.05	excluded	5	0.32	used in sample preparation (stopcock, lids)
poly(dially isophtalate)		2	0.02	excluded	2	0.13	poor spectral fit
alkyl		1	0.01	<5% in any sample, 'other'	0		
polyacrylamide		1	0.01	<5% in any sample, 'other'	1	0.06	
Total number		10085			1588		

__bold__: plastic types that constitute ≥5% in any sample*

Supplementary Figure S3. Example of the absorbance spectra of a particle classified as polypropylene in comparison to reference spectra for polypropylene and 'fake polypropylene', likely organic matter.

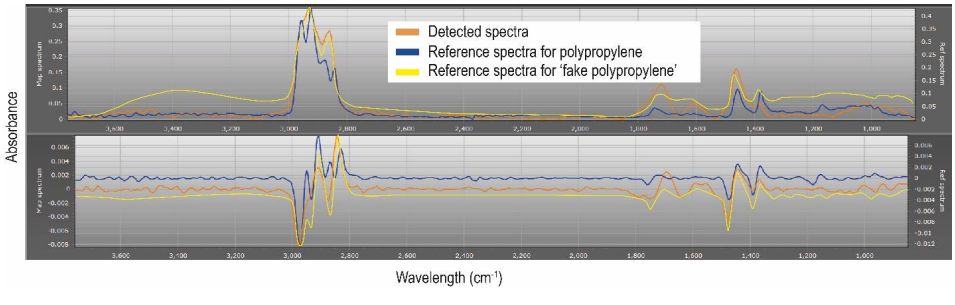

SUPPLEMENTARY MATERIAL S5. OVERVIEW OF SOFTWARE AND R PACKAGES USED FOR DATA PROCESSING

Supplementary Table S9. Softwares and R packages used for data processing of Py-GC/MS and µ-FT-IR imaging data, including references.

Dataset	Type	Name	Reference
Py-GC/MS	Software	OpenChrom	Wenig, P.; Odermatt, J. OpenChrom: A Cross-Platform Open Source Software for the Mass Spectrometric Analysis of Chromatographic Data. BMC Bioinformatics 2010, 11, 405. https://doi.org/10.1186/1471-2105-11-405.
	R package	magrittr	Bache, S., Wickham, H. (2022). _magrittr: A Forward-Pipe Operator for R_. R package version 2.0.3, https://CRAN.R-project.org/package=magrittr.
	R package	data.table	Dowle, M., Srinivasan, A. (2021). _data.table: Extension of `data.frame`_. R package version 1.14.0, https://CRAN.R-project.org/package=data.table.
	R package	envalysis	Steinmetz, Z. (2021). _envalysis: Miscellaneous Functions for Environmental Analyses_. R package version 0.5.1, https://CRAN.R-project.org/package=envalysis.
	R package	readxl	Wickham, H., Bryan, J. (2023). _readxl: Read Excel Files_. R package version 1.4.3, https://CRAN.R-project.org/package=readxl.
	R package	multcomp	Hothorn, T., Bretz, F., Westfall, P. (2008). Simultaneous Inference in General Parametric Models. Biometrical Journal 50(3), 346--363.
	R package	xtable	Dahl, D., Scott, D., Roosen, C., Magnusson, A., Swinton, J. (2019). _xtable: Export Tables to LaTeX or HTML_. R package version 1.8-4, https://CRAN.R-project.org/package=xtable.
	R package	ggsignif	Ahlmann-Eltze, C., & Patil, I. (2021). ggsignif: R Package for Displaying Significance Brackets for 'ggplot2'. PsyArxiv. doi:10.31234/osf.io/7awm6
	R package	ggrepel	Slowikowski, K. (2023). _ggrepel: Automatically Position Non-Overlapping Text Labels with 'ggplot2'_. R package version 0.9.3, https://CRAN.R-project.org/package=ggrepel.
	R package	patchwork	Pedersen, T. (2020). _patchwork: The Composer of Plots_. R package version 1.1.1, https://CRAN.R-project.org/package=patchwork.
	R package	viridis	Garnier, S., Ross, N., Rudis, R., Camargo, A.P., Sciaini, M. and Scherer , C. (2021). Rvision - Colorblind-Friendly Color Maps for R. R package version 0.6.2.
	R package	OpenSpecy	Cowger, W., Steinmetz, Z. (2021). _OpenSpecy: Analyze, Process, Identify, and Share, Raman and (FT)IR Spectra_. R package version 0.9.2, https://CRAN.R-project.org/package=OpenSpecy.
µ-FT-IR	software	siMPle	Primpke, S.; Cross, R. K.; Mintenig, S. M.; Simon, M.; Vianello, A.; Gerdts, G.; Vollertsen, J. Toward the Systematic Identification of Microplastics in the Environment: Evaluation of a New Independent Software Tool (siMPle) for Spectroscopic Analysis. Appl. Spectrosc. 2020, 0003702820917760. https://doi.org/10.1177/0003702820917760.
	R package	dplyr	Wickham, H., François, R., Henry, L., Müller K, Vaughan D (2023). _dplyr: A Grammar of Data Manipulation_. R package version 1.1.2, https://CRAN.R-project.org/package=dplyr.
	R package	scales	Wickham H, Seidel, D. (2022). _scales: Scale Functions for Visualization_. R package version 1.2.1, https://CRAN.R-project.org/package=scales.
	R package	readr:	Wickham, H., Hester, J., Bryan, J. (2023). _readr: Read Rectangular Text Data_. R package version 2.1.4, https://CRAN.R-project.org/package=readr.

	R package	tidyverse	Wickham, H., Averick, M., Bryan, J., Chang, W., McGowan, L.D., François, R., Grolemund, G., Hayes, A., Henry, L., Hester, J., Kuhn, M., Pedersen, T.L., Miller, E., Bache, S.M., Müller, K., Oom, J., Robinson, D., Seidel, D.P., Spinu, V., Takahashi, K., Vaughan, D., Wilke, C., Woo, K., Yutani, H. (2019). "Welcome to the tidyverse." _Journal of Open Source Software_, *4*(43), 1686. doi:10.21105/joss.01686, https://doi.org/10.21105/joss.01686.
	R package	cowplot	Wilke, C. (2020). _cowplot: Streamlined Plot Theme and Plot Annotations for 'ggplot2'_. R package version 1.1.1, https://CRAN.R-project.org/package=cowplot.
Data visualization	R package	ggplot2	Wickham. H. ggplot2: Elegant Graphics for Data Analysis. Springer-Verlag New York, 2016.

SUPPLEMENTARY MATERIAL S6. ESTIMATING MASS CONCENTRATIONS BASED ON PARTICLE METRICS

Supplementary Table S10: Comparison of averages of measured mass concentration (Py-GC/MS based, <2 mm), particle concentration (µ-FT-IR based, <500 µm) and estimated mass concentration following particle-to-mass conversion (mg kg^{-1}) with µ-FT-IR derived parameters. The conversion method integrated in the siMPle software (Primpke *et al*., 2019, 2017) was used, based on particle size and type-specific density (PE: 0.935 g cm^{-3}; PP: 0.905 g cm^{-3} and PS 1.048 g cm^{-3}) as given by Simon *et al.* (2018).

Sewage sludge treated soil			
Depth (cm)	**Py-GC/MS based: measured (mg kg^{-1})**	**µ-FT-IR based: measured (particles kg^{-1})**	**µ-FT-IR based: estimated (mg kg^{-1})**
	PE		
0-20	1.1±0.4	8000±3700	2.1±0.4
20-30	0.7±0.4	4600±400	1.3±0.7
30-40	0.7±0.8	3600±1400	0.6±0.3
	PP		
0-20	0.2±0.3	6500±2300	0.9±0.5
20-30	0.1±0.1	4100±600	0.4±0.2
30-40	0±0	4000±1100	0.09±0.04
	PS		
0-20	0.1±0.1	2500±1000	0.2±0.1
20-30	1.5±2.9	2400±700	0.09±0.04
30-40	0.02±0.01	1500±900	0.09±0.06
Mineral fertilizer treated soil			
	PE		
0-20	0.04±0.04	1600±1300	0.4±0.2
20-30	0.04±0.05	1800±1100	0.2±0.3
30-40	0.00±0	900±600	0.04±0.04
	PP		
0-20	0.00±0	9200±16500	0.5±0.8
20-30	0.04±0.08	1800±1600	0.1±0.1
30-40	0.00±0	1200±900	0.1±0.1

Supplementary Table S10 (continued)

	PS		
0-20	0.02±0.04	3500±3600	0.2±0.3
20-30	0.04±0.06	1200±1300	0.04±0.04
30-40	0.10±0.07	230±100	0.02±0.01

REFERENCES

Primpke, S., Dias, P., Gerdts, G., 2019. Automated Identification and Quantification of Microfibres and Microplastics. Anal. Methods 11. https://doi.org/10.1039/C9AY00126C

Primpke, S., Lorenz, C., Rascher-Friesenhausen, R., Gerdts, G., 2017. An automated approach for microplastics analysis using focal plane array (FPA) FTIR microscopy and image analysis. Anal Methods 9, 1499–1511. https://doi.org/10.1039/C6AY02476A

Simon, M., Alst, N. van, Vollertsen, J., 2018. Quantification of microplastic mass and removal rates at wastewater treatment plants applying Focal Plane Array (FPA)-based Fourier Transform Infrared (FT-IR) imaging. Water Res. 142, 1–9. https://doi.org/10.1016/j.watres.2018.05.019

Steinmetz, Z., Kintzi, A., Muñoz, K., Schaumann, G.E., 2020. A simple method for the selective quantification of polyethylene, polypropylene, and polystyrene plastic debris in soil by pyrolysis-gas chromatography/mass spectrometry. J. Anal. Appl. Pyrolysis 104803. https://doi.org/10.1016/j.jaap.2020.104803

II

Environmental Science & Technology

pubs.acs.org/est

Article

Nanoplastic Transport in Soil via Bioturbation by *Lumbricus terrestris*

Wiebke Mareile Heinze, Denise M. Mitrano, Elma Lahive, John Koestel, and Geert Cornelis*

Cite This: *Environ. Sci. Technol.* 2021, 55, 16423−16433

Read Online

ACCESS | Metrics & More | Article Recommendations | Supporting Information

ABSTRACT: Plastic pollution is increasingly perceived as an emerging threat to terrestrial environments, but the spatial and temporal dimension of plastic exposure in soils is poorly understood. Bioturbation displaces microplastics (>1 μm) in soils and likely also nanoplastics (<1 μm), but empirical evidence is lacking. We used a combination of methods that allowed us to not only quantify but to also understand the mechanisms of biologically driven transport of nanoplastics in microcosms with the deep-burrowing earthworm *Lumbricus terrestris*. We hypothesized that ingestion and subsurface excretion drives deep vertical transport of nanoplastics that subsequently accumulate in the drilosphere, i.e., burrow walls. Significant vertical transport of palladium-doped polystyrene nanoplastics (diameter 256 nm), traceable using elemental analysis, was observed and increased over 4 weeks. Nanoplastics were detected in depurated earthworms confirming their uptake without any detectable negative impact. Nanoplastics were indeed enriched in the drilosphere where cast material was visibly incorporated, and the reuse of initial burrows could be monitored via X-ray computed tomography. Moreover, the speed of nanoplastics transport to the deeper soil profile could not be explained with a local mixing model. Earthworms thus repeatedly ingested and excreted nanoplastics in the drilosphere calling for a more explicit inclusion of bioturbation in nanoplastic fate modeling under consideration of the dominant mechanism. Further investigation is required to quantify nanoplastic re-entrainment, such as during events of preferential flow in burrows.

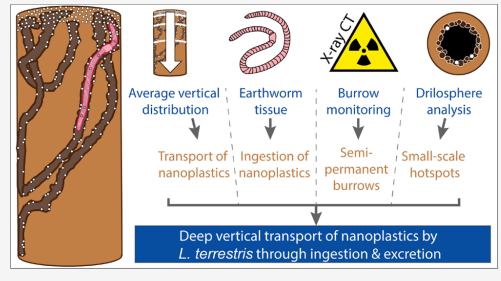

KEYWORDS: *Microplastic, transport, fate, exposure, X-ray computed tomography, earthworms*

INTRODUCTION

While plastic pollution has been acknowledged as a major challenge for the marine environment,[1] recent material flow estimates suggest that comparably more plastic is emitted to soils.[2,3] Plastics can make their way into soils from diffuse sources, such as mismanaged waste, littering, or as secondary particles from plastic products fragmenting during their use or originating from traffic.[2,4−7] Agricultural soils are exposed to plastics via application of sewage sludge,[8−11] compost,[12] manure,[13] or other biosolids as soil amendments[14] and with irrigation water[4] or when microplastics are released from macroplastics used in agriculture such as mulching films[15] or packaging material.[16] Of the emitted plastic, micro- (≤5 mm) and nanoplastics (≤1 μm) are considered problematic due to their potential mobility and susceptibility to ingestion by soil organisms.[5,17−19] Moreover, there is increasing evidence that these plastic particles can induce changes in soil properties[20−23] or exert effects on terrestrial microbial communities,[24] plants,[21,25] or other soil biota either directly or indirectly.[26−32]

Effects on terrestrial organisms exposed to micro- or nanoplastics are often expressed as a function of average concentrations in the soil, but the smaller scale spatial distribution of contaminants in soils is often more important than average concentrations for their bioavailability and subsequent effects.[20,33] Our understanding of the terrestrial fate and spatial distribution of microplastics and particularly nanoplastics within the soil profile is still fragmentary,[5,34] making it challenging to reliably assess the exposure of soil organisms or the long-term fate of these particles. At the same time, the abundance of nonbiodegradable nanoplastics in soils is expected to increase over time as plastic emissions continue and larger particles already present in the soil gradually fragment.[35] Understanding the spatial distribution and mobility of nanosized plastics in soil will therefore become more important in the future.

Advective transport of nanoplastics with water has been studied comparably well, usually using packed column tests.[36−41] These tests tend to find low particle mobility when the water content of the soil is low,[42−44] because particles tend to accumulate at air−water interfaces that are numerous in nonsaturated soils.[45] However, soils are rarely

Received: August 20, 2021
Revised: October 25, 2021
Accepted: November 15, 2021
Published: December 8, 2021

https://doi.org/10.1021/acs.est.1c05614
Environ. Sci. Technol. 2021, 55, 16423−16433

water saturated, making transport mechanisms other than advective transport potentially more relevant. A transport process that has been largely neglected in terrestrial exposure assessments is bioturbation, the restructuring of the soil by burrowing soil organisms. In particular, the role of deep-burrowing (anecic) earthworms may be important, as they break down and incorporate organic matter in the soil and their burrowing behavior facilitates soil aeration and drainage.[46−49] In doing so, they contribute to the movement of particles in the soil, not only organic matter[50,51] but also pollutants sorbed to mineral surfaces or particulate pollutants,[50−53] including inorganic nanoparticles.[54]

Particle transport by earthworm bioturbation is a combined result of mechanical soil mixing, particles attaching and detaching from the organism surface, and ingestion and excretion dynamics.[52−55] The contributions of the different bioturbation mechanisms may have implications for the resulting spatiotemporal distribution pattern within the soil profile. Local mixing has been previously used to model transport of engineered nanomaterials and is considered to result in gradual redistribution patterns resembling diffusion.[54,56] In contrast, ingestion and subsurface excretion may result in longer transport distances at a shorter time span.[57] First investigations have given qualitative indications that earthworms cause vertical transport of microplastics in the soil profile.[29,53,58] Earthworms were observed to ingest microplastics[59] and incorporate them into the soil.[58] Some authors have suggested nanoplastics would be similarly transported, albeit without providing empirical evidence.[60] Considering that initial investigations on microplastics showed increasing transport with decreasing size,[53] it appears reasonable that nanoplastics could be more susceptible to biologically driven transport and, in particular, ingestion/excretion dynamics. However, experimental evidence for nanoplastics uptake by earthworms and biologically mediated transport is still lacking. This is in part due to the challenges associated with the extraction and detection of nanoplastics in materials that contain organic carbon such as soils.[61−63] Established detection methods for microplastics either omit the nanosized fraction because of size limitations in the case of spectroscopic methods[64,65] or experience difficulties in detecting small mass concentrations in the case of thermoanalytical methods.[66]

The aim of this study was to assess the impact of earthworms on nanoplastics in soil, with a particular focus on the spatiotemporal dynamics and mechanisms of biologically mediated nanoplastics transport. We hypothesized that nonlocal transport by ingestion and excretion is the main mechanism causing vertical redistribution of nanoplastics in soil profiles. To this end, we performed process studies in microcosms with a deep-burrowing earthworm species, *Lumbricus terrestris*, using a combination of methods that would allow us to more closely understand the mechanisms of biologically mediated transport. We used metal-doped spherical polystyrene nanoplastics to allow for quantitative analysis in soil samples even at dilute concentrations. In a first step, we quantified the time-dependent vertical redistribution of nanoplastics within soil profiles. In a second step, we used X-ray computed tomography (CT) to monitor the earthworm burrow system development and thus mechanistically investigate how bioturbation transports nanoplastics. Finally, the presence of nanoplastics in the drilosphere versus the soil matrix was investigated to explore the potential formation of plastic hotspots following bioturbation. A better quantitative understanding of the transport mechanisms of nanoplastics in soils will provide more accurate estimations of exposure over more extended time periods, which in turn will enable more robust risk assessment and better informed environmental regulation.

MATERIALS AND METHODS

Nanoplastics. We synthesized metal-doped spherical polystyrene nanoplastics, as described in detail by Mitrano et al.,[67] for investigating transport of nanoplastics by bioturbation. Using the palladium (Pd) label as a proxy to measure the plastic allowed us to more easily measure plastic transport. Pd was incorporated into the center of the particle, so that the surface of the particle was composed entirely of polymer material. Only negligible Pd leaching from these nanoplastic particles was found in experimental systems in previous studies,[10,41,68] ensuring that Pd is a conservative tracer for nanoplastic particles. Moreover, we consider the particles to remain intact throughout the study period, because polystyrene has negligible biodegradation rates in soils.[69,70] The content of the metal tracer corresponded to 0.24% w/w of the plastic particles, determined based on dry weight of the nanoplastic suspension (after drying 48 h at 60 °C, $n = 3$) and microwave-assisted *aqua regia* extraction of Pd as described below. A Z-average hydrodynamic diameter of 256 ± 4 nm and a polydispersivity index of 0.096 ± 0.02 ($n = 12$) were found using dynamic light scattering (Malvern Zetasizer Nano ZS), confirming previous measurements on similar batches. Details on particle characterization are provided in the Supporting Information (Supplementary Table S1).

Soil. We used topsoil from the plough layer of a former agricultural site in Sprowston, UK (WGS 84:387724, 5835408). The soil selection was based on earthworm habitat requirements and the high relevance of plastic pollution for agricultural soils. The soil was classified as a sandy loam (60% sand, 28% silt, 12% clay), with a pH of 7.2−7.6 and 5.0% w/w organic matter. According to the measured soil properties (Table S2), we considered the soil typical for an agricultural plough layer affected by common management practices. The background concentration of Pd in this soil, measured after *aqua regia* digestion, was 32 ± 4 $\mu g\ kg^{-1}$ ($n = 6$).

Earthworms. Adult individuals of the deep-burrowing (anecic) earthworm species *Lumbricus terrestris* were purchased for bioturbation experiments (Wormsdirect, UK). Before being introduced to the microcosms, earthworms were depurated for 48 h. Individuals were rinsed with water, placed in Petri dishes with damp filter paper and kept in the dark at 13 °C to allow them to void their gut. Earthworm casts, i.e., excreted material, were regularly removed to avoid re-eating.[71] The wet weight of depurated individuals was documented before and after the experiment.

Bioturbation Microcosms. Two bioturbation experiments were established, addressing the two distinct aims of this study. The first experiment (Exp 1) served to determine the average vertical redistribution of nanoplastics in the soil profile. The second experiment (Exp 2) aimed at shedding light on the associated transport mechanisms by measuring nanoplastics concentrations in the drilosphere versus soil matrix, while also monitoring burrow development. The drilosphere is the soil layer around the burrows, where earthworm activity directly changes the soil structure and composition, and can extend to up to 8 mm from the burrow wall for *L. terrestris*.[72] Microcosms with earthworms were established in an identical

https://doi.org/10.1021/acs.est.1c05614
Environ. Sci. Technol. 2021, 55, 16423−16433

manner in both experiments but sampled differently according to the aims of the study.

The microcosms consisted of polyvinyl chloride (PVC) cylinders (10 cm diameter) packed with moistened soil to a total depth of 30 cm with an average bulk density of 1.24 ± 0.03 g cm^{-3} (Figure S1). At the bottom of each cylinder, a thin layer of sand (1 cm) and an aluminum mesh (1 mm mesh size) allowed free water drainage and aeration. A glass-fiber mesh (2 mm) prevented earthworms from escaping through the top. For treatments with plastics, the uppermost 2 cm of soil were spiked with nanoplastics before addition to the soil column. The spiking was done by thoroughly mixing a fraction of the soil with the nanoplastics suspension and then sequentially adding and mixing in the remaining soil. The total nanoplastic concentration for each microcosm was 0.56 g kg^{-1} or 0.06% (equivalent to 10.8 g kg^{-1} or 1.08% in the spiked layer). While these concentrations are relatively high within the spiked layer, they allowed for the detection of nanoplastics in low concentrations when transported into previously uncontaminated soil. Moreover, our concentrations were still lower than in other bioturbation and effect studies[14,28−30,58] because we aimed to use concentrations which were likely to be present in the environment. Soil moisture was kept at 40%−50% of the water holding capacity corresponding to habitat preferences of earthworms. The water content was maintained via recurring applications of ultrapure water (18.3 mΩ) via spraying, corresponding to an average precipitation of 8.3 ± 1.3 mm per week distributed over two to three application instances (Table S3). Convective transport of nanoplastics either in micro- or macropores is unlikely in these conditions because of the relatively low precipitation rate applied in this study[73] and unsaturated conditions that enhance particle deposition.[45] Three depurated earthworms were introduced into each column, corresponding to a density of 382 individuals m^{-2}. Although this stocking density is relatively high, it is not uncommon for some land uses, such as temperate pastures.[71] The columns were kept in a growth chamber (CLF Plant Climatics) at 13 °C with 60% relative humidity and continuous daylight (24 h) to minimize the risk of earthworms escaping. A litter layer of oven-dried, crushed leaves (*Tilia cordata*) was added on top as feed at the beginning of the study (4 g). An additional 2 g were added after 2 weeks. For the second experimental set (Exp 2), the leaf litter composition was changed due to seasonal availability (*Fagus sylvatica*).

Measuring the Average Vertical Redistribution of Nanoplastics in Microcosms (Exp 1). In the first set of experiments, treatments comprised microcosms with *L. terrestris* and plastic-spiked soil (n = 12) and control microcosms with nanoplastics but no earthworms (n = 3). At weekly intervals, i.e., after 7, 14, 21, 28 days, three replicate microcosms were destructively sampled by pressing the soil column out of the PVC cylinder and sectioning at depths 0−2, 2−6, 6−15, and 15−29 cm, hereafter referred to as layers 1−4 (Figure S1). The bottom 1 cm of soil was discarded to avoid dilution effects from the sand. We selected a greater vertical resolution at the top of the column since we anticipated a larger change in nanoplastic concentrations closer to the spiked top layer. Control microcosms with added nanoplastics but without earthworms were sampled after 28 days to assess nanoplastics transport induced only by water applications.

Association of Nanoplastics with Earthworm Burrows (Exp 2). During the second set of experiments, X-ray computed tomography (CT) scans were performed weekly to monitor the earthworm burrow system development. Treatments included control microcosms without worms and plastics (n = 3), microcosms with *L. terrestris* (n = 3), and microcosms with *L. terrestris* and plastics (n = 3). After the final X-ray CT scan, i.e., after 28 days, the microcosms were frozen, followed by targeted sampling of the drilosphere and soil matrix to better understand the local spatial distribution of plastics within each sampling layer. Here, soil matrix is defined as being at least 1.5 cm away from any burrow and visually showing no structures indicative of previous earthworm presence. For accessing burrows and unaffected soil matrix, the frozen soil columns were removed from the PVC cylinder. The drilosphere was sampled by carefully scratching off the burrow walls with a metal spoon during thawing at selected sites, where the burrow was intact and accessible, resulting in the analysis of four and three burrows for replicates 1 and 2, respectively. Figure 1 shows an example of the burrow systems,

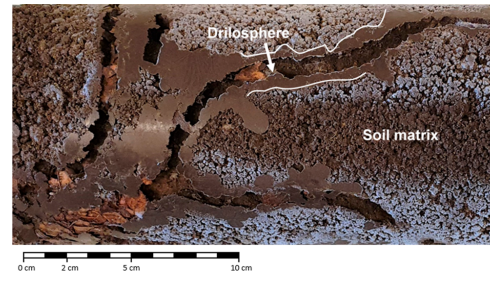

Figure 1. Example of burrows in a soil column after 28 days showing the drilosphere and soil matrix (Exp 2). The different texture of material around burrows is due to casts of earthworms and shows excretion occurs throughout burrows.

while the exact sampling locations are documented in Figure S2. One replicate was accidentally dropped and destroyed on day 22, so sampling for drilosphere and matrix was only done for two column replicates. The soil matrix samples were taken near the column wall and in the center of the column. The samples were categorized according to the layers they were extracted from.

X-ray CT Image Acquisition, Processing and Analysis. X-ray CT has been previously successfully applied to determine biopore volume and monitor earthworm burrow development.[54,55,74] We scanned the microcosms using an industrial X-ray scanner (GE Phoenix v|tome|x 240) in quick scan mode to minimize the radiation exposure of earthworms (see Table S4 for details). The acquired projections were reconstructed into a sequence (image stacks) of cross-sectional images of the column (GE software datos|x, version 2.1). The cross-sectional images (slices) are grids of voxels of 150 μm size, each with a specified gray value that reflects the attenuation of the X-rays by the material present inside a given voxel. As a result, image parts corresponding to specific materials can be extracted, such as air-filled macropores.

Image processing and analyses were carried out using the ImageJ/FIJI software[75,76] together with the SoilJ plug-in.[77] First, the imaged columns were moved to the center of the 3-D image canvas, and the coordinates of the PVC wall were detected. The gray values in all horizontal image cross sections were then normalized to standardized values for air-filled pores

https://doi.org/10.1021/acs.est.1c05614
Environ. Sci. Technol. 2021, 55, 16423−16433

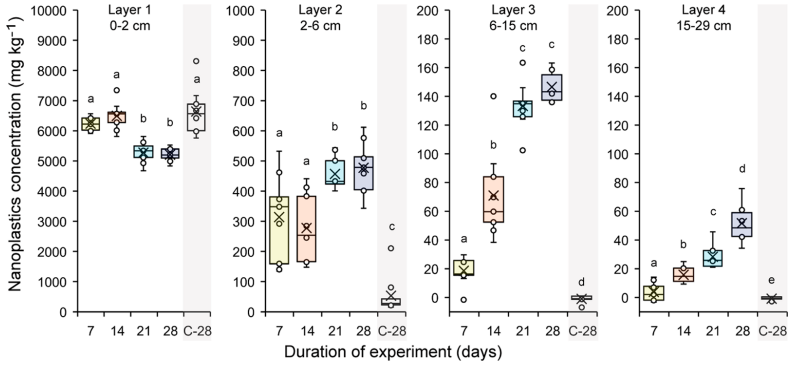

Figure 2. Concentrations of nanoplastics at different soil profile depths across burrowing times by *Lumbricus terrestris* (7, 14, 21, 28 days) and for control columns without *L. terrestris* sampled after 28 days shaded in gray (C-28). Box plots represent the distribution of the first to third quartile. Whiskers display the minimum and maximum (excluding outliers). Points represent individual data points. The lines within the box plots mark the median, and crosses mark the mean. Observations with the same letters do not show significant differences across the respective depth layer ($p > 0.05$).

and the column material.[77] A joint histogram of the gray values in all 3-D images was compiled on which we determined a joint segmentation threshold as described in Koestel et al.[78] (Figure S3). The following image segmentation resulted in binary images with voxels assigned to one of the two material classes,[77,79] i.e., soil pores or soil matrix, the latter also including organic material and earthworms. When earthworms were present inside the burrows in the segmented images, they were manually removed in slice-by-slice editing. For each column, approximately identical regions of interest were analyzed to monitor changes in the earthworm burrow structure across the four measurement instances, with a final average soil column length of 28.6 ± 0.3 cm considered for analysis (0.75 ± 0.34 cm below soil surface, 0.54 ± 0.22 cm cut off at the bottom). Using the PoreSpaceAnalyzer tool in SoilJ,[77] a 3-D map depicting the pores color coded by diameter was computed and used to filter out pores which were too small to be associated with earthworm burrows. A minimum pore-diameter threshold (≥3.5 mm spherical size) and a volume threshold (≥0.084 cm^3) were visually determined and applied to all images. We then quantified the burrow volume (cm^3) per depth layer and in total for each soil column. The respective share of the burrow pore volume per depth layer in relation to the total burrow pore volume of the soil column was then calculated, hereafter referred to as biomacroporosity. This allowed us to compare the spatial distribution of the burrows between the treatments with and without plastics. The visualization of the burrow system was done with the software Drishti (v2.7).[80] The processing workflow is provided in Figure S4.

Detection of Nanoplastics in Earthworm Tissue, Soil from Depth Layers, and Drilosphere Samples. Soil and drilosphere samples were oven dried (105 °C, 3 days), homogenized, and subsamples taken in triplicate for analysis by successive halving into half-lots. During the first set of experiments (Exp 1), earthworms collected from columns were rinsed, depurated, and weighed, rinsed again, sacrificed by freezing, and dried in a freeze dryer. Dried earthworm tissue was pretreated with 1.5 mL hydrogen peroxide (H_2O_2) overnight. Soils and pretreated earthworm tissue samples were then digested using *aqua regia*[81] in a closed microwave-assisted system (Milestone Ethos Easy, MAXI-44, 80 mL PTFE vessels) following EPA 3051a guidelines.[82] Pd was measured in digests (diluted 1:10 times for soil samples and 1:5.6 times for earthworm samples) using inductively coupled plasma mass spectrometry (ICP-MS, PerkinElmer Nexion 350D) with a detection limit of 0.09 μg L^{-1} and a quantification limit of 0.29 μg L^{-1} (n = 5). The calibration standards were matrix matched to diluted *aqua regia*, and ^{115}In was used as an internal standard. Detected Pd concentrations were corrected for procedural blanks and background concentration of the respective matrix (Supporting Information S1). Plastic concentrations were then derived from the measured Pd concentrations using the known Pd-to-plastic ratio. General quality assessment measures, i.e., procedural blanks and spike recoveries, were routinely included. For ensuring detectability of Pd in digests, spike recovery of Pd after digestion was tested in digestion vessels without any matrix (99 ± 8%), and in the presence of soil (83 ± 8%) or earthworm tissue (88 ± 4%). Similarly, the extraction efficiency of plastic-incorporated Pd for the optimized method remained above 91% when spiked into soil (Figure S5). Details on solvents and specifics of the digestion protocols can be found in the Supporting Information S1.

Statistical Analysis. Two-tailed t tests assuming equal variance were run for testing statistical significance of differences between detected plastic concentrations in earthworm tissues and in soil samples across different sampling time points, as well as in drilosphere and soil matrix samples. Additionally, the significance of differences in burrow pore volume in microcosms in the presence versus absence of plastics was tested. Significance tests were executed in Microsoft Excel choosing significance levels of 95%. Nanoplastic mass balances were calculated using the dry weight and the detected nanoplastic concentrations for the respective soil layer in comparison to the initial spike added to each column.

Modeling Nanoplastic Transport. Vertical nanoplastics transport by bioturbation was modeled using the simple one-dimensional bioturbation model developed by Rodriguez,[83] which was previously successfully applied for silver sulfide

https://doi.org/10.1021/acs.est.1c05614
Environ. Sci. Technol. 2021, 55, 16423−16433

nanoparticles.[54] The model is described in detail elsewhere,[54,83] and relevant equations are provided in Supporting Information S2. In brief, the model allows for the prediction of the depth-dependent concentrations for a substance as a function of time based on soil mixing rates. Mixing occurs only between adjacent soil depth segments and is assumed to be proportional to earthworm density. The mixing rate is determined semiempirically using the earthworm density and a fitting parameter that was derived by minimizing the sum of squared differences between experimental and modeled logarithmic concentrations. Thus, vertical transport in the model resembles advective transport but is dependent on earthworm density. Logarithmic concentrations were used to ensure that relatively low concentrations in deeper soil layers had similar weight than higher concentrations in top layers during fitting.

RESULTS AND DISCUSSION

Earthworms Are Drivers for Significant Nanoplastic Transport in soil. Deep-burrowing earthworms, *L. terrestris*, were responsible for significant vertical downward transport of nanoplastics in the soil profile (Exp 1, Figure 2). After 1 week, detectable nanoplastic quantities were transported from the uppermost 2 cm of the soil down to the lowest sampling layer. While microcosms in this experiment were limited to 30 cm depth, maximum burrowing depths of *L. terrestris* observed in the field commonly exceed 100 cm.[84] It is thus reasonable to expect that in field conditions the burrowing of anecic earthworm species such as *L. terrestris* can transport nanoplastics deeper in the soil profile than measured here.

Water applications to the columns were purposefully small to keep the focus on the contribution of bioturbation to nanoplastics transport opposed to advective transport. The soil columns were thus far from water saturated. Preferential flow in macropores is only relevant near water saturation.[85] Moreover, nanoplastics tend to interact strongly with air−water interfaces limiting their transport in micropores of nonsaturated soils as well.[45] Accordingly, water-driven nanoplastic transport via earthworm burrows can be considered highly unlikely in our setup. Nanoplastic concentrations in the control columns that were only exposed to water applications without earthworms remained below the Pd background concentration in soil layers deeper than 6 cm even after 28 days of treatment (Figure 2), confirming that, as intended, advective transport was not a major factor in our system. Some nanoplastics were detected in the second layer of these control columns, but these may in part be owed to sampling inaccuracies at the boundary between layer 1, i.e., the initial spike layer, and layer 2. The absence of nanoplastics below 6 cm depth in the control columns is in stark contrast to the nanoplastics measured in deeper soil layers when earthworms were present (Figure 2). Accordingly, it is necessary to explicitly account for bioturbation when investigating nanoplastic fate for unsaturated soils to avoid underestimating their mobility in terrestrial ecosystems.

Our findings on nanoplastics transport complement previous studies that confirmed transport of microplastics (>1 μm) by earthworm burrowing.[53,58] Previous research was generally limited to single time point measurements, neglecting the temporal dimension of transport processes. In our case, nanoplastics were detectable at a depth of 15−29 cm after the first sampling time point (7 days), and extending time led to higher total concentrations of nanoplastics being transferred into the lower soil profile (Figure 2, Table S5). The absolute share of nanoplastics in the lower two layers increased from 1.3% after 7 days to as much as 11.0% after 28 days (Table S6). Rillig et al. found that 50% of the microplastics (710−850 μm) applied to litter was transferred to depths of 7.0−10.5 cm after 21 days.[53] The faster mixing observed in their study may be a combined result of spatial confinement, as only 10.5 cm columns were used by these authors, and the fact that the microplastics were applied to litter. These particles were thus more susceptible for ingestion/excretion because litter serves as feeding source for *L. terrestris*.

Interestingly, we observed that the net influx of nanoplastics into layer 3 was not significantly different between 21 and 28 days ($p > 0.05$), while nanoplastic concentrations significantly increased for layer 4 over the course of the experiment. This could indicate that vertical transport of nanoplastics through bioturbation may not necessarily decrease monotonously with depth. These results also illustrate that bioturbation experiments, in general, should not be conducted as one time point measurements and be extended even beyond 4 weeks for capturing potential temporal variations and longer-term trends.

Earthworms Ingested Nanoplastics, But No Negative Effects Were Observed. Earthworms create their burrows through ingesting soil or moving it mechanically.[49] In our case, the analysis of depurated earthworms confirmed that nanoplastics initially present in the uppermost 2 cm of the soil were ingested, with some residual plastic found in the gut or tissue of individuals (Table S7). The ingestion and excretion of plastic particles, including nanoplastics, by earthworms have similarly been documented elsewhere.[86−88] It is unclear whether these nanoplastics were accumulated in tissues or whether they were still present in the gut due to incomplete depuration, but considering that depuration times of *L. terrestris* can extend beyond the 48 h used in this study, the latter is possible.[89] Earthworms from microcosms that were sampled after 7 days contained higher concentrations of nanoplastics as compared to those sampled in the subsequent weeks (Table S7). During this first week, earthworms needed to establish their burrows, which means they may have spent more time in the top layer of the column where the nanoplastics concentration was highest. In addition, earthworms were starved before the onset of the experiment and were thus more likely to frequent the upper layer to access the leaf litter on the soil surface. Hence, feeding ecology may have contributed to a higher exposure to nanoplastics during the first week of the experiment. Transitions of larger microplastics such as polyethylene beads (710−1400 μm)[53] or polyester fibers (361 ± 387 μm)[90] through the gut and excretion by earthworms have been reported. Thus, the decrease of nanoplastics found in earthworm tissue after prolonged experimental time are likely the result of the majority of ingested nanoplastics being excreted again, in conjunction with earthworms ingesting less of the surface layer of soil because burrows were already established. Overall, neither earthworm mortality nor a significant decrease in earthworm weight were noted in this study despite the uptake of nanoplastics and the higher exposure at the onset of the experiment (Table S7). Additionally, no other visible negative effects such as avoidance of the top layer due to nanoplastics contamination were observed as discussed in the following paragraph.

Earthworm Burrowing Is Not Significantly Altered in the Presence of Nanoplastics. The burrow systems derived from the X-ray CT measurements allowed for the assessment

https://doi.org/10.1021/acs.est.1c05614
Environ. Sci. Technol. 2021, 55, 16423−16433

of the activity of *L. terrestris* in the microcosms contaminated by nanoplastics compared to uncontaminated soil (Exp 2, Figure 3). Earthworms established their principal burrow

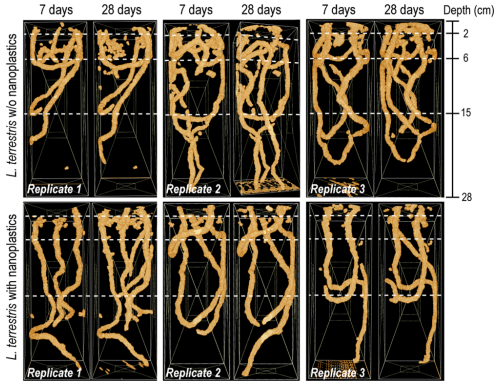

Figure 3. 3-D images of the burrow system of *L. terrestris* derived from X-ray CT analysis in experiment 2 (Exp 2) for each replicate column after 7 and 28 days of bioturbation without (top) and in the presence of nanoplastics (bottom). White dotted lines indicate layer boundaries. Note that for replicate 3 with plastics the later image represents 21 days exposure.

system within the first week, a system that generally remained intact over time, in particular, in the lower part of the soil profile. Over the course of the experiment, existing burrows were expanded, but only a limited number of new burrows were produced (Figure 3). *L. terrestris* are known to inhabit semipermanent burrow systems, and their behavior in the columns typified this.[51] Irrespective of the treatment, more burrows were created in the upper parts of the soil column. This was confirmed by the spatial distribution of the biomacroporosity within the soil columns as can be seen in Figure 4, with 60%−90% of earthworm burrows present in the upper half of the soil columns (Table S8).

Visual inspection of the burrow system development (Figure 3) suggested that earthworms were overall less active in the presence of nanoplastics, particularly in close vicinity to the areas initially spiked with nanoplastics (0−6 cm column depth, corresponding to layers 1 and 2) at the onset of the experiment. We therefore compared the biomacropores for the different depth segments of the soil profile between the treatments to assess whether there was quantitative evidence to support the avoidance behavior this pattern suggested. This analysis showed that the absolute biomacropore volume was indeed lower in the presence of nanoplastics, a difference that could mostly be attributed to a lower biomacropore volume encountered in the 0−6 cm depth fraction (19 ± 9 cm^3 with plastics versus 35 ± 8 cm^3 without plastics) (Table S8). However, the difference between the treatments was not significant ($p > 0.05$), and after prolonged bioturbation (i.e., within 14 days), apparent differences in total burrow pore volume and depth distribution fully disappeared (Figure 4). Moreover, burrow expansion in the presence of nanoplastics during that time was mostly occurring in the uppermost two layers (Table S8).

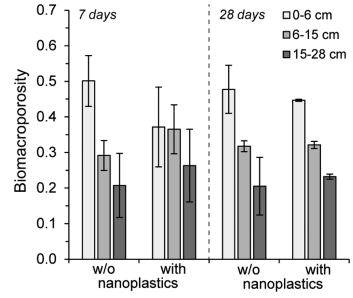

Figure 4. Biomacroporosity in different column segments of experiment 2 after 7 and 28 days of bioturbation without (w/o nanoplastics, $n = 3$) and in the presence of nanoplastics (with nanoplastics, $n = 3$ except after 28 days $n = 2$). Biomacroporosity represents the relative share of the total biopore volume of the respective microcosm soil column for each designated depth layer. The soil column was divided according to sampling layers, with the top two layers merged. Error bars represent standard deviations.

The absence of active avoidance behavior of nanoplastics is in line with observations from another study that used microplastic fibers in an avoidance-specific assay.[90] Note that quantifying ecotoxicological effects was not the primary goal of this study, which may have confounded accurate observation of an avoidance behavior. Avoidance-specific assays are typically carried out with contaminated and uncontaminated soils in equal volumes side by side, allowing the organism to move freely between the soils.[90] At the same time, exposure scenarios in the field are more likely to resemble the approach taken in our study, where the application of plastics would occur at the surface in a shallow layer. Hence, soil biota in the field which typically come to the surface to access food will not necessarily be able to avoid contact with incorporated micro- or nanoplastics, as mimicked in our study.

Ingestion−Excretion Is the Primary Transport Mechanism Causing Vertical Displacement of Nanoplastics in soils. Transport via bioturbation is generally a combined effect of local mechanical mixing resulting from the movement of soil during burrowing, ingestion and excretion of material and through the adhesion of particles to the surface of organisms as they move through the soil. However, the individual contributions of these different transport mechanisms may result in different spatial patterns of nanoplastics distribution within the soil profile, in particular, transport distances.[52] The results of Exp 2 confirm that nanoplastic transport was primarily occurring within the burrows of *L. terrestris*. After 4 weeks, drilosphere samples were analyzed for their nanoplastics concentration in comparison to the soil matrix (Figure 5). Nanoplastics were highly enriched within the drilosphere, whereas concentrations within the soil matrix were orders of magnitude lower and often lower than the Pd background concentration. To our knowledge, this is the first evidence that nanosized plastics can be incorporated into the drilosphere by earthworms, as has been previously observed for microplastics.[58,91]

We infer that nonlocal transport by ingestion and excretion was the dominant mechanism causing the deeper vertical redistribution of nanoplastics in the burrow system for three reasons. First, we confirmed that nanoplastics were ingested and thus also excreted by *L. terrestris*. Second, visual inspection

https://doi.org/10.1021/acs.est.1c05614
Environ. Sci. Technol. 2021, 55, 16423−16433

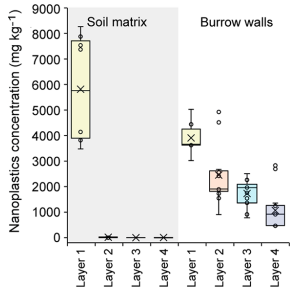

Figure 5. Concentrations of nanoplastics in burrow walls (drilosphere) and unaffected soil matrix at different soil depths after 28 days of soil column exposure to bioturbation by *Lumbricus terrestris*, experiment 2. Results are sorted according to sampling layer. Layer depths correspond to layer 1:0−2 cm, layer 2:2−6 cm, layer 3:6−15 cm, layer 4:15−29 cm. Box plots represent the distribution of the first to third quartile. Whiskers display the minimum and maximum (excluding outliers). Points represent individual data points. The lines within the box plots mark the median, and crosses mark the mean.

confirmed that casts of *L. terrestris* were incorporated into the drilosphere throughout the burrow system, which were easily distinguishable by their fine texture and density (Figure 1). This reworking of burrow walls with cast material is well documented for *L. terrestris*,[47,92,93] and similar hotspot-like patterns have been observed for redistributed organic matter by earthworms.[46] Gut transit times of *L. terrestris* have been estimated at approximately 11.6 h.[94] Earthworms could thus easily have reached deeper soil layers and excreted ingested material.

Finally, local transport through mixing is unlikely to explain the observed deep vertical transfer that was observed after the relatively short experimental times of 7−28 days. At first glance, the significant decline ($p \leq 0.05$) of average nanoplastics concentrations in the drilosphere with increasing burrow depth (Figure 5) suggests local transport through the mechanical movement of soil, i.e., mixing. However, our X-ray CT data shows that mixing after 1 week was mostly restricted to the top of the soil columns where burrows were more actively produced (0−6 cm), and correspondingly, more soil material was moved around (Figure 3). In contrast, vertical burrows reaching down to the lower layers remained intact until the end of the experiment, with only limited expansions or additions (Figure 3, Table S8). Nevertheless, plastic concentrations increased continuously in the bottom two layers of the column (Figure 2) despite this limited mixing. We fitted a bioturbation model based on local mixing, previously found suitable for other nanoparticles,[54] to the observed time- and depth-dependent nanoplastic concentrations. The fitted local transport model correctly estimated the concentrations in the deepest soil layer but systematically overestimated nanoplastic transport to the second and third soil layer (Figure S6, Table S9). In other words, an unusually high soil turnover rate of ca. 25 cm year^{-1} had to be assumed to predict the concentrations in the bottom layer. In comparison, typical turnover rates are in the order of 0.5 cm year^{-1}.[83] The transport of nanoplastics into the deepest soil layer thus proceeds at a faster rate than to the overlying soil layers (Figure S6). As a result, the local mixing model was unable to account for the observed spatial and temporal pattern of nanoplastic transport (Figure S7). Indeed, the distribution of nanoplastics did not always follow a strict depth-dependent trend within an individual burrow crossing different depth segments (Figure S7). In some cases, plastic concentrations in the burrow walls in the lower layer were similar to or exceeded those in the layers above, resulting in small-scale hotspots that indicate nonlocal transport processes. Consequently, ingestion and excretion dynamics are likely the major cause for the deeper vertical transfer that occurred over a timespan as short as 28 days.

Environmental Implications and Limitations. A better understanding of the temporal and spatial dynamics of fate processes affecting nanoplastics is a crucial step toward assessing long-term exposure levels within soils and also understanding the terrestrial contribution to aquatic plastic pollution. Our results show that ingestion and excretion by earthworms transport nanoplastics to the deeper soil layers in relatively short timespans from 7 to 28 days. While the transport of nanoplastics by bioturbation in our study was limited to only 30 cm depth due to restraints in our experimental setup, their transport will likely expand beyond this depth considering the deep burrowing behavior of *L. terrestris*. These results emphasize the need to account explicitly for bioturbation when characterizing nanoplastic fate in soil, but they also suggest that the dominant bioturbation mechanism is relevant. While we did not compare transport of nanoplastics with microplastics, we hypothesize the dominant bioturbation mechanism to be size specific. Ingestion and excretion of nanoplastics are more likely than for larger microplastics.[53] Hence, earthworms likely transport higher numbers of nanoplastics and, at least initially, over larger distances.[57]

Similarly, our observations call for a more critical assessment of exposure assessments, in particular, field sampling approaches for quantifying plastic pollution in soils. The most current studies reporting environmental concentrations of microplastics only analyze the uppermost part of the topsoil, ignoring the potential transport of plastic particles within the soil profile. For more accurate mass estimates and balances on larger scales in the future, considering the vertical distribution in monitoring schemes for micro- and nanoplastics is of importance.

While we only used one soil type under constant climatic conditions, it is important to note that field bioturbation rates differ highly between different localities. Bioturbation rates are highly dependent on the number of bioturbating organisms and species. These in turn depend on climatologic circumstances, physical and chemical soil properties, and land management.[95]

The redistribution of nanoplastics may also carry important implications for local exposure levels. Exposure levels to nanoplastics in the field are likely very heterogeneous as we observed that nanoplastics were highly enriched within the drilosphere. Earthworm burrows and the associated drilosphere can thus become hotspots of nanoplastic pollution. Earthworm species such as *L. terrestris* that move repeatedly through the same burrows and reingest burrow material[46,51] and other organisms that use earthworm burrows and the drilosphere as habitats may be more exposed even if average concentrations within the soil matrix are comparatively lower. Acute negative impacts were not observed in this study, whereas effects of chronic long-term exposure are still unknown.

https://doi.org/10.1021/acs.est.1c05614
Environ. Sci. Technol. 2021, 55, 16423−16433

An enrichment of plastics within the drilosphere may also result in combined effects of water- and bioturbation-driven transport processes. Earthworm burrows serve as pathways for preferential flow of water where flow rates, and thus shear rates, are higher than in micropores.[96] During heavy rainfall events, preferential flows may more easily remobilize nanoplastics and transport them to deeper soil layers and potentially even to shallow groundwater layers or nearby freshwater systems. Such preferential flows in earthworm burrows have been observed for microplastics in one study.[97] Similar tests would therefore be useful to gain a better understanding of the remobilization potential of the nanosized plastic fraction to reliably assess the associated risk of plastic transfers.

At the current time, it is still uncertain how different plastic shapes, sizes, earthworm species, or soil properties may affect bioturbation transport dynamics in terms of transport mechanisms and ultimately transport depth and rate. However, our study emphasizes that a more systematic understanding of bioturbation-driven transport of micro- and nanoplastics could not only advance our knowledge on the long-term fate of micro- and nanoplastics and flows between different environmental compartments but could also inform decisions made for in-field measurements and monitoring.

■ ASSOCIATED CONTENT

Supporting Information

The Supporting Information is available free of charge at https://pubs.acs.org/doi/10.1021/acs.est.1c05614.

> Nanoplastic characterization and soil properties, microcosm setup and sampling, X-ray CT measurement and workflow, digestion protocol, bioturbation model description and results, earthworm weight and uptake of nanoplastics, sampling procotol for drilosphere sampling, detected nanoplastic concentrations in soil samples (Exp 1) and drilosphere and soil matrix samples (Exp 2) (PDF)

■ AUTHOR INFORMATION

Corresponding Author

Geert Cornelis − *Department of Soil and Environment, Swedish University of Agricultural Sciences, 75007 Uppsala, Sweden;* orcid.org/0000-0003-0078-6798; Email: geert.cornelis@slu.se

Authors

Wiebke Mareile Heinze − *Department of Soil and Environment, Swedish University of Agricultural Sciences, 75007 Uppsala, Sweden;* orcid.org/0000-0003-1884-6664

Denise M. Mitrano − *Department of Environmental Systems Science, ETH Zurich, 8092 Zürich, Switzerland;* orcid.org/0000-0001-8030-6066

Elma Lahive − *UK Centre for Ecology and Hydrology, Wallingford OX10 8BB, United Kingdom*

John Koestel − *Department of Soil and Environment, Swedish University of Agricultural Sciences, 75007 Uppsala, Sweden; Agroscope − Standort Reckenholz, Soil Quality and Soil Use, 8046 Zürich, Switzerland*

Complete contact information is available at: https://pubs.acs.org/10.1021/acs.est.1c05614

Notes

All raw data has been prepared for upload to a dryad digital repository (doi: 10.5061/dryad.x69p8czjv).

The authors declare no competing financial interest.

■ ACKNOWLEDGMENTS

We thank Astrid Taylor and Kaisa Torrpa for their logistic support with the earthworms, Marta Baccaro for advice on the experimental setup, Zacharias Steinmetz, Francesco Parrella, and Roman Schefer for valuable discussions about the manuscript. Financial support for this project was provided by ACEnano (EU Horizon 2020, Grant Agreement No. 720952), the Swedish Research Council FORMAS (Project No. 2018-01080), the Swiss National Science Foundation (PZ00P2_168105 and PCEFP2_186856), and the Swedish University of Agricultural Sciences, UK Centre for Ecology and Hydrology, the Swiss Federal Insitute of Technology (ETH Zürich) and Agroscope.

■ REFERENCES

(1) *UNEP Year Book 2021: Emerging Issues in Our Global Environment*; United Nations Environment Programme, 2014.

(2) Kawecki, D.; Nowack, B. Polymer-Specific Modeling of the Environmental Emissions of Seven Commodity Plastics as Macro- and Microplastics. *Environ. Sci. Technol.* **2019**, *53* (16), 9664−9676.

(3) Nizzetto, L.; Futter, M.; Langaas, S. Are Agricultural Soils Dumps for Microplastics of Urban Origin? *Environ. Sci. Technol.* **2016**, *50* (20), 10777−10779.

(4) Bläsing, M.; Amelung, W. Plastics in Soil: Analytical Methods and Possible Sources. *Sci. Total Environ.* **2018**, *612*, 422−435.

(5) Horton, A. A.; Walton, A.; Spurgeon, D. J.; Lahive, E.; Svendsen, C. Microplastics in Freshwater and Terrestrial Environments: Evaluating the Current Understanding to Identify the Knowledge Gaps and Future Research Priorities. *Sci. Total Environ.* **2017**, *586*, 127−141.

(6) Bergmann, M.; Mützel, S.; Primpke, S.; Tekman, M. B.; Trachsel, J.; Gerdts, G. White and Wonderful? Microplastics Prevail in Snow from the Alps to the Arctic. *Sci. Adv.* **2019**, *5* (8), na DOI: 10.1126/sciadv.aax1157.

(7) Sommer, F.; Dietze, V.; Baum, A.; Sauer, J.; Gilge, S.; Maschowski, C.; Gieré, R. Tire Abrasion as a Major Source of Microplastics in the Environment. *Aerosol Air Qual. Res.* **2018**, *18* (8), 2014−2028.

(8) Mahon, A. M.; O'Connell, B.; Healy, M. G.; O'Connor, I.; Officer, R.; Nash, R.; Morrison, L. Microplastics in Sewage Sludge: Effects of Treatment. *Environ. Sci. Technol.* **2017**, *51* (2), 810−818.

(9) Corradini, F.; Meza, P.; Eguiluz, R.; Casado, F.; Huerta-Lwanga, E.; Geissen, V. Evidence of Microplastic Accumulation in Agricultural Soils from Sewage Sludge Disposal. *Sci. Total Environ.* **2019**, *671*, 411−420.

(10) Frehland, S.; Kaegi, R.; Hufenus, R.; Mitrano, D. M. Long-Term Assessment of Nanoplastic Particle and Microplastic Fiber Flux through a Pilot Wastewater Treatment Plant Using Metal-Doped Plastics. *Water Res.* **2020**, *182*, 115860.

(11) van den Berg, P.; Huerta-Lwanga, E.; Corradini, F.; Geissen, V. Sewage Sludge Application as a Vehicle for Microplastics in Eastern Spanish Agricultural Soils. *Environ. Pollut.* **2020**, *261*, 114198.

(12) Weithmann, N.; Möller, J. N.; Löder, M. G. J.; Piehl, S.; Laforsch, C.; Freitag, R. Organic Fertilizer as a Vehicle for the Entry of Microplastic into the Environment. *Sci. Adv.* **2018**, *4* (4), na DOI: 10.1126/sciadv.aap8060.

(13) Beriot, N.; Peek, J.; Zornoza, R.; Geissen, V.; Huerta Lwanga, E. Low Density-Microplastics Detected in Sheep Faeces and Soil: A Case Study from the Intensive Vegetable Farming in Southeast Spain. *Sci. Total Environ.* **2021**, *755*, 142653.

(14) Judy, J. D.; Williams, M.; Gregg, A.; Oliver, D.; Kumar, A.; Kookana, R.; Kirby, J. K. Microplastics in Municipal Mixed-Waste

Organic Outputs Induce Minimal Short to Long-Term Toxicity in Key Terrestrial Biota. *Environ. Pollut.* **2019**, *252*, 522−531.
(15) Steinmetz, Z.; Wollmann, C.; Schaefer, M.; Buchmann, C.; David, J.; Tröger, J.; Muñoz, K.; Frör, O.; Schaumann, G. E. Plastic Mulching in Agriculture. Trading Short-Term Agronomic Benefits for Long-Term Soil Degradation? *Sci. Total Environ.* **2016**, *550*, 690−705.
(16) Scarascia-Mugnozza, G.; Sica, C.; Russo, G. Plastic Materials in European Agriculture: Actual Use and Perspectives. *J. Agric. Eng.* **2011**, *42*, 15.
(17) Kim, H. M.; Lee, D.-K.; Long, N. P.; Kwon, S. W.; Park, J. H. Uptake of Nanopolystyrene Particles Induces Distinct Metabolic Profiles and Toxic Effects in Caenorhabditis Elegans. *Environ. Pollut.* **2019**, *246*, 578−586.
(18) Hartmann, N. B.; Hüffer, T.; Thompson, R. C.; Hassellöv, M.; Verschoor, A.; Daugaard, A. E.; Rist, S.; Karlsson, T.; Brennholt, N.; Cole, M.; Herrling, M. P.; Hess, M. C.; Ivleva, N. P.; Lusher, A. L.; Wagner, M. Are We Speaking the Same Language? Recommendations for a Definition and Categorization Framework for Plastic Debris. *Environ. Sci. Technol.* **2019**, *53* (3), 1039−1047.
(19) Mitrano, D. M.; Wick, P.; Nowack, B. Placing Nanoplastics in the Context of Global Plastic Pollution. *Nat. Nanotechnol.* **2021**, *16* (5), 491−500.
(20) de Souza Machado, A. A.; Lau, C. W.; Till, J.; Kloas, W.; Lehmann, A.; Becker, R.; Rillig, M. C. Impacts of Microplastics on the Soil Biophysical Environment. *Environ. Sci. Technol.* **2018**, *52* (17), 9656−9665.
(21) Lozano, Y. M.; Rillig, M. C. Effects of Microplastic Fibers and Drought on Plant Communities. *Environ. Sci. Technol.* **2020**, *54* (10), 6166−6173.
(22) Wan, Y.; Wu, C.; Xue, Q.; Hui, X. Effects of Plastic Contamination on Water Evaporation and Desiccation Cracking in Soil. *Sci. Total Environ.* **2019**, *654*, 576−582.
(23) de Souza Machado, A. A.; Lau, C. W.; Kloas, W.; Bergmann, J.; Bachelier, J. B.; Faltin, E.; Becker, R.; Görlich, A. S.; Rillig, M. C. Microplastics Can Change Soil Properties and Affect Plant Performance. *Environ. Sci. Technol.* **2019**, *53* (10), 6044−6052.
(24) Fei, Y.; Huang, S.; Zhang, H.; Tong, Y.; Wen, D.; Xia, X.; Wang, H.; Luo, Y.; Barceló, D. Response of Soil Enzyme Activities and Bacterial Communities to the Accumulation of Microplastics in an Acid Cropped Soil. *Sci. Total Environ.* **2020**, *707*, 135634.
(25) Khalid, N.; Aqeel, M.; Noman, A. Microplastics Could Be a Threat to Plants in Terrestrial Systems Directly or Indirectly. *Environ. Pollut.* **2020**, *267*, 115653.
(26) Zang, H.; Zhou, J.; Marshall, M. R.; Chadwick, D. R.; Wen, Y.; Jones, D. L. Microplastics in the Agroecosystem: Are They an Emerging Threat to the Plant-Soil System? *Soil Biol. Biochem.* **2020**, *148*, 107926.
(27) Lei, L.; Liu, M.; Song, Y.; Lu, S.; Hu, J.; Cao, C.; Xie, B.; Shi, H.; He, D. Polystyrene (Nano)Microplastics Cause Size-Dependent Neurotoxicity, Oxidative Damage and Other Adverse Effects in Caenorhabditis Elegans. *Environ. Sci.: Nano* **2018**, *5* (8), 2009−2020.
(28) Zhu, D.; Chen, Q.-L.; An, X.-L.; Yang, X.-R.; Christie, P.; Ke, X.; Wu, L.-H.; Zhu, Y.-G. Exposure of Soil Collembolans to Microplastics Perturbs Their Gut Microbiota and Alters Their Isotopic Composition. *Soil Biol. Biochem.* **2018**, *116*, 302−310.
(29) Huerta Lwanga, E.; Gertsen, H.; Gooren, H.; Peters, P.; Salánki, T.; van der Ploeg, M.; Besseling, E.; Koelmans, A. A.; Geissen, V. Microplastics in the Terrestrial Ecosystem: Implications for Lumbricus Terrestris (Oligochaeta, Lumbricidae). *Environ. Sci. Technol.* **2016**, *50* (5), 2685−2691.
(30) Ju, H.; Zhu, D.; Qiao, M. Effects of Polyethylene Microplastics on the Gut Microbial Community, Reproduction and Avoidance Behaviors of the Soil Springtail, Folsomia Candida. *Environ. Pollut.* **2019**, *247*, 890−897.
(31) Rodriguez-Seijo, A.; Lourenço, J.; Rocha-Santos, T. A. P.; da Costa, J.; Duarte, A. C.; Vala, H.; Pereira, R. Histopathological and Molecular Effects of Microplastics in Eisenia Andrei Bouché. *Environ. Pollut.* **2017**, *220*, 495−503.
(32) Lahive, E.; Walton, A.; Horton, A. A.; Spurgeon, D. J.; Svendsen, C. Microplastic Particles Reduce Reproduction in the Terrestrial Worm Enchytraeus Crypticus in a Soil Exposure. *Environ. Pollut.* **2019**, *255*, 113174.
(33) Krogh, P. H. Does a Heterogeneous Distribution of Food or Pesticide Affect the Outcome of Toxicity Tests with Collembola? *Ecotoxicol. Environ. Saf.* **1995**, *30* (2), 158−163.
(34) Qi, R.; Jones, D. L.; Li, Z.; Liu, Q.; Yan, C. Behavior of Microplastics and Plastic Film Residues in the Soil Environment: A Critical Review. *Sci. Total Environ.* **2020**, *703*, 134722.
(35) Rillig, M. C.; Kim, S. W.; Kim, T.-Y.; Waldman, W. R. The Global Plastic Toxicity Debt. *Environ. Sci. Technol.* **2021**, *55* (5), 2717−2719.
(36) Alimi, O. S.; Farner Budarz, J.; Hernandez, L. M.; Tufenkji, N. Microplastics and Nanoplastics in Aquatic Environments: Aggregation, Deposition, and Enhanced Contaminant Transport. *Environ. Sci. Technol.* **2018**, *52* (4), 1704−1724.
(37) Wu, X.; Lyu, X.; Li, Z.; Gao, B.; Zeng, X.; Wu, J.; Sun, Y. Transport of Polystyrene Nanoplastics in Natural Soils: Effect of Soil Properties, Ionic Strength and Cation Type. *Sci. Total Environ.* **2020**, *707*, 136065.
(38) Chinju, H.; Kuno, Y.; Nagasaki, S.; Tanaka, S. Deposition Behavior of Polystyrene Latex Particles on Solid Surfaces during Migration through an Artificial Fracture in a Granite Rock Sample. *J. Nucl. Sci. Technol.* **2001**, *38*, 439−443.
(39) Tufenkji, N.; Elimelech, M. Breakdown of Colloid Filtration Theory: Role of the Secondary Energy Minimum and Surface Charge Heterogeneities. *Langmuir* **2005**, *21* (3), 841−852.
(40) Quevedo, I. R.; Tufenkji, N. Mobility of Functionalized Quantum Dots and a Model Polystyrene Nanoparticle in Saturated Quartz Sand and Loamy Sand. *Environ. Sci. Technol.* **2012**, *46* (8), 4449−4457.
(41) Keller, A. S.; Jimenez-Martinez, J.; Mitrano, D. M. Transport of Nano- and Microplastic through Unsaturated Porous Media from Sewage Sludge Application. *Environ. Sci. Technol.* **2020**, *54* (2), 911−920.
(42) Fujita, Y.; Kobayashi, M. Transport of Colloidal Silica in Unsaturated Sand: Effect of Charging Properties of Sand and Silica Particles. *Chemosphere* **2016**, *154*, 179−186.
(43) Kumahor, S. K.; Hron, P.; Metreveli, G.; Schaumann, G. E.; Vogel, H.-J. Transport of Citrate-Coated Silver Nanoparticles in Unsaturated Sand. *Sci. Total Environ.* **2015**, *535*, 113−121.
(44) Torkzaban, S.; Bradford, S. A.; van Genuchten, M. Th; Walker, S. L. Colloid Transport in Unsaturated Porous Media: The Role of Water Content and Ionic Strength on Particle Straining. *J. Contam. Hydrol.* **2008**, *96* (1), 113−127.
(45) Flury, M.; Aramrak, S. Role of Air-Water Interfaces in Colloid Transport in Porous Media: A Review. *Water Resour. Res.* **2017**, *53* (7), 5247−5275.
(46) Jégou, D.; Cluzeau, D.; Balesdent, J.; Tréhen, P. Effects of Four Ecological Categories of Earthworms on Carbon Transfer in Soil. *Appl. Soil Ecol.* **1998**, *9* (1), 249−255.
(47) Don, A.; Steinberg, B.; Schöning, I.; Pritsch, K.; Joschko, M.; Gleixner, G.; Schulze, E.-D. Organic Carbon Sequestration in Earthworm Burrows. *Soil Biol. Biochem.* **2008**, *40* (7), 1803−1812.
(48) Bouché, M. B. Strategies Lombriciennes. *Ecol. Bull.* **1977**, No. 25, 122−132.
(49) Platt, B. F.; Kolb, D. J.; Kunhardt, C. G.; Milo, S. P.; New, L. G. Burrowing Through the Literature: The Impact of Soil-Disturbing Vertebrates on Physical and Chemical Properties of Soil. *Soil Sci.* **2016**, *181* (3/4), 175.
(50) Taylor, A. R.; Lenoir, L.; Vegerfors, B.; Persson, T. Ant and Earthworm Bioturbation in Cold-Temperate Ecosystems. *Ecosystems* **2019**, *22*, 981−994.
(51) Jégou, D.; Cluzeau, D.; Hallaire, V.; Balesdent, J.; Tréhen, P. Burrowing Activity of the Earthworms Lumbricus Terrestris and Aporrectodea Giardi and Consequences on C Transfers in Soil. *Eur. J. Soil Biol.* **2000**, *36* (1), 27−34.

https://doi.org/10.1021/acs.est.1c05614
Environ. Sci. Technol. 2021, 55, 16423−16433

(52) Jarvis, N. J.; Taylor, A.; Larsbo, M.; Etana, A.; Rosén, K. Modelling the Effects of Bioturbation on the Re-Distribution of 137Cs in an Undisturbed Grassland Soil. *Eur. J. Soil Sci.* **2010**, *61* (1), 24−34.
(53) Rillig, M. C.; Ziersch, L.; Hempel, S. Microplastic Transport in Soil by Earthworms. *Sci. Rep.* **2017**, *7* (1), 1362.
(54) Baccaro, M.; Harrison, S.; van den Berg, H.; Sloot, L.; Hermans, D.; Cornelis, G.; van Gestel, C. A.M.; van den Brink, N. W. Bioturbation of Ag2S-NPs in Soil Columns by Earthworms. *Environ. Pollut.* **2019**, *252*, 155−162.
(55) Capowiez, Y.; Sammartino, S.; Michel, E. Using X-Ray Tomography to Quantify Earthworm Bioturbation Non-Destructively in Repacked Soil Cores. *Geoderma* **2011**, *162* (1), 124−131.
(56) Astete, C. E.; Constant, W. D.; Thibodeaux, L. J.; Seals, R. K.; Selim, H. M. Bioturbation-Driven Particle Transport in Surface Soil: The Biodiffusion Coefficient Mobility Parameter. *Soil Sci.* **2015**, *180* (1), 2−9.
(57) Meysman, F. J. R.; Boudreau, B. P.; Middelburg, J. J. Relations between Local, Nonlocal, Discrete and Continuous Models of Bioturbation. *J. Mar. Res.* **2003**, *61*, 391−410.
(58) Huerta Lwanga, E.; Gertsen, H.; Gooren, H.; Peters, P.; Salanki, T.; van der Ploeg, M.; Besseling, E.; Koelmans, A. A.; Geissen, V. Incorporation of Microplastics from Litter into Burrows of Lumbricus Terrestris. *Environ. Pollut.* **2017**, *220*, 523−531.
(59) Huerta Lwanga, E.; Mendoza Vega, J.; Ku Quej, V.; Chi, J. d. l. A.; Sanchez del Cid, L.; Chi, C.; Escalona Segura, G.; Gertsen, H.; Salanki, T.; van der Ploeg, M.; Koelmans, A. A.; Geissen, V. Field Evidence for Transfer of Plastic Debris along a Terrestrial Food Chain. *Sci. Rep.* **2017**, *7* (1), 14071.
(60) Sanchez-Hernandez, J. C.; Capowiez, Y.; Ro, K. S. Potential Use of Earthworms to Enhance Decaying of Biodegradable Plastics. *ACS Sustainable Chem. Eng.* **2020**, *8* (11), 4292−4316.
(61) Thomas, D.; Schütze, B.; Heinze, W. M.; Steinmetz, Z. Sample Preparation Techniques for the Analysis of Microplastics in Soil—A Review. *Sustainability* **2020**, *12* (21), 9074.
(62) Li, J.; Song, Y.; Cai, Y. Focus Topics on Microplastics in Soil: Analytical Methods, Occurrence, Transport, and Ecological Risks. *Environ. Pollut.* **2020**, *257*, 113570.
(63) Wang, W.; Ge, J.; Yu, X.; Li, H. Environmental Fate and Impacts of Microplastics in Soil Ecosystems: Progress and Perspective. *Sci. Total Environ.* **2020**, *708*, 134841.
(64) Löder, M. G. J.; Kuczera, M.; Mintenig, S.; Lorenz, C.; Gerdts, G. Focal Plane Array Detector-Based Micro-Fourier-Transform Infrared Imaging for the Analysis of Microplastics in Environmental Samples. *Environ. Chem.* **2015**, *12* (5), 563−581.
(65) He, D.; Luo, Y.; Lu, S.; Liu, M.; Song, Y.; Lei, L. Microplastics in Soils: Analytical Methods, Pollution Characteristics and Ecological Risks. *TrAC, Trends Anal. Chem.* **2018**, *109*, 163−172.
(66) Dierkes, G.; Lauschke, T.; Becher, S.; Schumacher, H.; Földi, C.; Ternes, T. Quantification of Microplastics in Environmental Samples via Pressurized Liquid Extraction and Pyrolysis-Gas Chromatography. *Anal. Bioanal. Chem.* **2019**, *411* (26), 6959−6968.
(67) Mitrano, D. M.; Beltzung, A.; Frehland, S.; Schmiedgruber, M.; Cingolani, A.; Schmidt, F. Synthesis of Metal-Doped Nanoplastics and Their Utility to Investigate Fate and Behaviour in Complex Environmental Systems. *Nat. Nanotechnol.* **2019**, *14* (4), 362.
(68) Redondo-Hasselerharm, P. E.; Vink, G.; Mitrano, D. M.; Koelmans, A. A. Metal-Doping of Nanoplastics Enables Accurate Assessment of Uptake and Effects on Gammarus Pulex. *Environ. Sci.: Nano* **2021**, *8* (6), 1761−1770.
(69) Schlemmer, D.; Sales, M. J. A.; Resck, I. S. Degradation of Different Polystyrene/Thermoplastic Starch Blends Buried in Soil. *Carbohydr. Polym.* **2009**, *75* (1), 58−62.
(70) Kaplan, D.; Hartenstein, R.; Sutter, J. Biodegradation of Polystyrene, Poly(Methyl Methacrylate), and Phenol Formaldehyde. *Appl. Environ. Microbiol.* **1979**, *38*, 551−553.
(71) Fründ, H.-C.; Butt, K.; Capowiez, Y.; Eisenhauer, N.; Emmerling, C.; Ernst, G.; Potthoff, M.; Schädler, M.; Schrader, S. Using Earthworms as Model Organisms in the Laboratory: Recommendations for Experimental Implementations. *Pedobiologia* **2010**, *53* (2), 119−125.
(72) Andriuzzi, W. S.; Bolger, T.; Schmidt, O. The Drilosphere Concept: Fine-Scale Incorporation of Surface Residue-Derived N and C around Natural Lumbricus Terrestris Burrows. *Soil Biol. Biochem.* **2013**, *64*, 136−138.
(73) Jarvis, N. J. A Review of Non-Equilibrium Water Flow and Solute Transport in Soil Macropores: Principles, Controlling Factors and Consequences for Water Quality. *Eur. J. Soil Sci.* **2007**, *58* (3), 523−546.
(74) Balseiro-Romero, M.; Mazurier, A.; Monoshyn, D.; Baveye, P. C.; Clause, J. Using X-Ray Microtomography to Characterize the Burrowing Behaviour of Earthworms in Heterogeneously Polluted Soils. *Pedobiologia* **2020**, *83*, 150671.
(75) Schindelin, J.; Arganda-Carreras, I.; Frise, E.; Kaynig, V.; Longair, M.; Pietzsch, T.; Preibisch, S.; Rueden, C.; Saalfeld, S.; Schmid, B.; Tinevez, J.-Y.; White, D. J.; Hartenstein, V.; Eliceiri, K.; Tomancak, P.; Cardona, A. Fiji: An Open-Source Platform for Biological-Image Analysis. *Nat. Methods* **2012**, *9* (7), 676−682.
(76) Schneider, C. A.; Rasband, W. S.; Eliceiri, K. W. NIH Image to ImageJ: 25 Years of Image Analysis. *Nat. Methods* **2012**, *9* (7), 671−675.
(77) Koestel, J. SoilJ: An ImageJ Plugin for the Semiautomatic Processing of Three-Dimensional X-Ray Images of Soils. *Vadose Zone J.* **2018**, *17* (1), 170062.
(78) Koestel, J.; Dathe, A.; Skaggs, T. H.; Klakegg, O.; Ahmad, M. A.; Babko, M.; Giménez, D.; Farkas, C.; Nemes, A.; Jarvis, N. Estimating the Permeability of Naturally Structured Soil From Percolation Theory and Pore Space Characteristics Imaged by X-Ray. *Water Resour. Res.* **2018**, *54* (11), 9255−9263.
(79) Legland, D.; Arganda-Carreras, I.; Andrey, P. MorphoLibJ: Integrated Library and Plugins for Mathematical Morphology with ImageJ. *Bioinformatics* **2016**, *32* (22), 3532−3534.
(80) Limaye, A. Drishti: A Volume Exploration and Presentation Tool. *Proc. SPIE* **2012**, 85060X.
(81) *ISO 11466:1995. Soil Quality − Extraction of Trace Elements Soluble in Aqua Regia*; ISO: Geneva, 1995.
(82) *Method 3051A (SW-846): Microwave Assisted Acid Digestion of Sediments, Sludges, and Oils*; Revision 1; U.S. Environmental Protection Agency, 2007.
(83) Rodriguez, M. D. *The Bioturbation Transport of Chemicals in Surface Soils*; Master's Thesis, Louisiana State University, 2006.
(84) Pitkänen, J.; Nuutinen, V. Distribution and Abundance of Burrows Formed by Lumbricus Terrestris L. and Aporrectodea Caliginosa Sav. in the Soil Profile. *Soil Biol. Biochem.* **1997**, *29* (3), 463−467.
(85) Larsbo, M.; Koestel, J.; Jarvis, N. Relations between Macropore Network Characteristics and the Degree of Preferential Solute Transport. *Hydrol. Earth Syst. Sci.* **2014**, *18* (12), 5255−5269.
(86) Selonen, S.; Dolar, A.; Jemec Kokalj, A.; Skalar, T.; Parramon Dolcet, L.; Hurley, R.; van Gestel, C. A. M. Exploring the Impacts of Plastics in Soil - The Effects of Polyester Textile Fibers on Soil Invertebrates. *Sci. Total Environ.* **2020**, *700*, 134451.
(87) Kwak, J. I.; An, Y.-J. Microplastic Digestion Generates Fragmented Nanoplastics in Soils and Damages Earthworm Spermatogenesis and Coelomocyte Viability. *J. Hazard. Mater.* **2021**, *402*, 124034.
(88) Lahive, E.; Cross, R.; Saarloos, A. I.; Horton, A. A.; Svendsen, C.; Hufenus, R.; Mitrano, D. M. Earthworms Ingest Microplastic Fibres and Nanoplastics with Effects on Egestion Rate and Long-Term Retention. *Sci. Total Environ.* **2021**, 151022.
(89) Arnold, R. E.; Hodson, M. E. Effect of Time and Mode of Depuration on Tissue Copper Concentrations of the Earthworms Eisenia Andrei, Lumbricus Rubellus and Lumbricus Terrestris. *Environ. Pollut.* **2007**, *148* (1), 21−30.
(90) Prendergast-Miller, M. T.; Katsiamides, A.; Abbass, M.; Sturzenbaum, S. R.; Thorpe, K. L.; Hodson, M. E. Polyester-Derived Microfibre Impacts on the Soil-Dwelling Earthworm Lumbricus Terrestris. *Environ. Pollut.* **2019**, *251*, 453−459.

https://doi.org/10.1021/acs.est.1c05614
Environ. Sci. Technol. 2021, 55, 16423−16433

(91) Zhang, L.; Sintim, H. Y.; Bary, A. I.; Hayes, D. G.; Wadsworth, L. C.; Anunciado, M. B.; Flury, M. Interaction of Lumbricus Terrestris with Macroscopic Polyethylene and Biodegradable Plastic Mulch. *Sci. Total Environ.* **2018**, *635*, 1600−1608.
(92) Tiunov, A. V.; Bonkowski, M.; Bonkowski, M.; Tiunov, J. A.; Scheu, S. Microflora, Protozoa and Nematoda in Lumbricus Terrestris Burrow Walls: A Laboratory Experiment. *Pedobiologia* **2001**, *45* (1), 46−60.
(93) Jégou, D.; Schrader, S.; Diestel, H.; Cluzeau, D. Morphological, Physical and Biochemical Characteristics of Burrow Walls Formed by Earthworms. *Appl. Soil Ecol.* **2001**, *17* (2), 165−174.
(94) Taylor, A. R.; Taylor, A. F. S. Assessing Daily Egestion Rates in Earthworms: Using Fungal Spores as a Natural Soil Marker to Estimate Gut Transit Time. *Biol. Fertil. Soils* **2014**, *50* (1), 179−183.
(95) Spurgeon, D. J.; Keith, A. M.; Schmidt, O.; Lammertsma, D. R.; Faber, J. H. Land-Use and Land-Management Change: Relationships with Earthworm and Fungi Communities and Soil Structural Properties. *BMC Ecol.* **2013**, *13*, 46−46.
(96) Bergendahl, J.; Grasso, D. Colloid Generation during Batch Leaching Tests: Mechanics of Disaggregation. *Colloids Surf., A* **1998**, *135* (1), 193−205.
(97) Yu, M.; van der Ploeg, M.; Lwanga, E. H.; Yang, X.; Zhang, S.; Ma, X.; Ritsema, C. J.; Geissen, V. Leaching of Microplastics by Preferential Flow in Earthworm (Lumbricus Terrestris) Burrows. *Environ. Chem.* **2019**, *16* (1), 31−40.

https://doi.org/10.1021/acs.est.1c05614
Environ. Sci. Technol. 2021, 55, 16423−16433

Supporting information: Nanoplastic transport in soil through bioturbation of *Lumbricus terrestris*

Wiebke Mareile Heinze[a], Denise M. Mitrano[b], Elma Lahive[c], John Koestel[a,d], Geert Cornelis[a]

[a]Swedish University of Agricultural Sciences, Department of Soil and Environment, Box 7014, 75007 Uppsala, Sweden

[b]ETH Zurich, Department of Environmental Systems Science, Universitätsstrasse 16, 8092 Zürich, Switzerland

[c]UK Centre for Hydrology and Ecology, Benson Lane, Crowmarsh Gifford, Wallingford, OX10 8BB, UK

[d]Agroscope – Standort Reckenholz, Soil Quality and Soil Use, Reckenholzstrasse 191, 8046 Zürich, Switzerland

Note that the supporting information displayed here was reformatted for the purpose of this thesis. The content remains unchanged. The original is available free of charge at https://pubs.acs.org/doi/10.1021/acs.est.1c05614.

Supplementary materials

Supplementary materials S1. Digestion protocol for Pd-doped nanoplastics.

Palladium (Pd) doped nanoplastics nanoplastics (0.24% w/w) were used throughout the experiments, where Pd concentrations were determined in *aqua regia* extracts of soil (Exp 1), including drilosphere (Exp 2), and earthworm tissue using inductively coupled plasma mass spectrometry (ICP-MS) as a proxy for nanoplastics concentrations. Soil samples were oven-dried (105°C, 3 days), homogenized and ground by mechanical sieving (Exp 1) or manually in an agate mortar (Exp 2) due to differences in sample size. The bulk sample of each layer was subsampled by dividing the soil into half-lots by pouring the sample carefully over the edge of a container onto an even surface. This procedure was repeated until subsamples of approximately 2-3 g were achieved. For each sample triplicates of approximately 0.5-0.6 g were then transferred to the polytetrafluoroethylene (PTFE) digestion tubes (80 mL) using glass weighing floats. The exact weight of each sample was noted. For earthworms, the freeze-dried tissue was carefully divided into smaller pieces, added to digestion tubes (wich exact weight noted) and treated with 1.5 mL hydrogen peroxide (30 vol.% H_2O_2) overnight.

Aqua regia extraction of soils or earthworm tissue was done in a closed microwave-assisted system (Milestone Ethos Easy, MAXI-44). After sample addition, acids were sequentially applied to each sample: for soils 1.25 mL of 65 vol.% nitric acid (HNO_3) and 3.75 mL of 37 vol.% hydrochloric acid (HCl). For earthworm tissue, with weights of 0.5-1.0 g of dry material we applied a higher total volume composed of 1.875 ml HCl, and 5.625 ml HNO_3. The microwave digestion program followed EPA 3051 guidelines[2]: The temperature was ramped from 20°C to 175°C in 20 minutes (1800 W for > 9 vessels), kept constant at 175°C for 10 minutes and then cooled down for at least 50 minutes, or until temperatures were below 25°C. *Aqua regia* extracts were then transferred quantitatively to 50 mL volumetric flasks over a funnel and filter (Munktell filter paper) through repeatedly rinsing the tube with ultrapure water (18.3 Ω). Both filter and funnel were then rinsed with ultrapure water to dilute the sample to a total volume of 50 mL,

resulting in 10 times diluted extracts for soils and drilosphere, and 5.56 times for earthworms. The Pd-concentrations in the *aqua regia* extract were analyzed by inductively coupled plasma mass spectrometry (ICP-MS) (Perkin Elmer, Nexion 350D) with a detection limit of 0.026 µg L^{-1} (n=5). Pd-concentrations detected in the extracts were corrected for procedural blanks of the respective extraction set and for the respective background concentrations of Pd in the matrix. In case of soil samples, this was 32 ± 4 µg kg^{-1} (n=6) and for earthworm tissue this was 0.016 ± 0.012 µg kg^{-1} (n=3).

The extraction efficiency of plastic-incorporated Pd was optimized by testing different methods and digestion systems (Figure S5): 1) *aqua regia* digestion in an open-vessel hotplate system (n=3), 2) *aqua regia* digestion in a closed-vessel microwave-assisted system (n=3), 3) direct injection of diluted nanoplastic suspension (n=3). The highest extraction efficiencies were observed for the closed-vessel microwave-assisted *aqua regia* digestion (Figure S5), which was subsequently used for all further analysis throughout the experimental work.

Supplementary materials S2. Description of bioturbation model used for simulating nanoplastics transport in soil.

The bioturbation model is a one-dimensional mathematical model which was developed by Rodriguez[3], and was applied here as has previously been done by Baccaro et al.[4]. The bioturbation rate constant (equation 1) was retrofitted by minimizing the sum of squared errors between the logarithm of experimental time- and depth dependent concentrations and calculated ones based on equation 2. For this equation, the soil profile is divided into discrete depth layers of length d_l (m). Concentrations C (mg kg^{-1}) are changed only by mixing between directly adjacent layers ($l+1$ and $l-1$). The bioturbation rate is thus a semi-empirical parameter, proportional to a soil turnover rate $v_{l:l+1}$ (m s^{-1}) that is proportional to earthworm density and dependent on a bioturbation fitting parameter β (m^4 s^{-1}) (Equation 3).

$$k_{bioturb,l:l+1} = \frac{v_{l:l+1}}{d_l} \qquad \text{(Equation 1)}$$

$$[C]_{l,t+x} = [C]_{l,t} + k_{bioturb,l:l+1,t}\,\delta t\left([C]_{l+1,t} - [C]_{l,t}\right) + k_{bioturb,l-1:l,t}\,\delta t([C]_{l-1,t} - [C]_{l,t}) \qquad \text{(Equation 2)}$$

$$v_{l:l+1} = \beta w_l \qquad \text{(Equation 3)}$$

$k_{bioturb,l:l+1}$: bioturbation rate (s^{-1})
$v_{l:l+1}$: soil turnover rate (m s^{-1})
d_l: depth of layer with an associated concentration (m)
$[C]$: concentration of substance (mg kg^{-1})
δt: time-step considered for model (s^{-1})
β: bioturbation fitting parameter (m^4 s^{-1})
w_l: earthworm density (individuals m^{-3})

The parameters applied for this study are shown in Table S9. Note that for obtaining average concentrations for the soil depth layers of different thickness as investigated in our study, the simulated concentrations for the corresponding model depth layers were summed together.

Supplementary Tables

Table S1. Properties of palladium-doped polystyrene nanoplastics[1] used for quantifying nanoplastics transport by bioturbation in soil, Experiment 1 (Exp 1) and Experiment 2 (Exp 2).

Nanoplastics properties									
Particle material									
Shell material		Polystyrene							
Core material		Polyacrylonitrile							
Shape		Spherical							
Surface morphology		Raspberry-shell							
Suspension solution		Traces of SDS from synthesis process							
Palladium content		0.24 %							
Particle size and charge									
Z-average diameter[a]	nm	256	±4				*n=12*		
PDI[a]		0.10	±0.02				*n=12*		
Zeta potential in ultrapure water[b]	mV	-60	±1				*n=3*		
Zeta potential in soil leachate[b]	mV	-38	±1				*n=3*		
Dilution series									
Particle concentration	mg L^{-1}	170		85		34		17	
Z-average diameter[a]	nm	255	±2	254	±6	258	±2	258	±3
PDI[a]		0.12		0.10		0.09		0.08	
Time series									
Time	days	0		6		15		35	
Z-average diameter[a]	nm	255	±2	254	±5	251	±6	251	±4
PDI[a]		0.12		0.07		0.07		0.07	

[a]*Measurement conditions: 3 replicates, 13 readings per replicate, 18 °C, 120 s equilibration time, signal-to-noise >0.9, >600 kcps, attenuator value 6-7*

[b]*Electrophoretic mobility calculated into Zeta potential using the Smoluchowski approximation*

Table S2. Selected details including physical and chemical soil properties for the topsoil used in microcosm studies, Exp 1 and Exp 2.

Soil characterization			
Land use history		Agricultural	
Soil type		Topsoil	
Location	Sprowston, Norfolk, UK	WGS84: 387724, 5835408	
Soil texture		Sandy loam	
Coarse fragments	2-20 mm	3	%
Sand	2.0-0.063 mm	60	%
Silt	0.063-0.002 mm	28	%
Clay	<0.002 mm	12	%
Water holding capacity		420	mL kg^{-1}
Palladium concentration		32 ± 4	mg kg^{-1}
pH		7.2-7.6	
Soil organic matter		5.0	w/w %

[a]*The English/Welsh soil classification uses 0.06 mm as a boundary between sand and silt*[5]

Table S3. Average water content (% of water holding capacity) and dry bulk density of soil columns (g cm^{-3}) for each layer for Exp 1. Water applications are provided as average (mm $week^{-1}$) for all replicates.

Parameter	Sampling layer	7 days		14 days		21 days		28 days		Control (28 days)	
Water content at sampling timepoint (% of WHC)	Layer 1	40	±1%	41	±3%	49	±2%	45	±0%	42	±1%
	Layer 2	42	±2%	43	±2%	46	±1%	46	±3%	41	±2%
	Layer 3	40	±2%	42	±2%	41	±1%	42	±4%	42	±2%
	Layer 4	36	±1%	36	±1%	35	±1%	35	±2%	36	±1%
Bulk density at sampling timepoint (g cm^{-3})	Layer 1	0.93	±0.14	0.98	±0.08	0.99	±0.08	0.99	±0.08	1.13	±0.07
	Layer 2	1.07	±0.09	1.14	±0.09	1.19	±0.08	1.25	±0.17	1.13	±0.02
	Layer 3	1.20	±0.12	1.21	±0.07	1.26	±0.02	1.28	±0.02	1.20	±0.01
	Layer 4	1.34	±0.04	1.29	±0.07	1.26	±0.07	1.23	±0.01	1.29	±0.06
Average water application per week (mm)		7.7	±0.7	8.8	±0.6	9.8	±1.4	7.0	±0.6	8.3	±1.3

Table S4. Measurement parameters and instrument specifications for X-ray computed tomography (CT) scans, Exp 2.

Measurement parameter		
Volt	150	kV
Current	700	µA
Exposure time per projection	250	ms
Number of projections	2000	
Average	1	
Images skipped	0	
Binning	2 x 2	
Voxel size	150	µm
Multi-scan	Yes	
Fast scan	Yes	

Table S5. Average nanoplastic concentrations (top) calculated from Pd concentrations measured in the soil profiles of microcosms (bottom), Exp 1. For each layer (layer 1-4, here L1-L4), triplicate soil samples (Soil rep 1-3) were analyzed. The average Pd background concentration was subtracted (32 µg kg^{-1}).

			Microcosm replicate 1			Microcosm replicate 2			Microcosm replicate 3					
			Soil rep 1	Soil rep 2	Soil rep 3	Soil rep 1	Soil rep 2	Soil rep 3	Soil rep 1	Soil rep 2	Soil rep 3	**Mean**	**Stdev**	**RSD**
Nanoplastic concentrations (mg kg^{-1})	7 days	L1	6554	5913	6023	6222	6566	6313	6419	5993	6108	6235	± 244	4%
		L2	159	140	135	533	462	381	292	373	348	314	± 144	48%
		L3	16.4	15.5	13.2	25.7	24.5	15.5	<bkg	29.7	27.7	18.5	± 9.7	52%
		L4	<bkg[a]	<bkg	<bkg	14.1	12.1	7.7	2.1	7	<bkg	3.9	± 6.5	280%
	14 days	L1	7344	6562	6398	6012	5814	6814	6614	6609	6279	6494	± 448	7%
		L2	441	245	254	148	166	164	383	412	284	278	± 112	40%
		L3	52	47	60	38	84	55	93	140	70	71	± 31.3	44%
		L4	11	10	9	14	15	15	20	25	22	15.7	± 5.6	34%
	21 days	L1	4675	4933	5123	5339	5358	5619	5117	5498	5814	5275	± 353	7%
		L2	424	425	447	432	543	400	537	405	501	457	± 55	12%
		L3	137	146	135	130	124	102	163	126	137	133.3	± 16.6	12%
		L4	33	29	21	33	21	46	22	26	25	28.3	±7.9	28%
	28 days	L1	5529	5302	5394	4836	5419	5099	5113	4988	5201	5209	± 223	4%
		L2	343	404	402	612	510	514	478	576	459	478	± 86	18%
		L3	n.a.[b]	n.a.	n.a.	136	163	136	142	158	144	146.6	± 11.6	8%
		L4	n.a.	n.a.	n.a.	76	61	53	34	42	44	51.6	± 15.0	29%
	Control (28 days)	L1	7170	8313	6671	5983	5758	6005	6888	6418	6569	6641	± 775	12%
		L2	81	211	43	28	23	21	25	33	15	53	± 62	117%
		L3	<bkg	<bkg	<bkg	<bkg	<bkg	0.9	0.9	1.1	<bkg	<bkg	± 2.4	-241%
		L4	<bkg	<bkg	<bkg	0.6	<bkg	<bkg	0.4	<bkg	0.3	<bkg	± 1.3	-138%

			Microcosm replicate 1			Microcosm replicate 2			Microcosm replicate 3				
			Soil rep 1	Soil rep 2	Soil rep 3	Soil rep 1	Soil rep 2	Soil rep 3	Soil rep 1	Soil rep 2	Soil rep 3	**Mean**	**Stdev**
Pd concentrations (µg kg^{-1})	7 days	L1	15757	14215	14479	14958	15786	15176	15432	14408	14685	14989	± 586
		L2	383	337	324	1280	1110	915	702	898	838	754	± 346
		L3	39.3	37.3	31.7	61.8	59.0	37.2	<bkg	71.4	66.6	44.5	± 23
		L4	<bkg	<bkg	<bkg	34.0	29.0	18.5	4.9	16.9	<bkg	9.3	± 26
	14 days	L1	17655	15775	15382	14453	13976	16381	15901	15888	15097	15612	± 1078
		L2	1060	590	610	356	400	395	921	990	683	667	± 268
		L3	125.8	112.3	143.7	92.2	201.8	132.0	223.6	336.8	167.7	170.7	± 75
		L4	27.0	23.6	22.2	32.8	37.1	35.3	48.8	60.0	53.1	37.8	± 13
	21 days	L1	11238	11859	12316	12837	12881	13509	12301	13218	13978	12682	± 848
		L2	1018	1022	1075	1040	1307	963	1290	973	1204	1099	± 133
		L3	328.3	350.9	324.2	312.2	298.4	246.3	392.9	302.7	328.6	320.5	± 40
		L4	78.3	68.8	50.7	79.3	50.8	109.9	52.5	62.2	61.0	68.2	± 19
	28 days	L1	13292	12748	12967	11626	13028	12258	12292	11991	12504	12523	± 537
		L2	824	972	966	1471	1225	1235	1150	1386	1103	1148	± 208
		L3	n.a.	n.a.	n.a.	326.3	392.2	326.7	341.2	381.0	347.2	352.4	± 28
		L4	n.a.	n.a.	n.a.	182.3	146.3	127.8	82.5	101.3	104.8	124.2	± 36
	Control (28 days)	L1	17239	19985	16038	14383	13842	14437	16560	15430	15793	15967.4	± 1864
		L2	194	507	103	66	54	51	60	79	35	127.8	± 150
		L3	<bkg	<bkg	<bkg	<bkg	<bkg	2.2	2.2	2.6	<bkg	<bkg	± 6
		L4	<bkg	<bkg	<bkg	1.5	<bkg	<bkg	1.0	<bkg	0.7	<bkg	± 3

[a] Lower than the background Pd-concentration of the soil; [b]Not available

Table S6. Total and per layer recovery of nanoplastics in microcosm soil columns at each time point, calculation based on average concentration and dry weight of soil per layer, Exp 1.

Layer ID	Depth	Recovery of spiked plastic (%)					
		7 days	14 days	21 days	28 days	Control – 28 days	
Layer 1	0-2 cm	56 %	61 %	50 %	50 %		72 %
Layer 2	2-6 cm	6.5 %	6.0 %	10.5 %	11.3 %		1.2 %
Layer 3	6-15 cm	1.0 %	3.8 %	7.3 %	8.1 %[a]		0.0 %
Layer 4	15-29 cm	0.3 %	1.4 %	2.4 %	2.9 %[a]		0.0 %
Total	0-29 cm	64 %	73 %	70 %	72 %		74 %
Layer ID	Depth	Recovery of spiked plastic (mg)					
		7 days	14 days	21 days	28 days	Control – 28 days	
Layer 1	0-2 cm	913.5	999.7	815.4	807.4		1177.7
Layer 2	2-6 cm	106	97.6	171.1	184.7		18.9
Layer 3	6-15 cm	15.6	61.5	118.6	132.3[a]		0.1
Layer 4	15-29 cm	5.5	22.2	39.2	46.5[a]		0
Total	0-29 cm	1040.6	1181	1144.2	1170.9		1196.7

[a]Based on triplicate samples from two replicates only

Table S7. Earthworm weight, weight change and incorporated nanoplastics concentrations, Exp 1. Values are averages for each microcosm with three individual earthworms. The significance of differences ($p \leq 0.05$) was tested for the depurated wet weight before and after the experiment.

Time (days)	Replicate	Initial worm weight wet (g)[a]		Final worm weight wet (g)[a]		Change in weight (g)	Change in weight (%)	t-test, p-values	Worm weight dry (g dw)[b]		Average plastic (µg/g dw)[c]		RSD (%)
7	R1	6.7	±1.1	6.2	±0.5	-0.6	-8.3	0.47	1.2	±0.3	1135	±776	68
	R2	6.1	±0.8	4.8	±0.3	-1.4	-22.1	0.52	0.9	±0.1	1048	±628	60
	R3	5.3	±0.3	5.1	±1.1	-0.3	-4.7	0.32	0.7	±0.0	n.a.		
Average[d]		6.0	±0.9	5.4	±0.8	-0.7	-11.7		1.0	±0.2	1090	±633	58
14	R1	5.5	±0.5	6.5	±1.2	1.0	17.5	0.25	0.8	±0.2	120	±90	73
	R2	6.3	±0.7	6.4	±0.9	0.0	0.1	1.00	0.9	±0.1	260	±176	67
	R3	6.7	±0.1	7.8	±0.3	1.1	16.2	0.01	1.1	±0.1	380	±272	71
Average		6.2	±0.7	6.9	±1	0.7	11.3		0.9	±0.2	253	±202	80
21	R1	6.2	±0.5	6.5	±0.8	0.3	4.0	0.65	0.9	±0.1	211	±143	67
	R2	6.3	±1.0	7.1	±0.7	0.8	13.4	0.31	0.9	±0.0	153	±101	66
	R3	5.3	±0.9	5.7	±0.9	0.5	8.6	0.56	0.7	±0.1	234	±83	35
Average		5.9	±0.9	6.4	±0.9	0.5	8.7		0.8	±0.1	199	±103	52
28	R1	5.8	±0.8	5.5	±0.3	-0.3	-4.9	0.61	0.8	±0.1	311	±142	45
	R2	6.0	±0.5	6.1	±0.5	0.1	2.1	0.76	0.9	±0.1	574	±363	63
	R3	5.8	±0.9	5.8	±1.1	0.0	0.1	1.00	0.8	±0.2	276	±254	91
Average		5.9	±0.7	5.8	±0.7	-0.1	-0.9		0.9	±0.1	387	±272	70

[a]Depurated during 48 h
[b]After freeze-drying
[c]Corrected for background concentration in blank earthworm tissue
[d]Results based on worms extracted from two replicates (n=6)

Table S8. X-ray CT derived biomacropore volume (cm³, biopores with ≥3.5 mm spherical diameter) and biomacroporosity (%, share of the total biopore volume inside the respective soil layer) in microcosm soil columns with and without plastics after 7 and after 28 days, Exp 2.

Treat-ment	Time (days)	Repli-cate (nbr)	Total	Layers 1 and 2 (0-6 cm)		Layer 3 (6-15 cm)		Layer 4 (15-30 cm)	
			Biomacroporevolume (cm³) and biomacroporosity (%)						
			(cm³)	(cm³)	(%)	(cm³)	(%)	(cm³)	(%)
without (w/o) nano-plastics	7	1	53	30	57 %	17	33 %	5	10 %
		2	86	44	51 %	21	24 %	21	25 %
		3	72	31	43 %	22	30 %	20	27 %
		Mean	70	35	50 %	20	29 %	15	21 %
		Stdev	17	8	7 %	2	4 %	9	9 %
without (w/o) nano-plastics	28	1	62	34	54 %	21	33 %	8	12 %
		2	82	33	41%	25	31 %	23	29 %
		3	83	40	48 %	26	31 %	17	20 %
		Mean	76	36	48 %	24	32 %	16	20 %
		Stdev	11.6	3.8	7 %	2.7	2 %	7.9	8 %
with (w) nano-plastics	7	1	55	18	32 %	17	31 %	20	37 %
		2	57	29	50 %	19	34 %	9	16 %
		3*	39	12	29 %	17	44 %	10	26 %
		Mean	50	19	37 %	18	37 %	13	26 %
		Stdev	10	9	11 %	1	7 %	6	10 %
with (w) nano-plastics	28	1	85	38	45 %	27	31 %	20	24 %
		2	65	29	44 %	21	33 %	15	23 %
		3 [a]	53	21	39 %	22	41 %	10	20 %
		Mean	75	34	45 %	24	32 %	17	23 %
		Stdev	13.7	6.4	0 %	3.6	1 %	3.7	1 %

[a] *Replicate 3 with nanoplastics was accidentally destroyed after 21 days, and not considered for the calculation of mean or standard deviation*

Table S9. Applied parameters used for modelling nanoplastic transport by bioturbation (Exp 1) using the bioturbation model developed by Rodriguez (2006)[3].

Model parameter	Applied values		
Bioturbation rate	$k_{bioturb,l:l+1}$	(s^{-1})	1.59×10^{-5}
Soil turnover rate	$v_{l:l+1}$	($m\ s^{-1}$)	7.95×10^{-8}
Depth of layer with an associated concentration	d_l	(m)	0.005
Initial concentration of substance in top layer	$[C]$	($mg\ kg^{-1}$)	10.84
Time-step considered for model	δt	(s)	1210
Bioturbation fitting parameter	β	($m^4\ s^{-1}$)	5.83×10^{-11}
Earthworm density	w_l	(individuals m^{-3})	1364

Supplementary Figures.

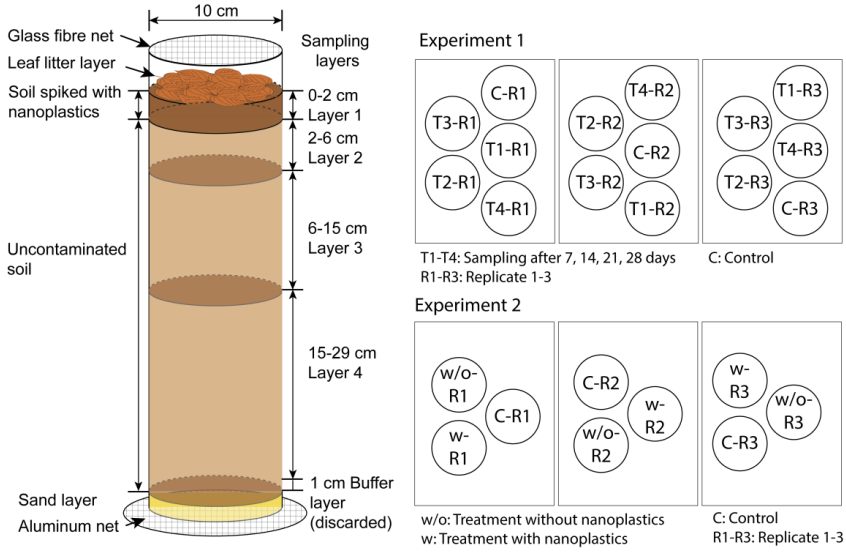

Figure S1. Schematic overview of setup and sampling scheme of microcosm columns for investigating bioturbation-induced transport of nanoplastics by *Lumbricus terrestris* (left) and arrangement of columns in the growth chamber (right), Exp 1 and Exp 2.

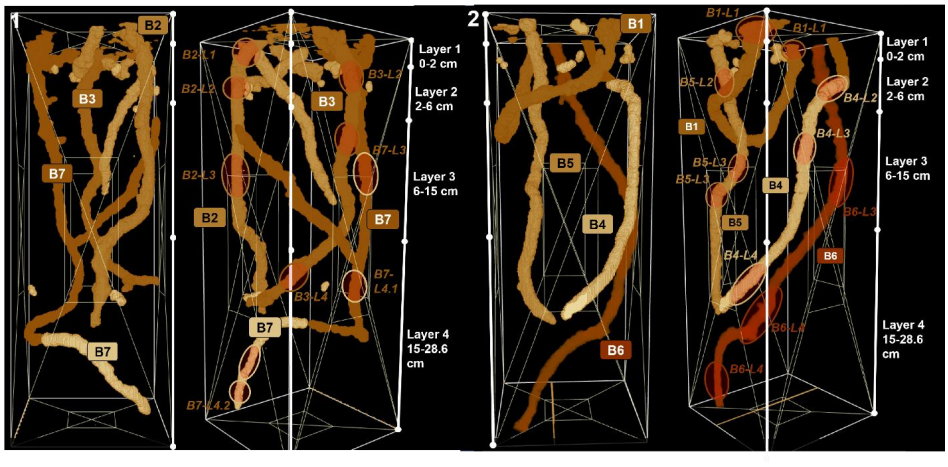

Figure S2. Sampling locations of drilosphere samples in replicate 1 (left, 1) and replicate 2 (right, 2), Exp 2. In total, 7 intact burrows were sampled (B1-B7), and classified according to the depth layer samples were taken from (L1-L4). In one case two samples for layer 4 were analyzed separately (L4.1 and L4.2).

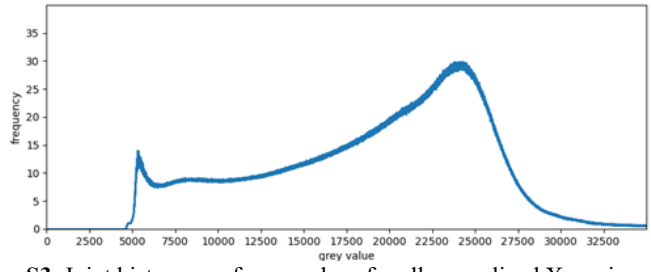

Figure S3. Joint histogram of gray-values for all normalized X-ray image sequences to determine a joint segmentation threshold, Exp 2.

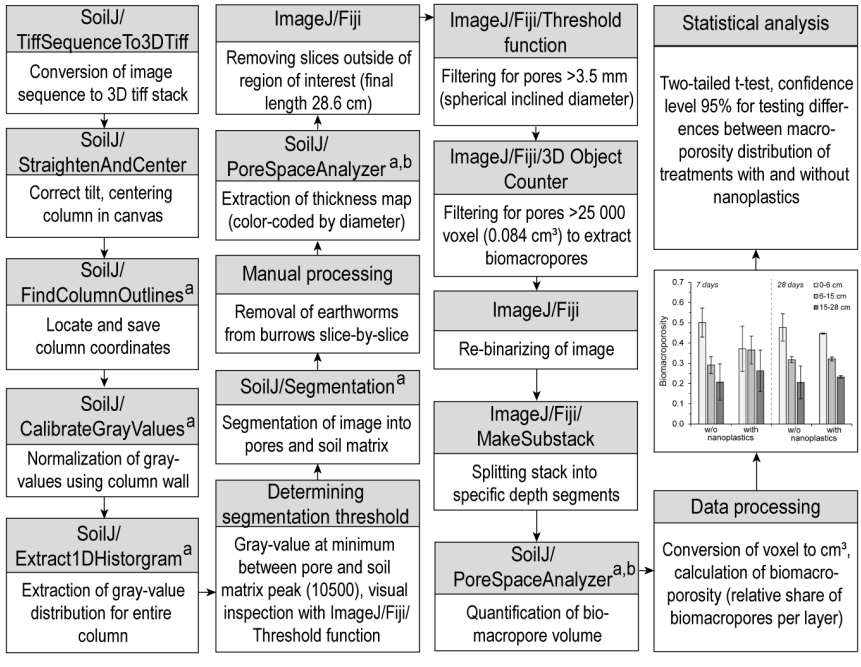

Figure S4: Detailed workflow of X-ray CT image processing and analysis, Exp 2, including applied tools and corresponding references in ImageJ/Fiji using the SoilJ plug-in. References for the corresponding tools are denoted with letters, a: Koestel (2018)[5], b: Legland, *et al.* (2016)[6].

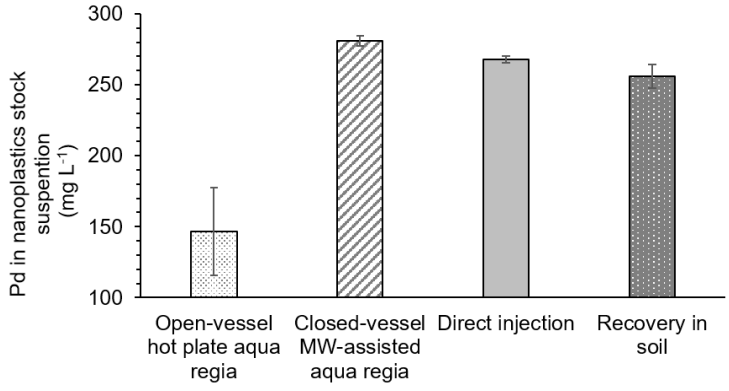

Figure S5. Results of optimization of analytical protocol for digesting nanoplastics and extracting incorporated palladium with *aqua regia*: open-vessel hot plate and closed-vessel microwave-assisted digestion, and direct injection of diluted nanoplastics suspension into ICP-MS. The recovery of nanoplastic-incorporated Pd in presence of soil is included for the final method.

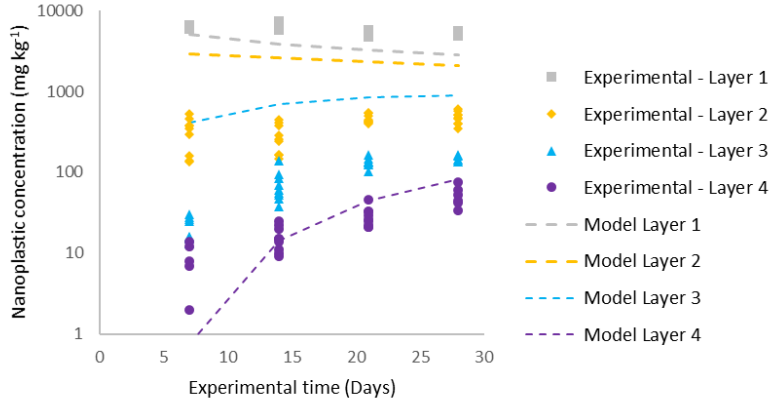

Figure S6. Experimental and modelled nanoplastics concentrations in the four depth layers (0-2, 2-6, 6-15, 15-28 cm) of Exp 1 using a simple bioturbation model developed by Rodriguez (2006)[3].

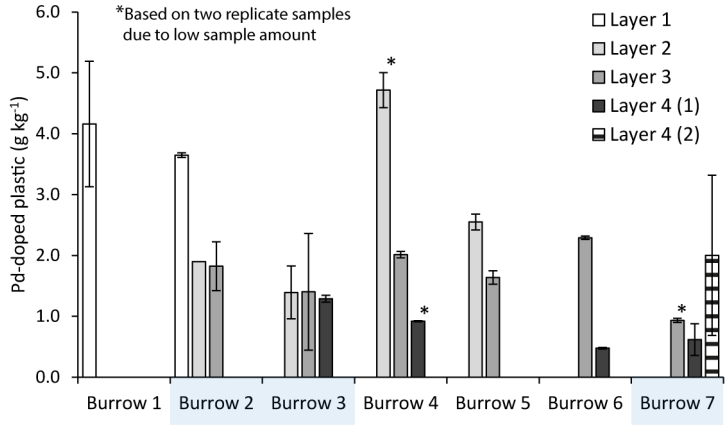

Figure S7. Nanoplastics concentrations detected in the drilosphere (burrow wall) samples (Exp 2), sorted according to burrow number and sampling layer. Highlighted (blue) are burrows from soil column replicate 1, without shading are burrows from replicate 2. Note that for Burrow 7 two separate samples from the lowest layer were analyzed.

References for supplementary information

(1) Mitrano, D. M.; Beltzung, A.; Frehland, S.; Schmiedgruber, M.; Cingolani, A.; Schmidt, F. Synthesis of Metal-Doped Nanoplastics and Their Utility to Investigate Fate and Behaviour in Complex Environmental Systems. *Nat. Nanotechnol.* **2019**, 9. https://doi.org/10.1038/s41565-018-0360-3.

(2) U.S. EPA. Method 3051A (SW-846): Microwave Assisted Acid Digestion of Sediments, Sludges, and Oils. **2007**, No. Revision 1.

(3) Rodriguez, M. D. The Bioturbation Transport of Chemicals in Surface Soils, Louisiana State University, 2006.

(4) Baccaro, M.; Harrison, S.; Berg, H. van den; Sloot, L.; Hermans, D.; Cornelis, G.; Gestel, C. A. M. van; Brink, N. W. van den. Bioturbation of Ag2S-NPs in Soil Columns by Earthworms. *Environ. Pollut.* **2019**, *252*, 155–162. https://doi.org/10.1016/j.envpol.2019.05.106.

(5) Martín, M. Á.; Pachepsky, Y. A.; García-Gutiérrez, C.; Reyes, M. On Soil Textural Classifications and Soil-Texture-Based Estimations. *Solid Earth* **2018**, *9* (1), 159–165. https://doi.org/10.5194/se-9-159-2018.

(6) Koestel, J. SoilJ: An ImageJ Plugin for the Semiautomatic Processing of Three-Dimensional X-Ray Images of Soils. *Vadose Zone J.* **2018**, *17* (1), 170062. https://doi.org/10.2136/vzj2017.03.0062.

(7) Legland, D.; Arganda-Carreras, I.; Andrey, P. MorphoLibJ: Integrated Library and Plugins for Mathematical Morphology with ImageJ. *Bioinformatics* **2016**, *32* (22), 3532–3534. https://doi.org/10.1093/bioinformatics/btw413.

Acta Universitatis Agriculturae Sueciae

Doctoral Thesis No. 2024:80

Micro- and nanoplastics are small plastic particles that can have potentially adverse effects on the soil ecosystem. This thesis investigated potential input pathways to soils as well as the subsequent redistribution of micro- and nanoplastics, involved transport mechanisms and transport limiting factors. The presented results are relevant for understanding the spatial distribution and spread of these persistent particles in soils and other ecosystems.

Wiebke Mareile Heinze received her graduate education at the Department of Soil and Environment, Swedish University of Agricultural Sciences (SLU), Sweden. She holds a M.Sc. degree in Environmental Sciences from the University of Copenhagen, Denmark, and the Swedish University of Agricultural Sciences, Sweden.

Acta Universitatis Agriculturae Sueciae presents doctoral theses from the Swedish University of Agricultural Sciences (SLU).

SLU generates knowledge for the sustainable use of biological natural resources. Research, education, extension, as well as environmental monitoring and assessment are used to achieve this goal.

ISSN 1652-6880
ISBN (print version) 978-91-8046-371-3
ISBN (electronic version) 978-91-8046-407-9